UNIVERSITY OF CALIFORNIA

Santa Barbara

Development of *In Vitro* Models to Study the Effects of Wound Repair and Aging in Retinal Pigmented Epithelium

A dissertation submitted in partial satisfaction of the
Requirements for the degree Doctor of Philosophy
in Molecular, Cellular, and Developmental Biology

By

Lindsay J. Bailey-Steinitz

Committee in charge:

Professor Pete J. Coffey, Co-Chair

Professor Anthony W. De Tomaso, Co-Chair

Professor Dennis O. Clegg

Professor Stuart C. Feinstein

September 2021

The dissertation of Lindsay J. Bailey-Steinitz is approved.

_____

Dennis O. Clegg

_____

Stuart C. Feinstein

_____

Anthony W. De Tomaso, Committee Co-Chair

_____

Pete J. Coffey, Committee Co-Chair

July 2021

Development of *In Vitro* Models to Study the Effects of
Wound Repair and Aging in Retinal Pigmented Epithelium

Acknowledgments

These last six years have been some of the most stressful and most rewarding times of my life. To start a project with a crazy idea that may or may not work and see it through until completion has taken much blood, sweat and, tears but has absolutely been worth it. I could not have made it this far without the guidance and advice from Dr. Pete Coffey and Dr. Monte Radeke. The mentoring and advice both of you have given me has been invaluable and will help propel me throughout my scientific career, whichever way it may go. I would also like to thank my committee members Dr. Tony De Tomaso, Dr. Dennis Clegg, and Dr. Stu Feinstein, whose scientific advice and support have helped steer me using outside knowledge.

Many thanks to Carolyn Radeke, who keeps the lab up and running and whose experience in cell culture has helped me tremendously throughout my Ph.D. Past graduate students Dr. Elson Shih and Dr. Amanda Hurley Timm played a critical role in my first few years, helping create a friendly yet inquisitive atmosphere to discuss science, life, and future scientific career goals. I would also like to thank Luke Crinson for your invaluable drafting skills, which made a large portion of my disease modeling possible, and Renato Minopoli, whose work has helped a tremendous amount this last year. Dr. Rachael Warrington, your friendship and scientific advice have been incredibly helpful these last few years, and I cannot thank you enough.

Thank you to my wife, Ronnie. Your unwavering support played the most significant role in helping me achieve this milestone. You believed in me and reminded me of the light

at the end of the tunnel, even when I could not see it. You made sure I made it through all the roughest times and made me even stronger on the other side. I could not have done this without you. Thank you to my family, who provided support throughout this whole process and was always willing to fill our cupboards and fridge when we needed it. Finally, thank you to the one and only Gizmo and your trusty sidekick, Gadget. Both of your silly and strange personalities have made me laugh every day and have made my life brighter.

VITA of Lindsay J. Bailey-Steinitz

July 2021

EDUCATION

Ph.D. University of California, Santa Barbara 2021
Major: Molecular, Cellular, and Developmental Biology

M.S. University of California, San Diego 2012
Major: Biology

B.S. University of California, San Diego 2010
Major: Human Biology

RESEARCH EXPERIENCE

University of California, Santa Barbara **Graduate Research Assistant** 2015-Present
The Effect of Aging and Wound Repair on Differentiated Human Retinal Pigmented Epithelial Cells. Use of novel techniques combined with transcriptome profiling to dissect potential pathways driving age-related macular degeneration.
Dr. Pete J. Coffey, *pjc@ucsb.edu*

University of California, San Diego **Laboratory Assistant** 2012-2015
Analysis of the role of RNA binding proteins during reproductive development of *Arabidopsis thaliana*. Analysis of the role of microRNA function in *Arabidopsis* growth and development.
Dr. Juan-José Ripoll and Dr. Marty Yanofsky, *jjripoll@ucsd.edu*

University of California, San Diego **Masters Student** 2010-2012
Analysis of upstream and downstream targets of master regulatory genes involved in fruit development in *Arabidopsis thaliana*. Assisted in the development of tools to perform a genome-wide approach termed "Promoter Hiking" in collaboration with the lab of Dr. José Pruneda-Paz.
Dr. Juan-José Ripoll and Dr. Marty Yanofsky, *jjripoll@ucsd.edu*

PUBLICATIONS

Bailey-Steinitz LJ, Shih YH, Radeke MJ, Coffey PJ. An *in vitro* model of chronic wounding and its implication for age-related macular degeneration. *PLoS One*. **2020** Jul 23. doi:10.1371/journal.pone.0236298. PMID: 32701996.

Rodríguez-Cazorla E, Ortuño-Miquel S, Candela H, **Bailey-Steinitz LJ**, Yanofsky MF, Martínez-Laborda A, Ripoll JJ, Vera A. Ovule identity mediated by pre-mRNA processing in Arabidopsis. PLoS Genetics. 2018 Jan 12. doi: 10.1371/journal.pgen.1007182. PMID: 29329291.

Gaillochet C, Stiehl T, Wenzl C, Ripoll JJ, **Bailey-Steinitz LJ**, Li L, Pfeiffer A, Miotk A, Hakenjos JP, Forner J, Yanofsky MF, Marciniak-Czochra A, Lohmann JU. Control of plant

cell fate transition by transcriptional and hormonal signals. Elife. 2017 Oct 23;6. pii: e30135. doi: 10.7554/eLife.30135. PMID: 29058667.

Guan P, Ripoll JJ, Wang R, Vuong L**, Bailey-Steinitz LJ**, Ye D, Crawford N. Interacting TCP and NLP transcription factors control plant responses to nitrate availability. PNAS. 2017 Feb 15. doi:10.1073/pnas.1615676114.

Rodríguez-Cazorla E, Andújar A, Ripoll JJ, **Bailey LJ**, Martínez-Laborda A, Yanofsky MF, Vera A. 3' Rapid amplification of cDNA ends (3'RACE) using Arabidopsis samples. Bio Protoc. 2015 Oct 5;5(19):e1604. PMID: 27034968.

Ripoll JJ, **Bailey LJ**, Mai QA, Wu SL, Hon CT, Chapman EJ, Ditta GS, Estelle M, Yanofsky MF. MicroRNA regulation of fruit growth. Nat Plants. 2015 Mar 30;1(4):15036. doi: 10.1038/nplants.2015.36. PMID: 27247036.

Rodrigues-Cazorla E, Ripoll JJ, Andújar A, **Bailey LJ**, Martínez-Laborda A, Yanofsky MF, Vera A. K-homology nuclear ribonucleoproteins regulate floral organ identity and determinacy in Arabidopsis. PLoS Genetics. 2015 Feb 6;11(2):e1004983. doi: 10.1371/journal.pgen.1004983. eCollection 2015 Feb. PMID: 25658099.

ABSTRACTS

Bailey-Steinitz, L.J., Shih, Y.H., Radeke, M.J, Coffey, P.J. "Cell culture platforms to model AMD Pathogenesis." Talk given at the Neuroscience Research Symposium, UCSB, Santa Barbara, California (2019).

Bailey-Steinitz, L.J., Shih, Y.H., Radeke, M.J, Coffey, P.J., "ECIS as a platform for uncovering AMD therapeutics." Poster presented at the Ocular Diseases Drug Discovery, GTCbio, San Diego, California (2018).

Bailey-Steinitz, L.J., Shih, Y.H., Radeke, M.J., Coffey, P.J., "ECIS as a platform to discover therapeutics for RPE regeneration in geographic atrophy." Talk given and poster presented at The Biology of Regenerative Medicine, Wellcome Genome Campus, Hinxton, United Kingdom (2017).

Bailey, L.J., Ripoll, J.J., Yanofsky, M.F., "miRroring the importance of post-transcriptional regulation in *Arabidopsis* fruit." Poster presented at the Division of Biology Student Research Showcase, UCSD, San Diego, California (2011).

AWARDS

Best Graduate Student Talk at Neuroscience Research Symposium, UCSB 2019.
Best Poster Award at Ocular Diseases Drug Discovery Conference, San Diego 2018.

TEACHING EXPERIENCE

University of California, Santa Barbara Teaching Assistant 2020
Course: Molecular Genetics of Eukaryotes

University of California, Santa Barbara Course: Molecular Genetics of Prokaryotes	Teaching Assistant	2017, 2020
University of California, Santa Barbara Course: Introductory Biology I Laboratory	Teaching Assistant	2015
University of California, San Diego Course: Genetics	Teaching Assistant	2011-2012
University of California, San Diego Course: AIDS Science and Society	Teaching Assistant	2011
University of California, San Diego Course: Human Reproduction and Development	Teaching Assistant	2010-2012

Abstract

Development of *In Vitro* Models to Study the Effects of
Wound Repair and Aging in Retinal Pigmented Epithelium
By
Lindsay J. Bailey-Steinitz

Age-related macular degeneration (AMD) is the leading cause of blindness in people over the age of 50 in the western world. Nearly 2 million people in the U.S. were affected in 2010, and as life expectancy increases, the number of people with AMD will also increase. By the year 2030, it is estimated that over 3 million people in the U.S. alone will be diagnosed with AMD. Although early signs of AMD can be identified easily by a fundus photograph taken by an ophthalmologist, little can be done to cure the disease. Once AMD progresses to advanced stages, irreversible central vision loss can occur, eventually resulting in blindness. In addition to the effect on quality of life, the economic burden of AMD is estimated to be over $340 billion globally.

Early AMD can progress into two advanced stages termed wet or dry AMD based on the presence of choroidal neovascularization. Although wet and dry AMD are clinically distinct, they both are triggered by the degeneration of the retinal pigmented epithelium in the macula, the area responsible for central vision. Retinal pigmented epithelial (RPE) cells are a cuboidal, polarized, and highly pigmented monolayer located between the visual photoreceptors and the vascular choroid. They are an essential cell type in the retina as they provide nutrients, support the visual cycle, and remove waste and fluids from the retina, among other functions. Degeneration and the failure of this single layer of cells to repair can have devastating impacts on retinal function and can ultimately result in the death of the

overlaying photoreceptors. The pathogenesis driving AMD is not entirely clear, but numerous risk factors have been identified including genetic variants and environmental stressors, but the number one risk factor is age. The lack of treatments for early and advanced stages of AMD can in part be explained by the lack of appropriate cell culture and animal models which recapitulate the progression of the disease.

My Ph.D. research focuses on the development of novel *in vitro* wounding platforms to analyze the innate ability of human RPE to repair. In chapter II, we discuss the development of a platform to induce a state of chronic wounding in RPE monolayers. Chronic wounding resulted in several AMD phenotypes including enlarged cell size and multinucleation, along with an increased inflammatory response. In chapter III, we examine a large macula-sized wounding platform. In this system, RPE cells failed to adequately repair, resulting in loss of cuboidal morphology, loss of pigmentation, and regions of RPE atrophy. Finally, in chapter IV, we use a transcriptomic approach to analyze age-related changes in RPE and how it may affect the ability of RPE to repair wounds in the monolayer. Taken together, the work presented here further our knowledge of RPE wound repair and may also allow for the identification of therapeutics which can improve the ability of RPE to repair.

Table of Contents

List of Figures

Abbreviations

AGEs	Advanced glycation end products
ALEs	Age-related lipoxidation end products
ALK5	Activin-like kinase 5
AMD	Age-related macular degeneration
BRB	Blood-retinal-barrier
CDK	Cyclin-dependent kinase
CHIR	CHIR-99021
CID	Chemical inducer of dimerization
CNV	Choroidal neovascularization
DEGs	Differentially expressed genes
DISC	Death-inducing signaling complex
ECIS	Electric cell-substrate impedance sensing
ECM	Extracellular matrix
EdU	5-ethynyl-2´-deoxyuridine
EMT	Epithelial-to-mesenchymal transition
FACS	Fluorescence activated cell sorting
FAK	Focal adhesion kinase
FGF	Fibroblast growth factor
GA	Geographic atrophy
GFP	Green fluorescent protein
GO	Gene ontology
GSK3	Glycogen synthase kinase 3
HSPGs	Heparan sulfate proteoglycans
IAPs	Inhibitors of apoptosis proteins
ICAM-1	Intracellular adhesion molecule-1
iCaspase9	Inducible Caspase-9
IPM	Interphotoreceptor matrix
iPS	Induced pluripotent stem cells

IRBP	Interphotoreceptor protein
LRAT	Lecithin retinol acyl transferase
MDS	Multidimensional scaling
MMPs	Matrix metalloproteinases
MPs	Mononuclear phagocytes
PBS	Phosphate buffer saline
POS	Photoreceptor outer segments
RCS	Royal College of Surgeons
RDH	Retinol dehydrogenase
ROCK	Rho-dependent protein kinase
ROS	Reactive oxygen species
RPE	Retinal pigmented epithelial

Chapter I: Introduction

A. Retinal pigmented epithelial cells

First identified in the 1790s as a net-shaped membrane composed of interlinked, black globules, the retinal pigment epithelial (RPE) cell monolayer is located at the base of the retina and serves as an essential support cell for the overlaying neural retina [1,2]. Situated between the light-sensitive photoreceptors and Brüch's membrane, this polarized, cuboidal, pigmented layer has many significant functions in the eye. Critical functions of RPE include forming the blood-retinal barrier (BRB), polarized secretion of growth factors, transport of nutrients, removal of waste, completion of the visual cycle, phagocytosis of photoreceptor-outer segments (POS), and absorption of stray light [3–5]. Degeneration of this single layer of cells can ultimately result in death of the overlaying photoreceptors and irreversible loss of vision [4,6,7].

B. Visual cycle

The light sensitivity of the eye is made possible by the presence of the chromophore 11-*cis* retinal, which covalently links to G-protein coupled receptors known as opsins located within the outer segments of photoreceptors [8]. In rods, the highly sensitive photoreceptor responsible for low-acuity and low-light vision, the opsin retinal complex is known as rhodopsin, while in cones, the photoreceptors responsible for high acuity and color vision, it is referred to as photopsin. Upon exposure with light, rhodopsin and photopsin undergo photoisomerization where 11-*cis* retinal isomerizes to all-*trans* retinal and causes a conformational change in the opsin that triggers visual transduction [9]. Subsequently, all-*trans* retinal is released from the opsin and replaced with new 11-*cis* retinal to allow for continued detection of light. Once released, all-*trans* retinal is transported to the underlying

RPE where it is converted back into 11-*cis* retinal and transported back to the photoreceptors in a process known as the visual cycle [10,11].

Several key proteins are involved in the classical visual cycle, many of which when mutated cause blinding diseases [12]. Within the photoreceptor, all-*trans* retinal is transported by the ATP binding cassette transporter ABCA4 into the cytoplasm where it is reduced to all-*trans* retinol (vitamin A) by all-*trans* retinol dehydrogenase (RDH12 or RDH8) [13–18]. Vitamin A then is bound to the interphotoreceptor protein (IRBP), transported out of the photoreceptor, across the interphotoreceptor matrix (IPM) and into the RPE where it is esterified into all-*trans* retinyl ester by lecithin retinol acyl transferase (LRAT) [19,20] . Retinol esters are isomerized and hydrolyzed into 11-*cis* retinol by RPE65 and oxidized by RDH5, RDH10, or RDH11 to form 11-*cis* retinal [21–24]. Finally, 11-*cis* retinal is rebound to IRBP and diffuses back across the IPM into the photoreceptor where it is loaded back into an opsin to complete the visual cycle.

C. Photoreceptor outer segment phagocytosis

A single RPE cell supports between 30-50 photoreceptors by providing nutrients and removing waste [25]. Microvilli on the apical surface of RPE interact with the distal ends of rod and cone photoreceptors, help keep the neural retina attached and are used to engulf the membranous outer segment discs [26,27]. This process is carried out daily, at first light, where roughly 5% of the photoreceptor outer segment (POS) mass is shed [25,28]. Phagocytosis of shed POS is essential for photoreceptor health. Disruption of this process ultimately leads to accumulation of outer segment debris and photoreceptor apoptosis, as seen in the Royal College of Surgeons (RCS) rat [6,29,30].

The RCS rat carries a mutation in the retinal dystrophy (rdy) locus, corresponding to the receptor tyrosine kinase MerTK, one of the two essential receptors required for POS phagocytosis [31]. The process of POS phagocytosis in RPE is composed of three distinct stages including binding, internalization, and digestion. The initiation of POS binding is mediated by the integrin receptor αvβ5, expressed on the apical surface of RPE, its secreted ligand MFG-E8, and phosphatidylserine exposed on distal POS [32–34]. MerTK can be activated by binding of its secreted ligands Gas6 or protein S with shedding outer segments and is further activated by downstream activation of focal adhesion kinase (FAK) by integrin αvβ5, allowing for internalization of POS [32,33,35].

Once internalized, shed POS are trafficked to the basal region of the RPE, mediated in part by two F-actin associated proteins, myosin VIIa and annexin A2, for digestion [36,37]. The internalized POS fuses with endosomes and lysosomes to begin degradation and recycling of POS components [3,33,38,39]. Cathepsin D, an aspartyl protease, is thought to be the primary protease involved in breakdown of opsins, which account for more than 80% of the protein content of POS, while lipid hydrolases phospholipase A_1 and A_2 break down POS lipids [40–42]. Some POS components are recycled for re-use while others are secreted basally through Brüch's membrane into the choroid. Failure to digest POS results in the accumulation of lipofuscin, composed of lipids, proteins, and fluorescent compounds, which build up in the lysosome and can ultimately lead to RPE dysfunction [43,44].

D. Blood-retinal barrier

While the apical surface is specialized to interact with overlaying photoreceptors, the basal surface of RPE consists of infoldings to attach to the underlying Brüch's membrane. Together, the RPE monolayer, Brüch's membrane, and the underlying capillary endothelial

cells form the outer BRB [45,46]. The outer BRB allows for separation between the neural retina and the high flow rate blood supply to the retina, the choroid.

The BRB regulates the movement of water, ions, proteins, and waste into and out of the retina. The ability of RPE to maintain tight junctions across cell-cell contacts is necessary in slowing the movement of molecules across the monolayer. This allows RPE to regulate the transepithelial transport of molecules across the RPE monolayer via facilitated diffusion, active transport, transcytosis, endocytosis, or across tight junctions themselves [46]. The maintenance of the BRB is critical for sustained retinal function and disruption can result in diseases such as diabetic retinopathy and age-related macular degeneration (AMD) [47,48].

BRB integrity is key to maintaining the eye as an immune privileged structure, so that excessive ocular inflammation is limited and vision is preserved [49,50]. Over activation or chronic activation of the immune system can result in a number of degenerative ocular disorders such as AMD, uveitis, and diabetic retinopathy [51]. Immune privilege of the eye is maintained using physical barriers, such as the BRB, and the inhibitory ocular environment where immunosuppressive factors, such as TGF-β, are expressed [52]. Microglial cells are the resident immune cell of the eye and provide surveillance of the retina to quickly clear debris and maintain homeostasis [53,54]

E. Brüch's membrane

Like the RPE, Brüch's membrane can also restrict the movement of molecules from the choroid. Situated between the RPE monolayer and the vascular choroid, this acellular structure anchors both the RPE monolayer and the choroidal endothelial cells. Brüch's membrane is comprised of five layers; (anterior to posterior) RPE basal lamina, inner collagenous layer, elastic layer, outer collagenous layer, and choriocapillaris basal lamina. As

an acellular structure, the dense protein structures are produced and maintained by the overlaying RPE and underlying choriocapillaris [55,56].

The RPE basal lamina is composed of collagen IV and V, laminins 1, 5, and 11, nidogen-1, heparan sulfate and chondroitin sulfate [57–59]. The inner collagenous layer and outer collagenous layers are composed of collagens I, II, and V, fibronectin, proteoglycans, vitronectin, lipoproteins and apolipoprotein E (apoE) [55,60,61]. The elastic layer is composed of a dense network of elastin fibers and calcium phosphate, which has some antiangiogenic barrier properties [62,63]. Interestingly, the dense fibers are more discontinuous in the macula, offering one explanation of why the macula region is more prone to choroidal neovascularization (CNV) [64]. The outer collagenous layer is composed of collagens type I, II, and V, fibulin-5, fibronectin, chondroitin and dermatan sulfate, lipoproteins, apoE, and clusterin [55,59,65,66]. The choriocapillaris basal lamina is composed of collagens IV, V, and VI, laminin, proteoglycans, and endostatin [57,67,68]. Although the underlying choriocapillaris are fenestrated, which may allow the movement of large molecules into Brüch's membrane, the dense networks of proteins layered in Brüch's membrane acts as a molecular sieve, preventing the movement of many large molecules into the retina.

F. Age-related changes

Several age-related changes occur in Brüch's membrane which affect the overall flexibility and ability of molecules to flow through the membrane. Accumulation of lipoproteins, composed of neutral lipids and apolipoprotein B (apoB), in the elastic layer and inner collagenous layer is one of the most obvious age related changes [65,69]. Lipids begin to accumulate in the elastic layer and outer collagenous layer around the age of 30 [70,71].

As age progresses, lipids continue to accumulate into the inner collagenous layer, eventually forming a new sublayer in Brüch's membrane, termed the lipid wall, located between the inner collagenous layer and the RPE basal lamina. The formation of the lipid wall is thought to be a precursor to AMD-specific lesions, basal linear deposits and drusen, and may ultimately impair the ability of molecules to diffuse through the membrane [65,72].

Additional age-related changes include thickening, accumulation of debris, heme, cross-linking, and calcification [55]. Collagens are a long-lived protein but can be modified *in vivo* by free radicals to yield advanced glycation end products (AGEs) and lipid-derived reactive carbonyl species known as age-related lipoxidation end products (ALEs) [62,73,74]. The accumulation of AGEs may influence the lysosomal ability of the overlaying RPE and may contribute to lipofuscin accumulation [75]. The accumulation in AGEs and ALEs have been implicated as pathogenic agents in age-related retinal disease [75]. Cross-linking and thickening of Brüch's membrane results in reduced diffusion ability of molecules which may ultimately impact RPE function [76]. Finally, calcification of the elastic layer can render Brüch's membrane brittle, resulting in breakage leading to neovascularization [77]. The accumulation of these age-related changes of Brüch's membrane may play an important role in the pathogenesis of AMD.

In addition to the changes in Brüch's membrane, a number of age-related changes occur within the RPE such as loss of melanin granules, accumulation of lipofuscin, increased oxidative stress, and a reduced ability to phagocytose POS [25,78–80]. As the retina is constantly absorbing UV light, over time it can result in the accumulation of reactive oxygen species (ROS) and contribute to DNA damage, oxidative stress, and inflammation [81–85]. The age-related reduction in pigmentation, which acts as a photoprotectant, likely

exacerbates this effect [86]. The accumulation of lipofuscin, thought to be in part due to age-dependent reduction in activity of lysosomal enzymes and antioxidants in the RPE and may be influenced by in changes in Brüch's membrane, can also generate ROS and contribute to increased oxidative stress of the cell [44,80,87,88]. Several structural changes of aged RPE occur as well, including atrophy of the apical microvilli and disorganization of the basal infoldings [27,89]. These changes may result in the decreased absorption and transport of nutrients and reduced POS phagocytosis in aged RPE [25,90].

G. Age-related macular degeneration

Age-related macular degeneration affects an estimated 170 million people worldwide and is expected to rise to 288 million by 2040 [91,92]. It is the leading cause of blindness in developed countries and the global cost is estimated to be over $340 billion [93]. AMD generally affects people over the age of 60 with people of European descent being most at risk for developing AMD [91,94].

Early stages of AMD can be identified by a fundus photograph, a picture of the back of the eye taken by an ophthalmologist. The presence of drusen, yellow sub-RPE deposits, in the macular region are criteria for the diagnosis of early AMD. Drusen are the clinical hallmark of AMD and typically develop between the RPE basal lamina and the inner collagenous layer [95–97]. Drusen are composed of esterified cholesterol, phosphatidylcholine, and proteins including vitronectin, complement factor 8 and 9, apoB, apoE, amyloid-β, and clusterin [98]. Although drusen biogenesis is still not fully understood, the overlaying RPE are thought to contribute significantly to the formation [98]. Drusen can be described as hard, having well-defined borders and generally small, or soft, having

indistinct borders with a tendency to be larger. Although similar in composition, soft drusen may be more predictive of AMD development [99,100].

AMD can advance to intermediate stages where pigmentation abnormalities begin to appear and drusen enlarge. Most people do not experience perceptible vision loss at this stage. However, in advanced stages of AMD the RPE undergo dysfunction and degeneration which may ultimately result in loss of vision [101]. AMD can progress to two clinically distinct, but not mutually exclusive forms termed wet and dry AMD, depending on the presence of choroidal neovascularization. In dry AMD, also known as geographic atrophy (GA), death of the underlying RPE and eventually death of the overlaying photoreceptors results in areas of atrophy in the macula which expand over time. In wet AMD, also known as choroidal neovascularization (CNV), infiltration of new blood vessels into the retina leak fluid, resulting in death of the RPE and photoreceptors. Dry AMD accounts for 90% of diagnosed cases, and while wet AMD accounts for the remaining 10% of cases it accounts for 90% of legal blindness [94]. Interestingly, wet AMD is always preceded by dry AMD and thus it is thought that dry AMD is the primary form of the disease and wet AMD is a complication of underlying disease.

No treatment options have been found thus far to help prevent the onset or progression of AMD. Treatment with the ARES/AREDS2 nutritional supplement has been shown to reduce the progression of AMD from intermediate to advanced stages by 25% [102,103]. A few treatment options to slow the progression of CNV exist which aim to prevent or occlude new blood vessel growth into the retina, however no treatment options exist for treatment of GA [104–106]. Death of RPE cells in the retina are one common

feature of both CNV and GA, resulting in the ultimate degeneration of the overlaying photoreceptors and loss of vision.

H. Risk factors associated with AMD

Several risk factors, besides age, have been attributed to contribute to AMD and ultimate RPE degeneration including genetics, inflammation, and oxidative stress. A number of genetic variants in complement factor genes (*CFH*, *CFB*, *C2*, *C3*, and *CFI*) have been associated with AMD [107–112]. As part of the innate immune system, the complement system enhances the ability of the immune system to remove damaged tissues and pathogens from the body. The complement system can be activated through several pathways, including the classical, alternative or lectin pathways. All three pathways converge downstream to form C3 convertase and ultimately induce inflammation and form the membrane attack complex which can induce cell lysis [113,114].

The complement system is tightly regulated to avoid possible over activation of inflammation and cell death. Several regulatory proteins exist to help prevent erroneous activation of the pathway, including CFH and CFI which act together to inactivate C3 [115]. Interestingly, CFH can protect cellular surfaces, like Brüch's membrane, by binding to heparan sulfates and glycosaminoglycans. The Y402H CFH polymorphism results in a reduced protective effect to prevent complement activation and an impaired binding ability to Brüch's membrane [116]. It is thought that people with this polymorphism have increased levels of complement activity, particularly in Brüch's membrane and the choriocapillaris [116,117]. This can result in excessive complement activation and ultimate RPE degeneration.

Drusen are also thought to be potential sites of inflammation, considering their inflammatory contents [98,118,119]. As the earliest sign of AMD, it is possible that drusen can result in long term chronic inflammation for the overlaying RPE. RPE dysfunction may also result from prolonged restricted movement of molecules between the RPE and Brüch's membrane [120].

Smoking is known to promote chronic inflammation and oxidative stress and can significantly increase the risk of developing and the rate of progression of AMD [121,122]. When added to cultured RPE cells, cigarette smoke extract can induce oxidative damage, induce the production of ROS, promote senescence, and induce cell death [123,124]. Although ROS play many important roles modulating cellular homeostasis, excessive production of ROS can trigger inflammation, cellular dysfunction, and may contribute to the progression of AMD [125,126].

I. Current *in vitro* wound healing systems

To try and elucidate mechanisms which may be driving the pathology of AMD numerous *in vitro* systems have been developed. Advancing our understanding of how RPE repair after traumatic events, such as wounding, can help further our understanding of RPE wound repair. Cell culture models offer fast and relatively inexpensive alternatives to animal models. Although *in vitro* models generally do not recapitulate the intricacies formed between the choriocapillaris, Brüch's membrane, and the RPE, the simplicity allows for detailed analysis of potential mechanisms driving RPE degeneration. In this way, large scale therapeutic screens are easily achieved, expediting drug discovery.

Several wound healing models currently exist to study the ability of RPE to repair, including wounds generated mechanically or by enzymatic disruption. The scratch assay is

perhaps the most common, where pipette tips or pins are used to generate wounds in the monolayer. The disruption of RPE cell-cell contacts triggers a wound healing response where the cell undergoes an epithelial-to-mesenchymal transition (EMT) to migrate and proliferate to fill the wound [127–129]. Once mended, the RPE must undergo a mesenchymal-to-epithelial transition (MET) to differentiate back into a functional RPE monolayer, failure of which can result in a terminal mesenchymal fate.

The generation of streamlined pipelines used to create and analyze wound repair using this method are helpful for screening large quantities of compounds quickly. However, the wound size can be variable, and damage to the underlying basement membrane is common, impeding wound repair. To avoid damage to the basement membrane, wounds can be generated by removing plugs or plastic inserts from specialized cultureware. In this case, cells are plated and allowed to differentiate in specialized plates. The plugs or inserts are then removed to generate a defined wound in the monolayer to study wound repair. In both cases, mechanical force is used to generate wounds in the monolayer.

Wounds in the RPE monolayer can also be generated using enzymatic methods. In this system, enzymes such as trypsin are used to continuously disrupt the formation of a differentiated RPE monolayer [130]. The continual disruption of cell contacts, induced by serial passaging, induces a state of chronic wounding and triggers the switch to a persistent mesenchymal state [130]. Using this method, it is possible to screen therapeutics which can prevent or potentially reverse the induced mesenchymal state. However, this method generates a global wound in the RPE monolayer, which is at odds with the localized areas of RPE degeneration in the macula seen in AMD.

J. Specific goals

The goal of my Ph.D. research was to develop *in vitro* wound healing models using cultured human RPE. Developing additional wound repair systems with phenotypic and transcriptomic similarities to AMD may help us to further elucidate mechanisms driving AMD pathogenesis. In the next chapter, I describe a novel method to induce a state of localized chronic wounding in RPE monolayers. In the third chapter, I describe a method to induce macula-sized lesions in RPE monolayers. Finally, in the fourth chapter, I analyze age-related changes in RPE and discuss how they may affect the ability of aged RPE to repair wounds. Together, the results from these chapters provide further insight into RPE wound repair, and how it is affected during aging. These platforms can be used to screen therapeutic libraries for compounds which may improve the innate ability of RPE to regenerate, opening the door for AMD treatment.

K. References

1. Mondini C. [On the ocular pigment]. Bononiensi Sci artium Inst atque Acad Comment. 1791;7: 29–32.
2. De Jong PTVM. Elusive drusen and changing terminology of AMD. 2017. doi:10.1038/eye.2017.298
3. Strauss O. The Retinal Pigment Epithelium in Visual Function. Physiol Rev. 2005;85: 845–881. doi:10.1152/physrev.00021.2004
4. Sparrow JR, Hicks D, Hamel CP. The retinal pigment epithelium in health and disease. Curr Mol Med. 2010;10: 802–23. Available: http://www.ncbi.nlm.nih.gov/pubmed/21091424
5. Blaauwgeers HGT, Holtkamp GM, Rutten H, Witmer AN, Koolwijk P, Partanen TA, et al. Polarized vascular endothelial growth factor secretion by human retinal pigment epithelium and localization of vascular endothelial growth factor receptors on the inner choriocapillaris: Evidence for a trophic paracrine relation. Am J Pathol. 1999;155: 421–428. doi:10.1016/S0002-9440(10)65138-3
6. Bok D, Hall MO. The role of the pigment epithelium in the etiology of inherited retinal dystrophy in the rat. J Cell Biol. 1971;49: 664–682. doi:10.1083/jcb.49.3.664

7. Gal A, Li Y, Thompson DA, Weir J, Orth U, Jacobson SG, et al. Mutations in MERTK, the human orthologue of the RCS rat retinal dystrophy gene, cause retinitis pigmentosa. Nat Genet. 2000;26: 270–271. doi:10.1038/81555

8. Wald G. Carotenoids and the visual cycle. J Gen Physiol. 1935;19: 351–371. doi:10.1085/jgp.19.2.351

9. Hubbard R, Kropf A. THE ACTION OF LIGHT ON RHODOPSIN. Proc Natl Acad Sci. 1958;44: 130–139. doi:10.1073/pnas.44.2.130

10. Wright CB, Redmond TM, Nickerson JM. A History of the Classical Visual Cycle. Progress in Molecular Biology and Translational Science. Elsevier B.V.; 2015. pp. 433–448. doi:10.1016/bs.pmbts.2015.06.009

11. Sahu B, Maeda A. Retinol dehydrogenases regulate vitamin A metabolism for visual function. Nutrients. MDPI AG; 2016. p. 746. doi:10.3390/nu8110746

12. Tsin A, Betts-Obregon B, Grigsby J. Visual cycle proteins: Structure, function, and roles in human retinal disease. J Biol Chem. 2018;293: 13016–13021. doi:10.1074/jbc.AW118.003228

13. Maeda A, Maeda T, Imanishi Y, Sun W, Jastrzebska B, Hatala DA, et al. Retinol dehydrogenase (RDH12) protects photoreceptors from light-induced degeneration in mice. J Biol Chem. 2006;281: 37697–37704. doi:10.1074/jbc.M608375200

14. Illing M, Molday LL, Molday RS. The 220-kDa rim protein of retinal rod outer segments is a member of the ABC transporter superfamily. J Biol Chem. 1997;272: 10303–10310. doi:10.1074/jbc.272.15.10303

15. Allikmets R, Shroyer NF, Singh N, Seddon JM, Lewis RA, Bernstein PS, et al. Mutation of the Stargardt disease gene (ABCR) in age-related macular degeneration. Science (80-). 1997;277: 1805–1807. doi:10.1126/science.277.5333.1805

16. Sun H, Molday RS, Nathans J. Retinal stimulates ATP hydrolysis by purified and reconstituted ABCR, the photoreceptor-specific ATP-binding cassette transporter responsible for Stargardt disease. J Biol Chem. 1999;274: 8269–8281. doi:10.1074/jbc.274.12.8269

17. Molday RS, Zhong M, Quazi F. The role of the photoreceptor ABC transporter ABCA4 in lipid transport and Stargardt macular degeneration. Biochim Biophys Acta - Mol Cell Biol Lipids. 2009;1791: 573–583. doi:10.1016/j.bbalip.2009.02.004

18. Perrault I, Hanein S, Gerber S, Barbet F, Ducroq D, Dollfus H, et al. Retinal dehydrogenase 12 (RDH12) mutations in leber congenital amaurosis. Am J Hum Genet. 2004;75: 639–646. doi:10.1086/424889

19. Adler AJ, Severin KM. Proteins of the bovine interphotoreceptor matrix: Tissues of origin. Exp Eye Res. 1981;32: 755–769. doi:10.1016/0014-4835(81)90025-7

20. Saari JC, Bredberg DL. Lecithin:retinol acyltransferase in retinal pigment epithelial microsomes. J Biol Chem. 1989;264: 8636–8640. doi:10.1016/s0021-9258(18)81839-7

21. Hamel CP, Tsilou E, Harris E, Pfeffer BA, Hooks JJ, Detrick B, et al. A developmentally regulated microsomal protein specific for the pigment epithelium of the vertebrate retina. J Neurosci Res. 1993;34: 414–425. doi:10.1002/jnr.490340406

22. Jin M, Li S, Moghrabi WN, Sun H, Travis GH. Rpe65 is the retinoid isomerase in bovine retinal pigment epithelium. Cell. 2005;122: 449–459. doi:10.1016/j.cell.2005.06.042

23. Redmond TM, Poliakov E, Yu S, Tsai JY, Lu Z, Gentleman S. Mutation of key residues of RPE65 abolishes its enzymatic role as isomerohydrolase in the visual cycle. Proc Natl Acad Sci U S A. 2005;102: 13658–13663. doi:10.1073/pnas.0504167102

24. Parker RO, Crouch RK. Retinol dehydrogenases (RDHs) in the visual cycle. Experimental Eye Research. NIH Public Access; 2010. pp. 788–792. doi:10.1016/j.exer.2010.08.013

25. Bonilha VL. Age and disease-related structural changes in the retinal pigment epithelium. Clin Ophthalmol. 2008;2: 413–424. doi:10.2147/opth.s2151

26. Bok D. The retinal pigment epithelium: A versatile partner in vision. Journal of Cell Science. Company of Biologists Ltd; 1993. pp. 189–195. doi:10.1242/jcs.1993.supplement_17.27

27. Bonilha VL, Rayborn ME, Bhattacharya SK, Gu X, Crabb JS, Crabb JW, et al. The retinal pigment epithelium apical microvilli and retinal function. Advances in Experimental Medicine and Biology. NIH Public Access; 2005. pp. 519–524. doi:10.1007/0-387-32442-9_72

28. Young RW, Bok D. Participation of the retinal pigment epithelium in the rod outer segment renewal process. J Cell Biol. 1969;42: 392–403. doi:10.1083/jcb.42.2.392

29. Strauss O. The Royal College of Surgeons rat: An animal model for inherited retinal degeneration with a still unknown genetic defect. Acta Anatomica. S. Karger AG; 1998. pp. 101–111. doi:10.1159/000046474

30. Chaitin MH, Hall MO. Defective ingestion of rod outer segments by cultured dystrophic rat pigment epithelial cells - PubMed. Investig Ophthalmol Vis Sci. 1983;24: 812–820. Available: https://pubmed.ncbi.nlm.nih.gov/6345445/

31. D'Cruz PM, Yasumura D, Weir J, Matthes MT, Abderrahim H, LaVail MM, et al. Mutation of the receptor tyrosine kinase gene Mertk in the retinal dystrophic RCS rat. Hum Mol Genet. 2000;9: 645–651. doi:10.1093/hmg/9.4.645

32. Vollrath D, Feng W, Duncan JL, Yasumura D, D'Cruz PM, Chappelow A, et al. Correction of the retinal dystrophy phenotype of the RCS rat by viral gene transfer of Mertk. Proc Natl Acad Sci U S A. 2001;98: 12584–12589. doi:10.1073/pnas.221364198

33. Mazzoni F, Safa H, Finnemann SC. Understanding photoreceptor outer segment phagocytosis: use and utility of RPE cells in culture. Exp Eye Res. 2014;126: 51–60. doi:10.1016/j.exer.2014.01.010

34. Nandrot EF, Anand M, Almeida D, Atabai K, Sheppard D, Finnemann SC. Essential role for MFG-E8 as ligand for αvβ5 integrin in diurnal retinal phagocytosis. Proc Natl Acad Sci U S A. 2007;104: 12005–12010. doi:10.1073/pnas.0704756104

35. Finnemann SC. Focal adhesion kinase signaling promotes phagocytosis of integrin-bound photoreceptors. EMBO J. 2003;22: 4143–4154. doi:10.1093/emboj/cdg416

36. Gibbs D, Kitamoto J, Williams DS. Abnormal phagocytosis by retinal pigmented epithelium that lacks myosin VIIa, the usher syndrome 1B protein. Proc Natl Acad Sci U S A. 2003;100: 6481–6486. doi:10.1073/pnas.1130432100

37. Law AL, Ling Q, Hajjar KA, Futter CE, Greenwood J, Adamson P, et al. Annexin A2 regulates phagocytosis of photoreceptor outer segments in the mouse retina. Mol Biol Cell. 2009;20: 3896–3904. doi:10.1091/mbc.E08-12-1204

38. Bazan NG, Gordon WC, Rodriguez de Turco EB. Docosahexaenoic acid uptake and metabolism in photoreceptors: Retinal conservation by an efficient retinal pigment epithelial cell-mediated recycling process. Advances in Experimental Medicine and Biology. Adv Exp Med Biol; 1992. pp. 295–306. doi:10.1007/978-1-4615-3426-6_26

39. Baehr W, Wu SM, Bird AC, Palczewski K. The retinoid cycle and retina disease. Vision Research. Elsevier Ltd; 2003. pp. 2957–2958. doi:10.1016/j.visres.2003.10.001

40. Kwon W, Freeman SA. Phagocytosis by the Retinal Pigment Epithelium: Recognition, Resolution, Recycling. Frontiers in Immunology. Frontiers Media S.A.; 2020. p. 2985. doi:10.3389/fimmu.2020.604205

41. Papermaster DS, Dreyer WJ. Rhodopsin Content in the Outer Segment Membranes of Bovine and Frog Retinal Rods. Biochemistry. 1974;13: 2438–2444. doi:10.1021/bi00708a031

42. Swartz JG, Mitchell JE. Phospholipase Activity of Retina and Pigment Epithelium. Biochemistry. 1973;12: 5273–5278. doi:10.1021/bi00750a008

43. Dalvi S, Galloway CA, Winschel L, Hashim A, Soto C, Tang C, et al. Environmental stress impairs photoreceptor outer segment (POS) phagocytosis and degradation and induces autofluorescent material accumulation in hiPSC-RPE cells. Cell Death Discov. 2019;5: 96. doi:10.1038/s41420-019-0171-9

44. Kennedy CJ, Rakoczy PE, Constable IJ. Lipofuscin of the retinal pigment epithelium: A review. Eye. 1995;9: 763–771. doi:10.1038/eye.1995.192

45. Fields MA, Del Priore L V., Adelman RA, Rizzolo LJ. Interactions of the choroid, Bruch's membrane, retinal pigment epithelium, and neurosensory retina collaborate to form the outer blood-retinal-barrier. Progress in Retinal and Eye Research. Elsevier Ltd; 2020. p. 100803. doi:10.1016/j.preteyeres.2019.100803

46. Rizzolo LJ, Peng S, Luo Y, Xiao W. Integration of tight junctions and claudins with the barrier functions of the retinal pigment epithelium. Progress in Retinal and Eye Research Pergamon; Sep 1, 2011 pp. 296–323. doi:10.1016/j.preteyeres.2011.06.002

47. Xu HZ, Song Z, Fu S, Zhu M, Le YZ. RPE barrier breakdown in diabetic retinopathy: Seeing is believing. J Ocul Biol Dis Infor. 2011;4: 83–92. doi:10.1007/s12177-011-9068-4

48. Vinores SA. Breakdown of the blood-retinal barrier. Encyclopedia of the Eye. Elsevier; 2010. pp. 216–222. doi:10.1016/B978-0-12-374203-2.00137-8

49. Cunha-Vaz J. The Blood–Retinal Barrier in Retinal Disease. Eur Ophthalmic Rev. 2009;03: 105. doi:10.17925/eor.2009.03.02.105

50. Cunha-Vaz J. The blood-ocular barriers. Surv Ophthalmol. 1979;23: 279–296. doi:10.1016/0039-6257(79)90158-9

51. Murakami Y, Ishikawa K, Nakao S, Sonoda KH. Innate immune response in retinal homeostasis and inflammatory disorders. Progress in Retinal and Eye Research. Elsevier Ltd; 2020. p. 100778. doi:10.1016/j.preteyeres.2019.100778

52. Zhou R, Caspi RR. Ocular immune privilege. F1000 Biol Rep. 2010;2. doi:10.3410/B2-3

53. Rashid K, Akhtar-Schaefer I, Langmann T. Microglia in Retinal Degeneration. Front Immunol. 2019;10: 1975. doi:10.3389/fimmu.2019.01975

54. Ginhoux F, Greter M, Leboeuf M, Nandi S, See P, Gokhan S, et al. Fate mapping analysis reveals that adult microglia derive from primitive macrophages. Science (80-). 2010;330: 841–845. doi:10.1126/science.1194637

55. Curcio CA, Johnson M. Structure, Function, and Pathology of Bruch's Membrane. Retina Fifth Edition. Elsevier Inc.; 2012. pp. 465–481. doi:10.1016/B978-1-4557-0737-9.00020-5

56. Booij JC, Baas DC, Beisekeeva J, Gorgels TGMF, Bergen AAB. The dynamic nature of Bruch's membrane. Progress in Retinal and Eye Research. Prog Retin Eye Res; 2010. pp. 1–18. doi:10.1016/j.preteyeres.2009.08.003

57. Chen L, Miyamura N, Ninomiya Y, Handa JT. Distribution of the collagen IV isoforms in human Bruch's membrane. Br J Ophthalmol. 2003;87: 212–215. doi:10.1136/bjo.87.2.212

58. Aisenbrey S, Zhang M, Bacher D, Yee J, Brunken WJ, Hunter DD. Retinal pigment epithelial cells synthesize laminins, including laminin 5, and adhere to them through α3- and α6-containing integrins. Investig Ophthalmol Vis Sci. 2006;47: 5537–5544. doi:10.1167/iovs.05-1590

59. Call TW, Hollyfield JG. Sulfated proteoglycans in Bruch's membrane of the human eye: Localization and characterization using cupromeronic blue. Exp Eye Res. 1990;51: 451–462. doi:10.1016/0014-4835(90)90158-Q

60. Anderson DH, Ozaki S, Nealon M, Neitz J, Mullins RF, Hageman GS, et al. Local cellular sources of apolipoprotein E in the human retina and retinal pigmented epithelium: Implications for the process of drusen formation. Am J Ophthalmol. 2001;131: 767–781. doi:10.1016/S0002-9394(00)00961-2

61. Tezel TH, Geng L, Lato EB, Schaal S, Liu Y, Dean D, et al. Synthesis and secretion of hemoglobin by retinal pigment epithelium. Investig Ophthalmol Vis Sci. 2009;50: 1911–1919. doi:10.1167/iovs.07-1372

62. Beattie JR, Pawlak AM, Boulton ME, Zhang J, Monnier VM, McGarvey JJ, et al. Multiplex analysis of age-related protein and lipid modifications in human Bruch's membrane. FASEB J. 2010;24: 4816–4824. doi:10.1096/fj.10-166090

63. Davis WL, Jones RG, Hagler HK. An electron microscopic histochemical and analytical X-ray microprobe study of calcification in Bruch's membrane from human eyes. J Histochem Cytochem. 1981;29: 601–608. doi:10.1177/29.5.7252127

64. Chong NHV, Keonin J, Luthert PJ, Frennesson CI, Weingeist DM, Wolf RL, et al. Decreased thickness and integrity of the macular elastic layer of Bruch's membrane correspond to the distribution of lesions associated with age-related macular degeneration. Am J Pathol. 2005;166: 241–251. doi:10.1016/S0002-9440(10)62248-1

65. Huang JD, Presley JB, Chimento MF, Curcio CA, Johnson M. Age-related changes in human macular Bruch's membrane as seen by quick-freeze/deep-etch. Exp Eye Res. 2007;85: 202–218. doi:10.1016/j.exer.2007.03.011

66. Wang L, Li CM, Rudolf M, Belyaeva O V., Chung BH, Messinger JD, et al. Lipoprotein particles of intraocular origin in human bruch membrane: An unusual lipid profile. Investig Ophthalmol Vis Sci. 2009;50: 870–877. doi:10.1167/iovs.08-2376

67. Bhutto IA, Kim SY, McLeod DS, Merges C, Fukai N, Olsen BR, et al. Localization of collagen XVIII and the endostatin portion of collagen XVIII in aged human control eyes and eyes with age-related macular degeneration. Investig Ophthalmol Vis Sci. 2004;45: 1544–1552. doi:10.1167/iovs.03-0862

68. Lin WL, Essner E, McCarthy KJ, Couchman JR. Ultrastructural immunocytochemical localization of chondroitin sulfate proteoglycan in Bruch's membrane of the rat. | IOVS | ARVO Journals. Investig Ophthalmol Vis Sci. 1992;33: 2072–2075. Available: https://iovs.arvojournals.org/article.aspx?articleid=2161290&resultClick=1

69. Curcio CA, Johnson M, Huang JD, Rudolf M. Aging, age-related macular degeneration, and the response-to-retention of apolipoprotein B-containing lipoproteins. Prog Retin Eye Res. 2009;28: 393–422. doi:10.1016/j.preteyeres.2009.08.001

70. Pauleikhoff D, Sheraidah G, Marshall J, Bird AC, Wessing A. BIOCHEMISCHE UND HISTOCHEMISCHE ANALYSE ALTERSABHANGIGER LIPIDABLAGERUNGEN IN DER BRUCHSCHEN MEMBRAN. Ophthalmologe. 1994;91: 730–734. Available: https://europepmc.org/article/med/7849423

71. Pauleikhoff D, Harper CA, Marshall J, Bird AC. Aging Changes in Bruch's Membrane: A Histochemical and Morphologic Study. Ophthalmology. 1990;97: 171–178. doi:10.1016/S0161-6420(90)32619-2

72. Curcio CA, Johnson M, Rudolf M, Huang JD. The oil spill in ageing Bruch membrane. Br J Ophthalmol. 2011;95: 1638–1645. doi:10.1136/bjophthalmol-2011-300344

73. Ida H, Ishibashi K, Reiser K, Hjelmeland LM, Handa JT. Ultrastructural aging of the RPE-Bruch's membrane-choriocapillaris complex in the D-galactose-treated mouse. Investig Ophthalmol Vis Sci. 2004;45: 2348–2354. doi:10.1167/iovs.03-1337

74. Crabb JW, Miyagi M, Gu X, Shadrach K, West KA, Sakaguchi H, et al. Drusen proteome analysis: an approach to the etiology of age-related macular degeneration. Proc Natl Acad Sci U S A. 2002;99: 14682–7. doi:10.1073/pnas.222551899

75. Glenn J V., Mahaffy H, Wu K, Smith G, Nagai R, Simpson DAC, et al. Advanced glycation end product (AGE) accumulation on Bruch's membrane: Links to age-related RPE dysfunction. Investig Ophthalmol Vis Sci. 2009;50: 441–451. doi:10.1167/iovs.08-1724

76. Karwatowski WSS, Jeffries TE, Duance VC, Albon J, Bailey AJ, Easty DL. Collagen and ageing in Bruch's Membrane. Biochemical Society Transactions. Biochem Soc Trans; 1991. doi:10.1042/bst019349s

77. Spraul CW, Lang GKGE, Grossniklaus HE, Lang GKGE. Histologic and morphometric analysis of the choroid, Bruch's membrane, and retinal pigment epithelium in postmortem eyes with age-related macular degeneration and histologic examination of surgically excised choroidal neovascular membranes. Surv Ophthalmol. 1999;44: S10–S32. doi:10.1016/S0039-6257(99)00086-7

78. Gu X, Neric NJ, Crabb JS, Crabb JW, Bhattacharya SK, Rayborn ME, et al. Age-related changes in the retinal pigment epithelium (RPE). PLoS One. 2012;7: e38673. doi:10.1371/journal.pone.0038673

79. Datta S, Cano M, Ebrahimi K, Wang L, Handa JT. The impact of oxidative stress and inflammation on RPE degeneration in non-neovascular AMD. Prog Retin Eye Res. 2017;60: 201–218. doi:10.1016/j.preteyeres.2017.03.002

80. Weiter JJ, Delori FC, Wing GL, Fitch KA. Retinal pigment epithelial lipofuscin and melanin and choroidal melanin in human eyes - PubMed. Investig Ophthalmol Vis Sci. 1986;27: 145–152. Available: https://pubmed.ncbi.nlm.nih.gov/3943941/

81. Bellezza I. Oxidative stress in age-related macular degeneration: NRF2 as therapeutic target. Front Pharmacol. 2018;9. doi:10.3389/fphar.2018.01280

82. Rowe LA, Degtyareva N, Doetsch PW. DNA damage-induced reactive oxygen species (ROS) stress response in Saccharomyces cerevisiae. Free Radic Biol Med. 2008;45: 1167–1177. doi:10.1016/j.freeradbiomed.2008.07.018

83. Mahendra CK, Tan LTH, Pusparajah P, Htar TT, Chuah LH, Lee VS, et al. Detrimental Effects of UVB on Retinal Pigment Epithelial Cells and Its Role in Age-Related Macular Degeneration. Oxidative Medicine and Cellular Longevity. Hindawi Limited; 2020. doi:10.1155/2020/1904178

84. You YH, Lee DH, Yoon JH, Nakajima S, Yasui A, Pfeifer GP. Cyclobutane

Pyrimidine Dimers Are Responsible for the Vast Majority of Mutations Induced by UVB Irradiation in Mammalian Cells. J Biol Chem. 2001;276: 44688–44694. doi:10.1074/jbc.M107696200

85. Hollyfield JG, Bonilha VL, Rayborn ME, Yang X, Shadrach KG, Lu L, et al. Oxidative damage-induced inflammation initiates age-related macular degeneration. 2008 [cited 8 Aug 2018]. doi:10.1038/nm1709

86. Solano F. Photoprotection and skin pigmentation: Melanin-related molecules and some other new agents obtained from natural sources. Molecules. MDPI AG; 2020. doi:10.3390/molecules25071537

87. Höhn A, Jung T, Grimm S, Grune T. Lipofuscin-bound iron is a major intracellular source of oxidants: Role in senescent cells. Free Radic Biol Med. 2010;48: 1100–1108. doi:10.1016/j.freeradbiomed.2010.01.030

88. Berman ER. Retinal pigment epithelium: Lysosomal enzymes and aging. British Journal of Ophthalmology. BMJ Publishing Group; 1994. pp. 82–83. doi:10.1136/bjo.78.2.82

89. Beatty S, Koh HH, Phil M, Henson D, Boulton M. The role of oxidative stress in the pathogenesis of age-related macular degeneration. Surv Ophthalmol. 2000;45: 115–134. doi:10.1016/S0039-6257(00)00140-5

90. Boulton M, Dayhaw-Barker P. The role of the retinal pigment epithelium: Topographical variation and ageing changes. Eye. 2001;15: 384–389. doi:10.1038/eye.2001.141

91. Wong WL, Su X, Li X, Cheung CMG, Klein R, Cheng C-Y, et al. Global prevalence of age-related macular degeneration and disease burden projection for 2020 and 2040: a systematic review and meta-analysis. Lancet Glob Heal. 2014;2: e106–e116. doi:10.1016/S2214-109X(13)70145-1

92. Xu X, Wu J, Yu X, Tang Y, Tang X, Shentu X. Regional differences in the global burden of age-related macular degeneration. BMC Public Health. 2020;20: 1–9. doi:10.1186/s12889-020-8445-y

93. Age-Related Macular Degeneration: Facts & Figures | BrightFocus Foundation. [cited 25 Sep 2018]. Available: https://www.brightfocus.org/macular/article/age-related-macular-facts-figures

94. Macular Degeneration Prevention & Risk Factors | BrightFocus Foundation. [cited 30 Jun 2021]. Available: https://www.brightfocus.org/macular/prevention-and-risk-factors

95. Hageman GS, Luthert PJ, Victor Chong NHH, Johnson L V., Anderson DH, Mullins RF. An Integrated Hypothesis That Considers Drusen as Biomarkers of Immune-Mediated Processes at the RPE-Bruch's Membrane Interface in Aging and Age-Related Macular Degeneration. Prog Retin Eye Res. 2001;20: 705–732. doi:10.1016/S1350-9462(01)00010-6

96. Russell SR, Mullins RF, Schneider BL, Hageman GS. Location, substructure, and

composition of basal laminar drusen compared with drusen associated with aging and age-related macular degeneration. Am J Ophthalmol. 2000;129: 205–214. doi:10.1016/S0002-9394(99)00345-1

97. Coffey AJH, Brownstein S. The prevalence of macular drusen in postmortem eyes. Am J Ophthalmol. 1986;102: 164–171. doi:10.1016/0002-9394(86)90138-8

98. Wang L, Clark ME, Crossman DK, Kojima K, Messinger JD, Mobley JA, et al. Abundant Lipid and Protein Components of Drusen. Koch K-W, editor. PLoS One. 2010;5: e10329. doi:10.1371/journal.pone.0010329

99. Sarks JP, Sarks SH, Killingsworth MC. Evolution of soft drusen in age-related macular degeneration. Eye. 1994;8: 269–283. doi:10.1038/eye.1994.57

100. Spaide RF, Curcio CA. Drusen characterization with multimodal imaging. Retina. 2010;30: 1441–1454. doi:10.1097/IAE.0b013e3181ee5ce8

101. (UK) NI for H and CE. Age-related macular degeneration: diagnosis and management. 5th, Classification ed. National Institute for Health and Care Excellence (UK); 2018. Available: https://www.ncbi.nlm.nih.gov/books/NBK536465/

102. AREDS/AREDS2 Clinical Trials | National Eye Institute. [cited 6 Jul 2021]. Available: https://www.nei.nih.gov/research/clinical-trials/age-related-eye-disease-studies-aredsareds2/about-areds-and-areds2

103. The Age-Related Eye Disease Study (AREDS): design implications. AREDS report no. 1. Control Clin Trials. 1999;20: 573–600. doi:10.1016/S0197-2456(99)00031-8

104. da Cruz L, Fynes K, Georgiadis O, Kerby J, Luo YH, Ahmado A, et al. Phase 1 clinical study of an embryonic stem cell–derived retinal pigment epithelium patch in age-related macular degeneration. Nat Biotechnol. 2018;36: 328–337. doi:10.1038/nbt.4114

105. Kashani AH, Lebkowski JS, Rahhal FM, Avery RL, Salehi-Had H, Dang W, et al. A bioengineered retinal pigment epithelial monolayer for advanced, dry age-related macular degeneration. Sci Transl Med. 2018;10: eaao4097. doi:10.1126/scitranslmed.aao4097

106. Jian L, Panpan Y, Wen X. Current Choroidal Neovascularization Treatment. Ophthalmologica. 2013;230: 55–61. doi:10.1159/000351660

107. Gold B, Merriam JE, Zernant J, Hancox LS, Taiber AJ, Gehrs K, et al. Variation in factor B (BF) and complement component 2 (C2) genes is associated with age-related macular degeneration. Nat Genet. 2006;38: 458–462. doi:10.1038/ng1750

108. Yates JRW, Sepp T, Matharu BK, Khan JC, Thurlby DA, Shahid H, et al. Complement C3 Variant and the Risk of Age-Related Macular Degeneration. N Engl J Med. 2007;357: 553–561. doi:10.1056/nejmoa072618

109. Fagerness JA, Maller JB, Neale BM, Reynolds RC, Daly MJ, Seddon JM. Variation near complement factor I is associated with risk of advanced AMD. Eur J Hum Genet. 2009;17: 100–104. doi:10.1038/ejhg.2008.140

110. Hageman GS, Anderson DH, Johnson L V., Hancox LS, Taiber AJ, Hardisty LI, et al. From The Cover: A common haplotype in the complement regulatory gene factor H (HF1/CFH) predisposes individuals to age-related macular degeneration. Proc Natl Acad Sci. 2005;102: 7227–7232. doi:10.1073/pnas.0501536102

111. Edwards AO, Ritter R, Abel KJ, Manning A, Panhuysen C, Farrer LA. Complement factor H polymorphism and age-related macular degeneration. Science. 2005;308: 421–4. doi:10.1126/science.1110189

112. den Hollander AI, de Jong EK. Highly penetrant alleles in age-related macular degeneration. Cold Spring Harb Perspect Med. 2015;5. doi:10.1101/cshperspect.a017202

113. Lo MW, Woodruff TM. Complement: Bridging the innate and adaptive immune systems in sterile inflammation. Journal of Leukocyte Biology. John Wiley and Sons Inc.; 2020. pp. 339–351. doi:10.1002/JLB.3MIR0220-270R

114. Schartz ND, Tenner AJ. The good, the bad, and the opportunities of the complement system in neurodegenerative disease. Journal of Neuroinflammation. BioMed Central Ltd; 2020. pp. 1–25. doi:10.1186/s12974-020-02024-8

115. Noris M, Remuzzi G. Overview of complement activation and regulation. Semin Nephrol. 2013;33: 479–492. doi:10.1016/j.semnephrol.2013.08.001

116. Clark SJ, Perveen R, Hakobyan S, Morgan BP, Sim RB, Bishop PN, et al. Impaired binding of the age-related macular degeneration-associated complement factor H 402H allotype to Bruch's membrane in human retina. J Biol Chem. 2010;285: 30192–30202. doi:10.1074/jbc.M110.103986

117. Bhutto IA, Baba T, Merges C, Juriasinghani V, McLeod DS, Lutty GA. C-reactive protein and complement factor H in aged human eyes and eyes with age-related macular degeneration. Br J Ophthalmol. 2011;95: 1323–1330. doi:10.1136/bjo.2010.199216

118. Johnson L V, Leitner WP, Staples MK, Anderson DH. Complement Activation and Inflammatory Processes in Drusen Formation and Age Related Macular Degeneration. Exp Eye Res. 2001;73: 887–896. doi:10.1006/exer.2001.1094

119. Anderson DH, Mullins RF, Hageman GS, Johnson L V. A role for local inflammation in the formation of drusen in the aging eye. Am J Ophthalmol. 2002;134: 411–431. doi:10.1016/S0002-9394(02)01624-0

120. Balaratnasingam C, Yannuzzi LA, Curcio CA, Morgan WH, Querques G, Capuano V, et al. Associations between retinal pigment epithelium and drusen volume changes during the lifecycle of large drusenoid pigment epithelial detachments. Investig Ophthalmol Vis Sci. 2016;57: 5479–5489. doi:10.1167/iovs.16-19816

121. Lee J, Taneja V, Vassallo R. Cigarette smoking and inflammation: Cellular and molecular mechanisms. Journal of Dental Research. International Association for Dental Research; 2012. pp. 142–149. doi:10.1177/0022034511421200

122. Velilla S, García-Medina JJ, García-Layana A, Dolz-Marco R, Pons-Vázquez S,

Pinazo-Durán MD, et al. Smoking and age-related macular degeneration: Review and update. Journal of Ophthalmology. Hindawi Limited; 2013. p. 11. doi:10.1155/2013/895147

123. Bertram KM, Baglole CJ, Phipps RP, Libby RT. Molecular regulation of cigarette smoke induced-oxidative stress in human retinal pigment epithelial cells: Implications for age-related macular degeneration. Am J Physiol - Cell Physiol. 2009;297. doi:10.1152/ajpcell.00126.2009

124. Yu AL, Birke K, Burger J, Welge-Lussen U. Biological Effects of Cigarette Smoke in Cultured Human Retinal Pigment Epithelial Cells. PLoS One. 2012;7. doi:10.1371/journal.pone.0048501

125. Forrester SJ, Kikuchi DS, Hernandes MS, Xu Q, Griendling KK. Reactive oxygen species in metabolic and inflammatory signaling. Circulation Research. Lippincott Williams and Wilkins; 2018. pp. 877–902. doi:10.1161/CIRCRESAHA.117.311401

126. Finkel T. Signal transduction by reactive oxygen species. Journal of Cell Biology. J Cell Biol; 2011. pp. 7–15. doi:10.1083/jcb.201102095

127. Lamouille S, Xu J, Derynck R. Molecular mechanisms of epithelial-mesenchymal transition. Nature Reviews Molecular Cell Biology. Nat Rev Mol Cell Biol; 2014. pp. 178–196. doi:10.1038/nrm3758

128. Lee SC, Kwon OW, Seong GJ, Kim SH, Ahn JE, Kay EDP. Epitheliomesenchymal transdifferentiation of cultured RPE cells. Ophthalmic Res. 2001;33: 80–86. doi:10.1159/000055648

129. De Iongh RU, Wederell E, Lovicu FJ, McAvoy JW. Transforming growth factor-β-induced epithelial-mesenchymal transition in the lens: A model for cataract formation. Cells Tissues Organs. 2005;179: 43–55. doi:10.1159/000084508

130. Radeke MJ, Radeke CM, Shih Y-H, Hu J, Bok D, Johnson L V., et al. Restoration of mesenchymal retinal pigmented epithelial cells by TGFβ pathway inhibitors: implications for age-related macular degeneration. Genome Med. 2015;7: 58. doi:10.1186/s13073-015-0183-x

Chapter II: An *in vitro* Model of Chronic Wounding and its Implication for Age-Related Macular Degeneration

Lindsay J. Bailey-Steinitz, Ying-Hsuan Shih, Monte J. Radeke, Pete J. Coffey

A. Abstract

Degeneration of the retinal pigment epithelium (RPE) plays a central role in age-related macular degeneration (AMD). Throughout life, RPE cells are challenged by a variety of cytotoxic stressors, some of which are cumulative with age and may ultimately contribute to drusen and lipofuscin accumulation. Stressors such as these continually damage RPE cells resulting in a state of chronic wounding. Current cell-based platforms that model a state of chronic RPE cell wounding are limited, and the RPE cellular response is not entirely understood. Here, we used the electric cell-substrate impedance sensing (ECIS) system to induce a state of acute or chronic wounding on differentiated human fetal RPE cells to analyze changes in the wound repair response. RPE cells surrounding the lesioned area employ both cell migration and proliferation to repair wounds but fail to reestablish their original cell morphology or density after repetitive wounding. Chronically wounded RPE cells develop phenotypic AMD characteristics such as loss of cuboidal morphology, enlarged size, and multinucleation. Transcriptomic analysis suggests a systemic misregulation of RPE cell functions in bystander cells, which are not directly adjacent to the wound. Genes associated with the major RPE cell functions (*LRAT, MITF, RDH11*) significantly downregulate after wounding, in addition to differential expression of genes associated with the cell cycle (*CDK1, CDC6, CDC20*), inflammation (*IL-18, CCL2*), and apoptosis (*FAS*). Interestingly, repetitive wounding resulted in prolonged misregulation of genes, including *FAS, LRAT,* and *PEDF*. The use of ECIS to induce wounding resulted in an over-

representation of AMD-associated genes among those dysregulated genes, particularly genes associated with advanced AMD. This simple system provides a new model for further investigation of RPE cell wound response in AMD pathogenesis.

B. Introduction

Retinal pigment epithelium (RPE) cells are a monolayer of highly specialized pigmented cells residing between the retinal photoreceptors and Brüch's membrane. A single RPE cell maintains the health of approximately thirty photoreceptors by phagocytosing outer segments and supporting the visual cycle, among other functions [1]. As a layer of epithelium, RPE cells selectively transport substances across the blood-retinal-barrier (BRB) and secrete growth factors such as PEDF and VEGF to support the neural retina and choriocapillaris [2–4]. RPE cells play a vital role in the maintenance of retinal health; as such, degeneration of this simple layer of cells can cause an imbalance in the homeostasis of the subretinal space and may lead to permanent visual impairment [5,6].

The loss of RPE cells is believed to be a crucial step in the onset of age-related macular degeneration (AMD), the leading cause of irreversible blindness in the elderly population of the developed world. Early stages of AMD can be identified by the presence of drusen, extracellular deposits located between the RPE and Bruch's membrane, and RPE cell abnormalities, including changes in pigmentation [7–9]. As the disease advances to later stages, it can take on two clinically distinct yet not mutually exclusive forms commonly referred to as dry and wet AMD [10–13]. Approximately 12% of early AMD cases develop into an advanced subtype of dry AMD called geographic atrophy (GA), which is characterized by the progressive degeneration of the RPE cells, photoreceptors, and choroidal capillaries near the macular region [14–18]. Additional RPE cell abnormalities associated

with GA include enlarged and multi-nucleated cells at the margins of the regions of atrophy [19]. Alternatively, early AMD can progress to wet AMD, characterized by choroidal neovascularization (CNV), where neovascular tissues infiltrate the retina. Infiltration of these tissues can interfere with the RPE-photoreceptor interface leading to scarring and may leak fluid into the retina, causing further degeneration and transdifferentiation of RPE cells [20–22].

Although the exact mechanisms of AMD progression are under debate, chronic exposure to cytotoxic elements such as drusen, lipofuscin, and reactive oxygen species (ROS) can promote RPE cell death and increase the risk of AMD [23–27]. In the last decades, numerous cell-based wound healing assays, via chemical or mechanical ablation, have been developed to dissect the underlying mechanisms of RPE cell wound response and AMD pathogenesis [28–32]. Nevertheless, it is a technical challenge to create a chronic and localized wounding situation to recapitulate the progressive RPE degeneration seen in the macular region of AMD eyes. To overcome the challenge, we used the electric cell-substrate impedance sensing (ECIS) system to precisely and repetitively wound the same area on a differentiated human fetal RPE monolayer. Chronic wounding of the RPE monolayer using this system leads to significant changes in RPE morphology, behavior, and gene expression that are distinct from changes that occur after an acute wound.

C. Materials and Methods

Cell culture

Human fetal RPE cells were provided by Dean Bok (University of California, Los Angeles). Fetal cells were isolated from deidentified tissue that was obtained with written

informed consent by a third party tissue repository (Advanced Bioscience Resources, Alameda, CA, USA) and cultured according to previously described methods [28,33,34]. Cells were seeded at $1x10^5$ cells/cm^2 and allowed to differentiate for 32-40 days in a base medium described by Maminishkis [35]. ECIS 96-well 1E+ cultureware (Applied BioPhysics) were coated with filtered 10 mM cysteine hydrochloride (Fisher Scientific) in nanopure water for 10 minutes at room temperature. The plate was rinsed twice with nanopure water before coating with 20 ug/ml laminin (ThermoFisher Scientific Inc.) overnight at 4ºC. Wounds were delivered using ECIS Zθ (Applied BioPhysics) with a wound current of 3000 µA, frequency of 60000Hz, and a wound time of 15 sec. Dead cells were gently removed from electrode approximately two hours post wounding by pipetting. Palbociclib (40 µM, Selleckchem); Thiazovivin (2 µM, Cayman Chemical); human recombinant TGFβ-2 (50 ng/ml, PeproTech); RepSox (50 nM, Cayman Chemical); 5-ethynyl-2'-deoxyuridine (EdU, 30 µM, Invitrogen); DKK-1 (200 ng/ml, R&D Systems); Wnt3a (200 ng/ml, R&D Systems) was supplemented to cultures on a daily basis.

EdU labeling and immunocytochemistry

Proliferating cells were labeled using medium supplemented with 30 µM 5-ethynyl-2´-deoxyuridine (EdU) for 24-48 hours. Cells were fixed with 4% paraformaldehyde for 10-15 minutes. Specimens were incubated with 5% normal donkey serum at 4ºC overnight. Click-iT® Plus EdU reactions were conducted following the manufacturer's instructions (Invitrogen). Primary antibodies; Alexa Fluor 594 mouse anti-ZO-1 (7.5 µg/ml, Life Technologies), Anti-Fas clone CH11 (500 ng/ml, Sigma) were incubated overnight at 4ºC. Nuclei were stained using Hoechst 33342 (1:2000, Thermo Scientific) for 10 minutes at room temperature. ECIS wells were excised from the dish and mounded on CellVis #1.5H 12-well

dishes using ProLong Gold antifade mountant (Thermo Fisher). Images were obtained using a Cytation5 (BioTek) and processed using the Gen3.0 software to produce movies. Images taken to assess cell density and morphology were taken using auto exposure.

Transcriptomic analysis

Cells on and in the region adjacent to the 350 μm diameter electrodes were manually dissected using a 1.5 mm biopsy punch (Integra LifeSciences). RNA was harvested using NucleoSpin RNA XS Kit (Macherey-Nagel) and converted into cDNA using SMART-Seq v4 Ultra Low Input RNA Kit (Clontech Laboratories). DNA libraries were prepared with Ion Xpress™ Plus gDNA Fragment Library Preparation kit and sequenced by an Ion Proton next-generation sequencer (Thermo Fisher Scientific Inc.). The resulting sequences were aligned to the human transcriptome and genome (hg38) using a two-stage alignment pipeline employing STAR and TMAP read aligners [36]. The number of reads per protein-coding mRNA was determined using Partek Genomics Suite (Partek Inc.), and the dataset was normalized using the trimmed mean of the M-values method [37]. Genes with reads per million (RPM) ≥1 in three or more samples were selected (S1 Table), and differential expression and statistical analysis were carried out using the classic implementation of edgeR (S2 Table) [38]. The RNA-Seq data and methods can be accessed through the Gene Expression Omnibus (GEO: GSE146884).

D. Results

Differentiated human fetal RPE cells mend lesions within 24-hours

The integrity of the RPE monolayer along with the endothelial cells of Bruch's membrane are required to maintain the blood-retinal barrier [2]. To investigate the wound-

healing capacity of differentiated human RPE, electric cell-substrate impedance sensing (ECIS) Zθ technology was utilized [39–41]. In this system, cells are grown on gold electrodes located in the bottom of an ECIS cultureware plate where the electrical impedance imposed by those cells is monitored and recorded by the application of a low voltage alternating current Discrete paddle-shaped wounds in the monolayer can be created by delivering high current-high frequency pulses for several seconds, killing the cells overlaying and directly adjacent to the electrodes (Fig 2-1A). The kinetics of wound repair can be measured by monitoring the impedance as a function of time [42,43].

To determine the kinetics of repair in the differentiated RPE after a single acute wound, human fetal RPE cells plated at high density and cultured for 32 days to allow for the development of cuboidal morphology and pigmentation. Differentiated RPE cells maintained an impedance at 5000-6000 Ω at a frequency of 16,000 Hz as a confluent monolayer. Immediately following the delivery of a high current electrical pulse, the impedance dropped to a level comparable to an empty electrode (~2000 Ω; Fig 2-1B). A lag phase was apparent after the delivery of the pulse, where the impedance of an empty electrode was maintained. Using time-lapse imaging, we determined that the lag phase consisted of two events. In the first 300 minutes, bystander cells were maintained in a latent condition, where no obvious movement was observed (Fig 2-1A), followed by a vigorous ingrowth of bystander cells. However, it took approximately 200 minutes for RPE cells to migrate from the perimeter of the lesion to the margin of the electrode, where changes in impedance can be detected. Notably, the majority of the RPE migrated as a sheet, while cells distal to the lesion remained stationary (S1 Movie). Following the lag phase, the impedance steadily increased to a level

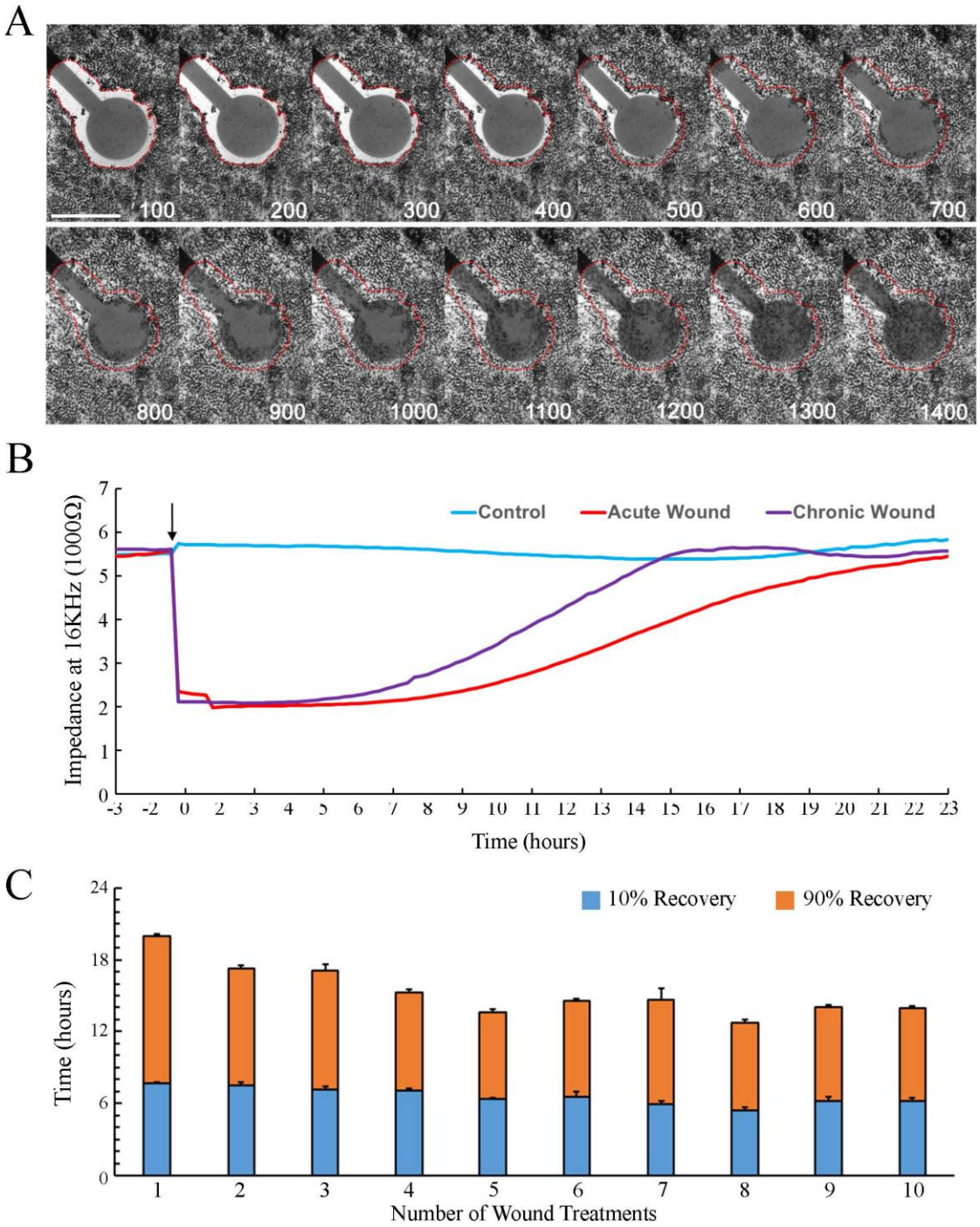

Figure 2-1. RPE cell wound repair kinetics. (A) Time-lapse phase contrast images of RPE cells wound healing. Red-dash lines indicate the original lesion border. Images were taken every 100 minutes post-wounding. Scale bar is 400 µm. (B) Real-time impedance recording of RPE wound healing. A rapid reduction in impedance occurs after delivery of a high current-high frequency electrical pulse (3 mA, 60 kHz, 15 sec.; arrow) to the monolayer. Over time, the impedance gradually recovers to a level similar to that of an intact monolayer. Impedance was plotted after the first wound for acute wound treatments (red) and after the tenth wound for chronic wound treatments (purple). Unwounded wells served as controls (blue). Trace is the average of four biological replicates. (C) Time for bystander cells to recover 10% and 90% of the maximum impedance showing a time reduction trend after daily treatments (mean ± SD, n=4).

comparable to the unwounded monolayer within 24 hours, which was confirmed by the continuous ingrowth of RPE cells using time-lapse imaging.

Repetitive wounding accelerates the rate of wound closure

One advantage of the ECIS system is the capability of delivering distinct and repetitive lesions to the same geographic location in a monolayer of cells while retaining the integrity of the basement membrane (S2-1 Fig). This feature allows for the development of a reliable method that can model chronically wounded RPE without hindering wound healing by physical damage of the extracellular matrix. Electrical pulses were delivered to create discrete wounds in the RPE cell monolayer every 24 hours for ten consecutive days to evaluate the capacity of differentiated human RPE to repair during a state of chronic wounding. We monitored changes in impedance between each daily treatment as the bystander RPE cells repaired the damaged areas. The time for cells to achieve a 10% and 90% level of recovery after each treatment were used as criteria to assess the rate of RPE wound healing. After the first treatment, it took an average of 7.91 hours to regain 10% of the lost impedance and approximately 19.55 hours total to reach 90% recovery (Fig 2-1C). Interestingly, the amount of time to repair wound closure decreased with repetitive treatments (Fig 2-1B). By the tenth wound treatment, the cells regained 10% and 90% of the maximum impedance after approximately 6.69 hours (11.6% reduction) and 14.48 hours total (25.9% reduction), respectively (Fig 2-1C).

Repetitive wounding promotes RPE proliferation but leads to hypotrophy of the monolayer

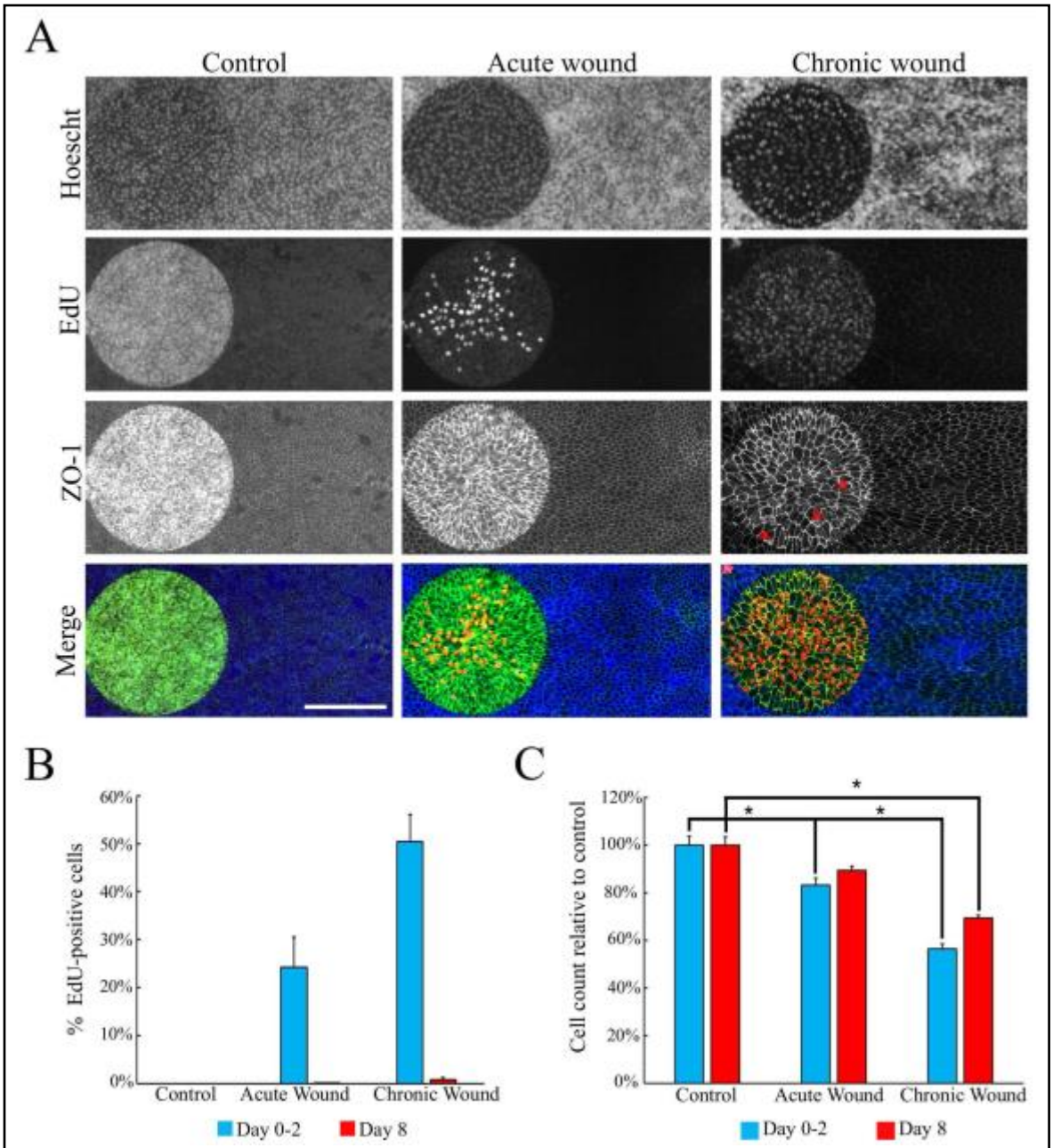

Figure 2-2. RPE cells fail to regenerate fully following repeated wounding. (A) Immunostaining of unwounded (control), acutely wounded, and chronically wounded RPE cells 48-hours after the last wound. Gold electrodes are located on the left side of each panel. Nuclei are labeled with Hoechst (blue); proliferating cells are labeled using EdU (red); cell-cell junctions are detected by ZO-1 staining (green). EdU was supplemented to the media for 48 hours post wounding. Both EdU-positive and -negative nuclei are observed in the enclosed wound, indicating that both proliferation and migration are involved in the wound closure process. Enlarged RPE cells seen after repetitive wounding are indicated by red arrows. Images were taken with auto exposure. Scale bar is 200 μm. (B) The percentage of EdU-positive cells on electrodes (mean ± SD, n=4). (C) The numbers of cells on the electrode relative to the control (mean ± SD, n=4, * indicates p-value<0.01, see S3 Table).

To investigate whether cell proliferation is involved in the repair process of a

wounded differentiated human RPE monolayer, EdU (5-ethynyl-2´-deoxyuridine) was added to label the proliferating population of cells after the last wound treatment. While an intact RPE monolayer maintained a quiescent state (Fig 2-2A), both EdU-positive and EdU–negative cells were observed over the round 350 μm area of the lesion, indicating RPE wound healing involves both cell proliferation and migration. The number of proliferating cells increased by nearly 2-fold in the chronic wounding condition, where cultures were wounded approximately every 24 hours for ten days, compared to cells in the acute wounding condition, which were wounded only once (Fig 2-2B). Notably, the EdU-positive population was typically restricted to the enclosed wound area, whereas most of the cells outside of the lesion remained in a quiescent state. However, even after chronic wounding, cell proliferation was not sustained. The proliferative population decreased to less than 1% of the total population in both acute and chronic wounding states by eight days after the last wound treatment (Fig 2-2B).

Although RPE monolayers appear to use both proliferation and migration to repair damaged areas, the RPE cells are incapable of restoring the original density after repetitive wounding. Two days after an acute wound treatment, the number of cells on the electrode was restored to roughly 85% of the control density (Fig. 2-2C). After eight days of recovery, the cell density increased to a similar number as the intact control. However, after repetitive wounding, the regenerative ability appeared to decline as the cell number only restored to 75% of the control even after eight days of recovery. The decline in cell density resulted in enlarged RPE cells over the lesioned area, which was observed using anti-ZO-1 immunostaining (red arrows in Fig. 2-2A).

Inhibition of the cell cycle does not affect the rate of RPE cell wound closure

To assess whether cell proliferation is an essential component of RPE wound closure, we blocked proliferation after wounding using palbociclib, a cyclin-dependent kinase (CDK) 4 and CDK6 inhibitor. Supplementation of palbociclib significantly decreased cell proliferation in wounded cultures (Figs 2-3A and 2-3B) but did not affect the rate of wound closure (Fig 2-3D). However, there was a significant reduction in cell density over the electrode compared to chronic wound controls (Fig 2-3C). This data suggests that although initiation of the cell cycle is not required for RPE wound closure, the loss of proliferation results in a further reduction in cell density over lesioned areas.

Modulation of bystander RPE cell transcriptome profile following acute or chronic wounding

Transcriptome analysis was employed to gain a more comprehensive understanding of how RPE respond to acute and chronic wounding. To enrich for cells in close proximity of the wounded area, we utilized a 1.5 mm biopsy punch (red circle in S2-2A Fig). While electrodes in a single well encompass just 0.6% of the total surface area, a single electrode encompasses 5.4% of a 1.5 mm biopsy punch, a 9-fold enrichment. Cells were harvested at 5-hours, 24-hours, and 8-days after the final acute or chronic wound treatment, and transcriptome profiles were compiled using RNA-Seq. Acute wounding consisted of one wound treatment while chronic wounding consisted of ten consecutive wounds, once every 24-hours, to determine whether repetitive wounding resulted in any prolonged misregulation of the transcriptome. The 5-hour time point coincides with the end of the lag phase and the onset of migration. The 24-hour sample captures the point in time shortly after wound closure. The 8-day time point assesses the residual effects of wounding after the completion of proliferation and migration. Samples collected from adjacent, non-wounded cultures

served as controls.

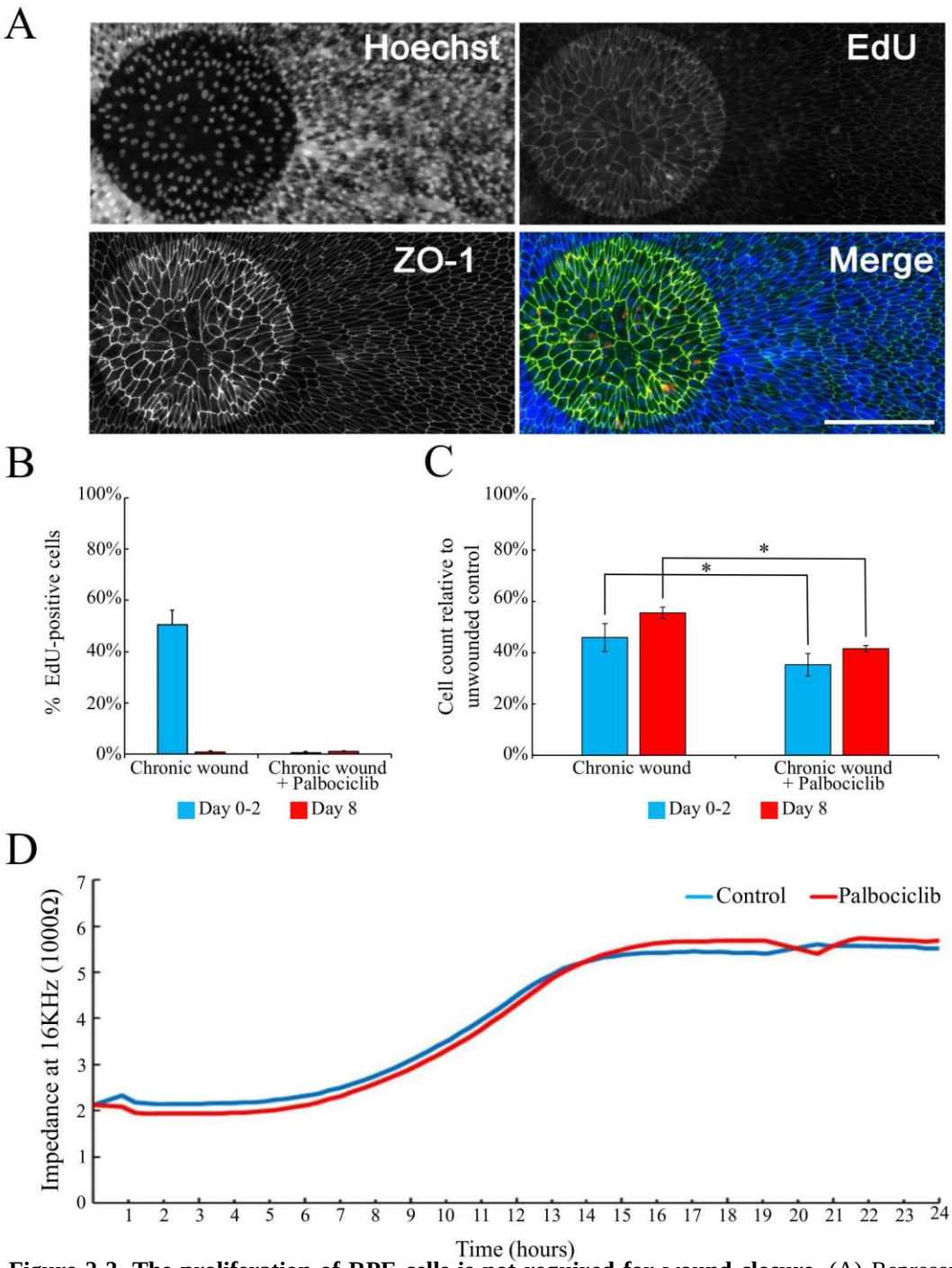

Figure 2-3. The proliferation of RPE cells is not required for wound closure. (A) Representative images of Hoescht, EdU, and ZO-1 labeled cell cultures two days after chronic wound treatments in the continual presence of 10 □M palbociclib. Scale bar is 200 μm. (B) Percent of EdU-positive cells 48-hours or 8-days after receiving chronic wounding treatments (mean ± SD, n=4). (C) Inhibition of cell proliferation by the addition of palbociclib decreases the capability of RPE cells to restore control cell density over the electrode (mean ± SD, n=3, * indicates p-value<0.01, see S3 Table). (D) Real-time impedance recording of RPE wound healing after chronic wound treatment in control and palbociclib treated cells. Trace is the average of three biological replicates.

As summarized in Fig 2-4A, roughly 2600 genes in total were differentially expressed (FDR $\leq$ 0.05 and $\geq$ 2-fold change) compared to controls following either acute or chronic wounding treatments across all time points (S2-4 Table). Over 1800 differentially expressed genes (DEGs) were detected in both acute and chronic wounding conditions, while roughly 700 distinct genes remained significantly altered in acute or chronically wounded cultures alone. A majority of the DEGs were detected 5-hours after wounding. Remarkably, the expression levels of most DEGs detected in the acutely wounded 5-hour samples were restored to levels comparable to unwounded controls by 24-hours (Fig 2-4B). In the acute wound samples, 3.8% of the DEGs at 5-hours remained differentially expressed at 24-hours and only 0.2% genes remained differentially expressed at all time points. In chronically wounded samples there was less recovery of expression after the last wound; 17.6% of the DEGs at 5-hours remained differentially expressed at 24-hours, and 1.2% of the genes remained differentially expressed at all time points.

After eight days of recovery, only 26 and 65 genes remained differentially expressed in the acute and chronic wound samples, respectively. Thirteen genes remained differentially expressed in both acute and chronic wound samples after 8-days of recovery, including proteins associated with cellular structures (*ACTA2, TAGLN, KRT7, IQCJ-SCHIP1*), signal transduction (*DKK1, JUN, PRLR, RASSF3, WDR83*), oxidoreduction (*OGFOD2*), protease activity (*PRSS12, SERPINE1*), and chromatin remodeling (*SETMAR*).

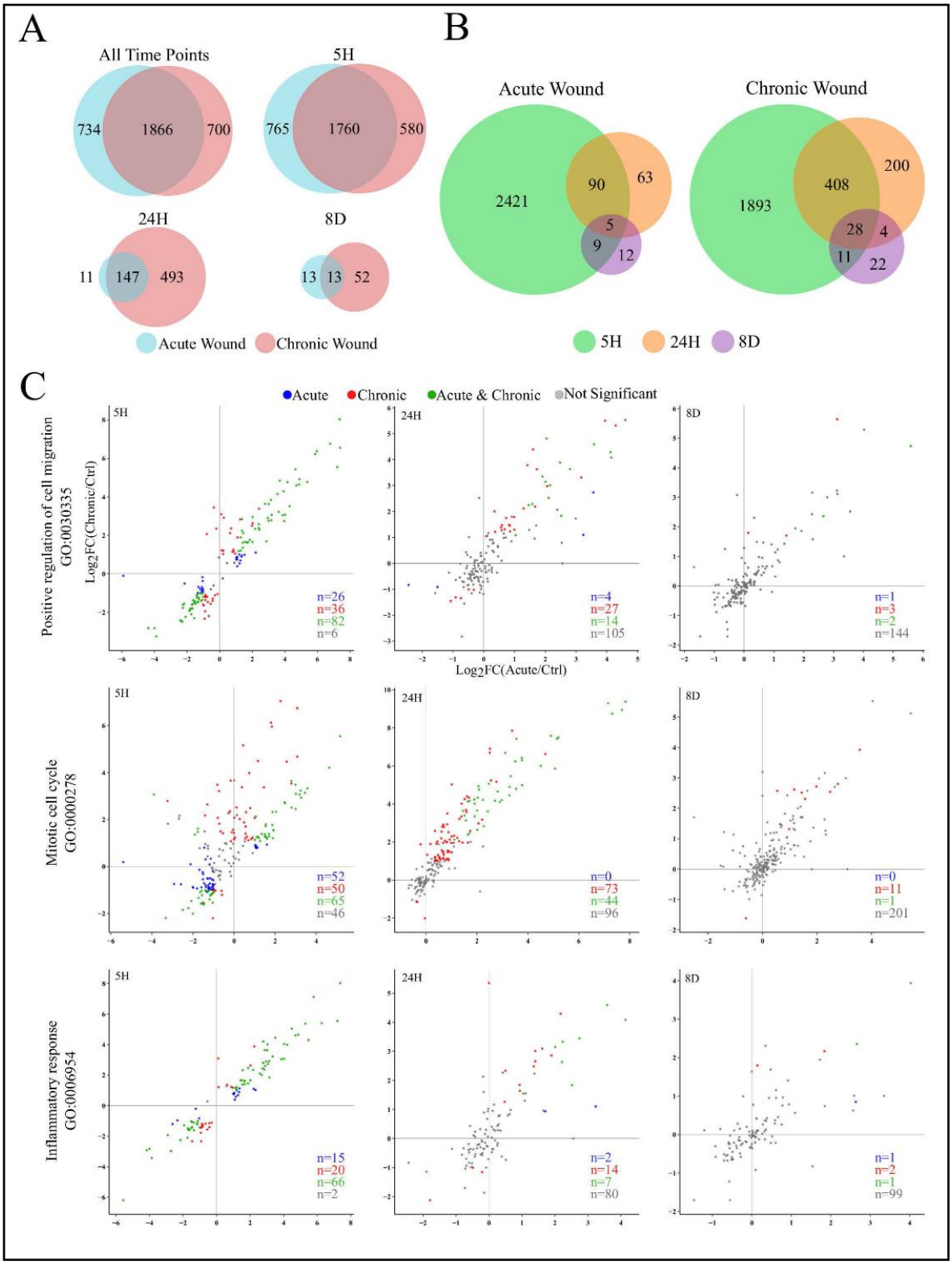
A
All Time Points
734
1866
700
5H
765
1760
580
24H
11
147
493
8D
13
13
52
Acute Wound
Chronic Wound
B
Acute Wound
2421
90
63
5
9
12
Chronic Wound
1893
408
200
28
4
11
22
5H
24H
8D
C
Acute
Chronic
Acute & Chronic
Not Significant
Positive regulation of cell migration GO:0030335
Mitotic cell cycle GO:0000278
Inflammatory response GO:0006954
Log2FC(Chronic/Ctrl)
Log2FC(Acute/Ctrl)
5H
24H
8D
n=26
n=36
n=82
n=6
n=4
n=27
n=14
n=105
n=1
n=3
n=2
n=144
n=52
n=50
n=65
n=46
n=0
n=73
n=44
n=96
n=0
n=11
n=1
n=201
n=15
n=20
n=66
n=2
n=2
n=14
n=7
n=80
n=1
n=2
n=1
n=99

Figure 2-4. Differential expression and gene ontology analysis. (A) Venn diagrams comparing the differentially expressed genes (DEG; FDR ≤ 0.05 and > 2-fold change) at three time points following acute or chronic wound treatments. (B) Venn diagrams showing the overlap of DEGs in the acute or chronic wounding condition alone after wounding. Chronic wounding results in prolonged misregulation of gene expression compared to acute wounding, as seen by the increase in the number of DEGs at both 24-hours and 8-days post wounding. (C) Scatter plots of DEGs showing $\log_2$ transformed fold change (Log2FC) of acute (X-axis) or chronic (Y-axis) compared to unwounded controls at 5 hours (5H), 24 hours (24H) and 8 days (8D) after wounding. DEGs in either acute wounding alone or chronic wounding alone are colored blue and red, respectively. DEGs in both wounding conditions are colored green, and genes that are not significantly changed (either FDR > 0.05 or > 2-fold change) are colored grey. All genes are differentially expressed in one or more time point. Gene ontology groups are significantly enriched based on the total number of differentially expressed genes.

Of the common differentially expressed genes, the upregulation of *DKK1* stands out due to its role as a Wnt signaling antagonist, which has been shown to modulate RPE cell wound healing in a CNV model [44,45]. However, the addition of recombinant DKK1 or Wnt3a to the culture medium did not affect the rate of wound healing or cell density of chronically wounded RPE monolayers (S2-3 Fig).

Using transcriptomic analysis, we showed that bystander RPE cells can rapidly adjust transcriptome profiles in response to sudden disruptions to the monolayer. Interestingly, the gene expression profile alters when the monolayer receives chronic damage compared to acute damage. For example, prolonged differential expression of genes is seen at 24-hours following chronic wounding in gene ontology groups involved in positive regulation of cell migration (GO:0030335), mitotic cell cycle (GO:0000278), and inflammatory response (GO:0006954) compared to acute wounding (Fig 2-4C). This observation corresponds to results showing an increased speed of wound closure and an increase in the proliferative population enclosing the lesioned area (Figs 2-1 and 2-2).

Prolonged misregulation of key genes involved in RPE cell functions following chronic wounding

To evaluate whether lesions on the monolayer affect the expression of key genes involved in RPE cell identity and function, we investigated the expression levels of the top 100 genes which are known to decrease in expression when RPE cells lose their epithelial identity and transdifferentiate into the mesenchymal cell fate (S2-5 Table) [28]. Expression levels of 81 genes were significantly altered (Benjamini & Hochberg correction, P-value<0.01 compared to controls) 5-hours post wounding, most of which have decreased expression in both acute and chronic wounding conditions (Fig 2-5A). All genes misregulated in the acute wound 5-hour samples were restored to control levels by 24-hours, but 26 genes remained significantly down-regulated after chronic wounding. After 8-days of recovery, expression levels of the top 100 RPE genes were not significantly different from intact control samples.

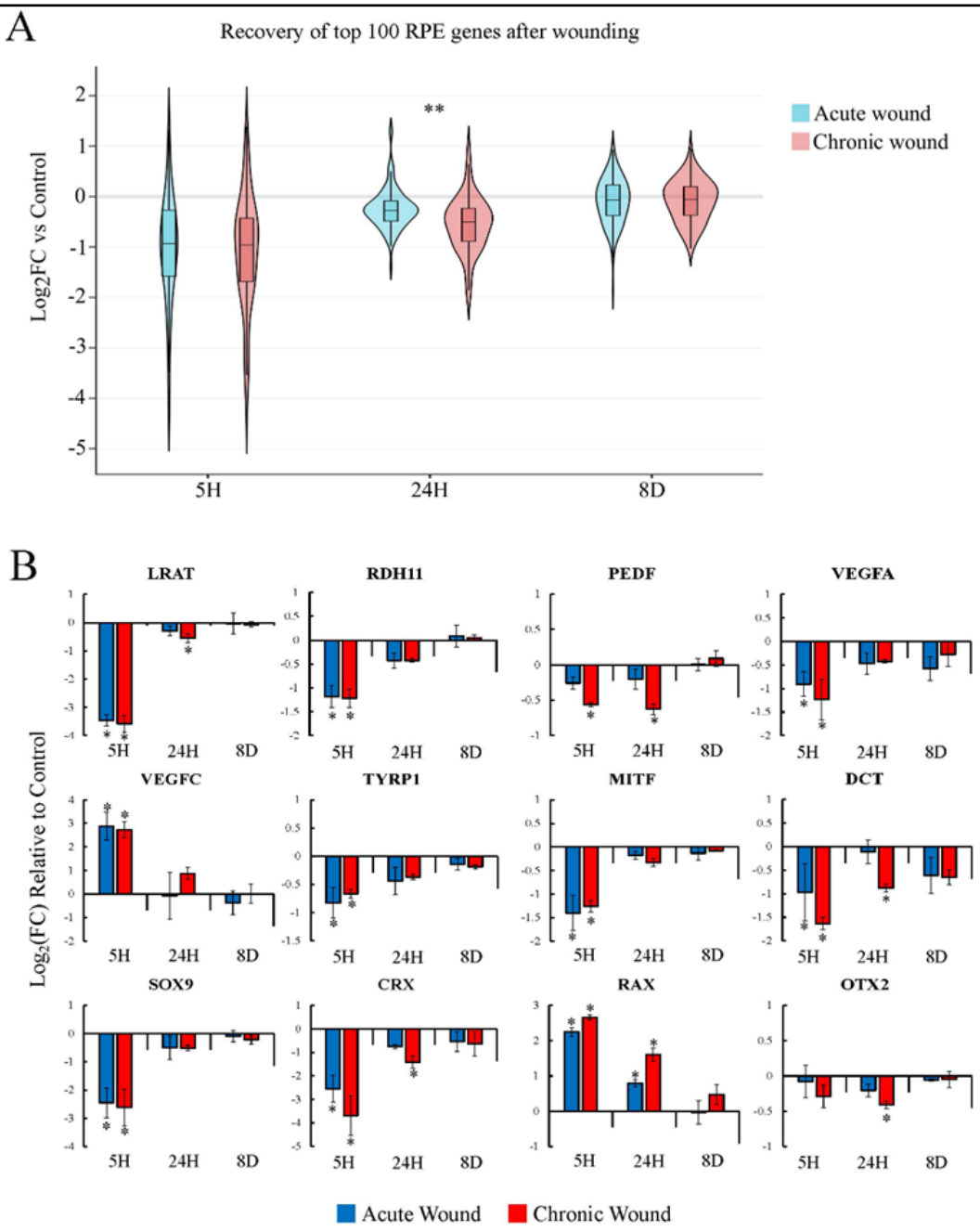

Figure 2-5. Systemic misregulation of RPE genes following wounding. (A) Violin plot showing Log2FC of the top 100 RPE genes in acutely wounded (blue) or chronically wounded (red) RPE cells (**=p-value<0.0001). (B) Bar graphs of select RPE genes showing Log2FC of acute or chronic wounding at 5H, 24H, and 8D compared to unwounded controls (mean ± SD, n=3,* indicates p-value<0.01, see S3 Table).

Next, we assessed the expression of genes associated with key RPE functions, including the visual cycle, growth factors, pigmentation, and retinal development. One such

critical process includes the isomerization of all-*trans* retinal to 11-*cis* retinal, misregulation of which can jeopardize the visual cycle, and lead to photoreceptor degeneration and vision loss [46]. This process is carried out by LRAT, RPE65, and RDH proteins. Here, we found that the expression levels of *LRAT* and *RDH11* were significantly diminished 5-hour post wounding (Fig 2-5B). *RPE65* expression decreased 24-hours post wounding but did not meet our DEG criteria. Despite the increase in expression of *LRAT* and *RDH11* 24-hours after wounding, expression levels of *LRAT* transcripts remained significantly reduced after chronic wounding, restoring to an average of less than 70% of control levels. Considering the entire lesioned area contributes to just 5.4% of the total area of the biopsy punch used for RNA isolation, the decrease in expression of LRAT suggests a broad decrease in expression levels across bystander cells; cells responding to the wound but not directly next to the lesion.

In addition to functioning in the visual cycle, RPE cells secrete PEDF and VEGF to support the photoreceptors and the choroid, respectively. Here, we found that the expression level of *PEDF* was minimally affected following acute wounding but significantly decreased with chronic wounding (Fig 2-5B). In our culture system, differentiated human fetal RPE cells express three *VEGF* isoforms, *A, B*, and *C*. *VEGFA* is the most abundant isoform averaging 905 RPM, *VEGFB* averages 125 RPM, and *VEGFC* is the least abundant isoform averaging 2 RPM. Previously, we have shown that *VEGFA* expression decreases while the expression of *VEGFC* increases when RPE cells terminally differentiated into a mesenchymal cell fate [28]. Here, a similar phenomenon was observed; expression levels of *VEGFA* were significantly decreased, and *VEGFC* was significantly increased in the 5-hour samples. Unlike the terminal epithelial to mesenchymal transdifferentiation seen in our previous work [28], expression levels of *VEGFA* and *VEGFC* can be restored 24 hours after

wounding in acutely and chronically wounded RPE monolayers. *VEGFB* transcripts were unaffected by wounding.

Pigmentation is one of the most definitive phenotypical characteristics of RPE cells. The pigment in RPE cells can absorb scattered light to improve visual acuity and, importantly, protect retinal cells from photo-oxidative stress [5,47]. MITF mediates the pigmentation of RPE and can also transactivate the expression of *TYR*, *TYRP1*, and *DCT*, essential enzymes for melanogenesis. Downregulation of *MITF*, *TYRP1*, and *DCT* was observed 5-hours after wounding while the expression of *TYR* was not affected. The expression levels of *MITF* and *TYRP1* restored to control levels 24 hours after wounding, but *DCT* remained downregulated in the chronic wounding condition (Fig 2-5B). In addition to MITF, the misregulation of other transcription factors associated with retinal development was also detected. Expression levels of *SOX9* and *CRX* decreased 5-hours after wounding and restored to control levels after 24 hours. After a single wound, the expression levels of *RAX* increased 5-hours and 24-hours after wounding but restored to control levels after 8-days. Prolonged upregulation of *RAX* was seen in the chronically wounded samples after 8-days.

Together, these results indicate that lesions on the RPE monolayer can lead to dysregulation of genes key to RPE specification and function in bystander RPE cells. Expression levels of a majority of the dysregulated genes restore by 24 hours in the acute wounding condition. However, many genes failed to fully recover after 24 hours in the chronic wounding condition, indicating that the ability of bystander RPE cells to regenerate diminishes following repetitive wounding. Due to the importance of RPE cells in maintaining

the subretinal environment, prolonged dysregulation of RPE functions can potentially lead to RPE and photoreceptor degeneration.

Association of RPE wound response with AMD pathogenesis

In addition to genes associated with RPE cell specification and function, several DEGs are important due to their potential roles in AMD pathogenesis, particularly genes which play a role in inflammation. In this study, we observed an increase of *CCL2*, *IL-18*, *and FAS* expression in wounded samples compared to unwounded controls (Fig 2-6A). Expression of both *CCL2* and *IL-18* increased 5-hours after acute or chronic wounding and restored to roughly normal levels 8-days post wounding.

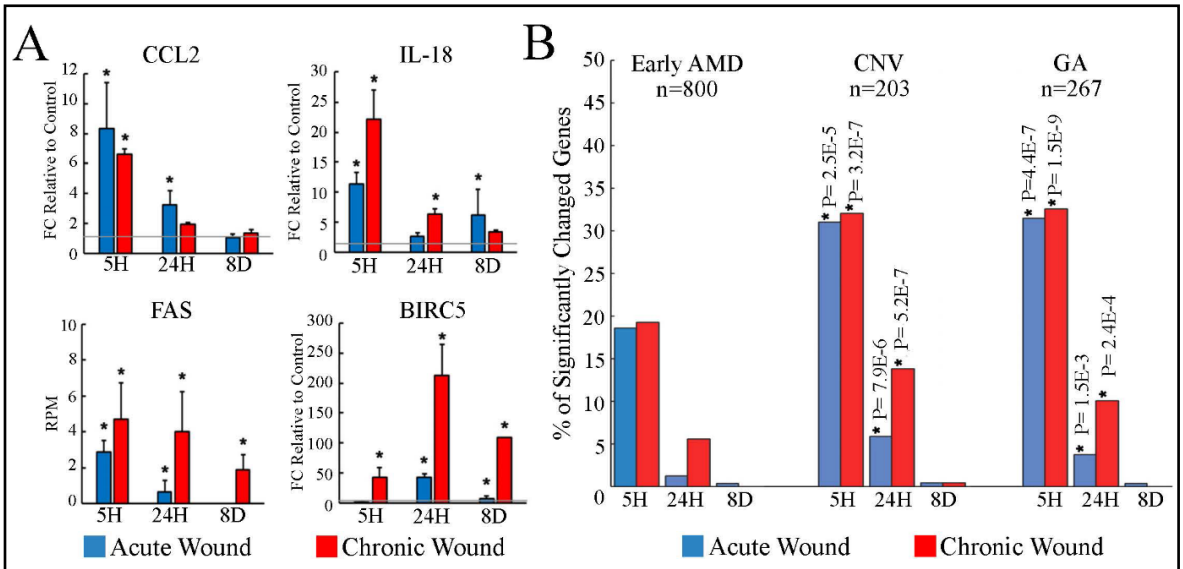

Figure 2-6. Correlation between RPE cell wounding and AMD. (A) Expression levels of selected genes. Grey line indicates the expression level of the unwounded control (mean ± SD, n=3, * indicates p-value<0.01, see S3 Table). (B) Bar graph indicates the percentage of early AMD, CNV, and GA associated genes, whose expression levels are significantly differentially expressed (Benjamini & Hochberg correction, p-value<0.01) following acute (blue) or chronic (red) wounding. An asterisk indicates significant over-representation of CNV and GA-associated genes in wounded samples (Fisher's exact test, p-value <0.01).

Unlike *CCL2* and *IL-18*, which were expressed at detectible levels even in unwounded RPE, *FAS* transcripts were absent or in a non-detectable range in intact controls.

Five-hours post wounding *FAS* was detected in both acute and chronically wounded samples (Fig 2-6A). In the acute wound cultures, the expression of *FAS* was reduced by 24 hours and non-detectable after 8-days. In contrast, chronically wounded RPE cells maintained upregulation of *FAS* after 8-days of recovery. Despite the confirmation of FAS expression by immunostaining, we did not observe a clear apoptotic effect on the bystander RPE cells using FAS activating IgM, as the impedance recovery profile and the cell density were comparable to unwounded controls (S2-3 Fig). Perhaps persistent upregulation of *BIRC5* (also known as Survivin), a member of the inhibitors of apoptosis proteins (IAPs), in the chronically wounded cells may protect bystander cells from FAS mediated cell death (Fig 2-6A).

Finally, we used Fisher's exact test to investigate whether using ECIS for acutely or chronically wounded RPE displays significant transcriptomic changes similar to transcriptomic profiles of AMD eyes [48]. Due to differences in the methodology, only genes expressed by *in vitro* RPE cells were considered amongst those previously detected by DNA microarray in the RPE-choroid AMD samples (S2-6 Table). As shown in Fig 2-6B, there was no significant correlation between *in vitro* RPE wounding and early AMD. Interestingly, however, a significant over-representation of genes associated with both types of advanced AMD was observed in both acute and chronically wounded samples, where chronically wounded RPE monolayers exhibited a higher correlation with both types of advanced AMD (Fig 2-6B).

E. Discussion

In this study, we investigated the wound healing response of acutely and chronically wounded differentiated human RPE monolayers. We report that differentiated human RPE cells repair lesions introduced by high current electrical pulses using the ECIS system and

can repair repetitively induced wounds. In response to a lesion on the monolayer, bystander RPE cells migrate and proliferate to repair the wound; whereas, cells distal to the lesion remain quiescent (Fig 2-2A). Compared to an acutely wounded monolayer, repetitive wounding accelerates the speed of wound closure and increases the proliferative population in conjunction with prolonging the differential expression of genes related to cell migration, cell cycle, RPE function and, inflammation.

Previous reports suggest the density of RPE in the macula to be 4,960 ± 1,040 cells/mm^2, with a loss rate of 0.54% per year [49]. In our system, the density of the unwounded controls fell within previous reports, while chronic wounding resulted in a reduced cell density of ~3,000 RPE cells/mm^2 (S2-2 Fig D and E). Despite an increase in the proliferative cell population following chronic wounding, chronically damaged RPE monolayers restore to just 75% of control density, resulting in enlarged cells over the lesion (Fig 2-2C). This seemingly conflicting result is likely due to the repetitive ablation of proliferative cells on the lesioned area and the lack of proliferation in the region distal to the lesion. It is possible that the RPE cells enlarge in the periphery, similar to enlarged cells seen on the electrode to compensate for cell loss while maintaining the coherence of the monolayer (S2-2 Fig).

Many features seen in RPE monolayers in a state of chronic wounding are strikingly similar to features seen in AMD. For instance, enlarged RPE has been reported previously in eyes with AMD, particularly near drusen [7]. The accumulation of drusen is the clinical hallmark of AMD, and it has been proposed that the presence of inflammation-associated proteins in drusen, such as complement factors, can lead to chronic immune responses in the subretinal space leading to RPE degeneration and AMD [50–53]. Using the ECIS system, we

observed an increase in RPE cell size only after chronic wounding. The generation of lesions in an RPE monolayer also elicited an inflammatory response. Interestingly, the chronic wounding state showed an even more prolonged misregulation of inflammatory genes compared to the acute wounding state (Fig 2-4C).

In addition to the inflammatory components of drusen, mononuclear phagocytes (MPs) has been observed in both forms of advanced AMD, further supporting the idea that that chronic low-grade inflammation may play a role in the progression of AMD [54–56]. MP activation has been shown to diminish the expression of genes critical for RPE function and can induce cell death [57,58]. CCL2 is a chemoattractant for MPs, recruiting and activating MPs to sites of CCL2 secretion. The upregulation of CCL2 expression can lead to the accumulation of MPs in the subretinal space, and CCL2 treated MPs can stimulate RPE cell apoptosis [59–62]. We observed a drastic upregulation of *CCL2* expression following both acute and chronic wounding (Fig 2-6A).

Apoptosis has been reported to contribute to AMD pathogenesis, particularly for RPE near drusen or GA lesions [63]. The FAS dependent apoptosis pathway is initiated by the engagement of FAS (receptor) with FASL (ligand), inducing the formation of the death-inducing signaling complex (DISC), activation of the caspase cascade, and ultimately causes DNA fragmentation [64]. Additionally, apoptosis has also been shown to be triggered in RPE cells via the IL-18 and FAS-mediated pathway, triggered by the misregulation of RNA processing [65,66]. We found that the RPE cell response to acute or chronic wounding results in a significant increase in both *IL-18* and *FAS* expression (Fig 2-6A). However, expression of FASL and the components of the IL-18 receptor, IL18R1 and IL18RAP, were in the low to non-detectable range. The expression of these three components are generally expressed

on immune cells such as MPs, T cells, B cells, natural killer cells, and has been reported in RPE *in vivo* [67–71].

Wounding of the RPE monolayer also caused a transient misregulation of genes key to the visual cycle, melanogenesis, growth factor expression, and RPE cell specification. Even though bystander RPE can restore the expression levels of these genes after 8-days of repair, the capacity to recover diminishes following chronic wounding. Because of the importance of RPE cells in the maintenance of the sub-retinal environment, prolonged dysregulation of bystander RPE after chronic wounding may lead to dysfunction of the RPE monolayer leading to photoreceptor death and loss of vision [7,19,72].

When investigating the differentially expressed genes from the acute and chronic wounding conditions, we found a significant overrepresentation of genes that have been shown previously to be differentially expressed in late AMD eyes [48]. Similar to the RPE genes, expression levels of most of the AMD associated genes are restored after 8-days of recovery. However, a greater number of AMD associated genes were differentially expressed in the chronically wounded samples, and the extent of recovery diminished following chronic wounding.

Despite the similarity of several features of chronically wounded RPE cells and AMD, there is a fundamental difference between the model presented in this study and the advanced stages of AMD. While we observed a productive wound healing process using ECIS, even while using a cell-cycle inhibitor, a productive wound healing process is seemingly absent in advanced stages of the disease. Tissue regeneration requires the proliferation of the progenitor or bystander cells, followed by differentiation of the newly produced cells. RPE cells can reenter the cell cycle in response to growth factor stimulations

such as PDGF, bFGF, TGFβ, and TNFα [73–77]. *In vitro*, primary adult and fetal human RPE cells can redifferentiate into a functional monolayer with a minimal amount of expansion. However, extensive passaging or low-density plating can direct RPE cells toward terminal mesenchymal transdifferentiation and give rise to fibrotic tissues [28]. Observations of RPE-derived fibrotic membranes in wet AMD eyes suggest that exposure to serum components may promote RPE hyperproliferation and transdifferentiation. In this study, although >50% of cells on the electrode were in a proliferative state after chronic wounding, we did not observe a clear sign of terminal mesenchymal transdifferentiation. This result is likely due to the magnitude of lesions created by the ECIS system being relatively small; therefore, an extensive propagation is not required to mend the gap.

In contrast, in GA, gross RPE proliferation and transdifferentiation are not observed. In GA, the decline in the nutrition supply due to degeneration of the choroidal capillaries together with enhanced cell apoptosis and chronic inflammation may prevent RPE regeneration. The decline in *VEGF*-A expression and the increase in the *CCL2*, *IL-18*, and *FAS* expression levels in chronically wounded bystander RPE suggest that lesions in the RPE monolayer may lead to the degeneration of choroidal capillaries and promote an inflammatory response, which can lead to further degeneration of RPE cells.

Using the ECIS system, we were able to generate an *in vitro* system to model a chronic wound state in a short amount of time with features distinct from that of an acute wounding state. However, there are limitations of this system which do not fully recapitulate the progression of AMD *in vivo*. For instance, high current is used to induce lesions by causing cell death in RPE cells overlaying the electrodes. Although this mechanism of RPE cell death is not physiologically relevant to AMD, we believe the study of the bystander

wound response has potential disease-related implications, as we see several similarities between known features of AMD and chronically wounded RPE.

Another limitation of this system is the lack of underlying choroid. While the RPE monolayer maintains the heath of the overlaying RPE, the underlying choroid plays an equally important role in maintaining the health of the RPE by providing nutrients and removing waste [78]. Degeneration of the choroid, specifically the choriocapillaris, often occurs during the early stages of AMD, although the exact timing of events is still under debate [79]. Perhaps future work combining RPE, choroidal epithelial cells, photoreceptor outer segments, and one of the many types of ECIS arrays may provide more insight into how these interconnected cell types change during wound repair. While our system does not recapitulate some aspects of an intact retina, *in vitro* models, such as this, are less expensive than *in vivo* experiments, quicker to perform, and can be efficiently scaled up.

Using ECIS as a platform for chronic wounding of RPE cells may be ideal for screening therapeutics that may enhance the ability of RPE cells to wound repair over time, which could potentially help increase the reparative capacity of RPE. In addition to the experiments presented here, this platform allows for the addition of other risk factors known to influence the onset of AMD, such as age, oxidative stress, inflammation, and mitochondrial health [80,81]. Although we do not fully understand the pathology that drives AMD progression, this system may lead to further insights into these mechanisms. Further investigations combining chronic wounding with additional AMD risk factors may be key in further elucidating mechanisms that influence RPE wound repair in advanced stages of AMD.

F. References

1. Volland S, Esteve-Rudd J, Hoo J, Yee C, Williams DS. A Comparison of Some Organizational Characteristics of the Mouse Central Retina and the Human Macula. Li T, editor. PLoS One. Public Library of Science; 2015;10: e0125631. doi:10.1371/journal.pone.0125631

2. Campbell M, Humphries P. The Blood-Retina Barrier. Springer, New York, NY; 2013. pp. 70–84. doi:10.1007/978-1-4614-4711-5_3

3. Blaauwgeers HGT, Holtkamp GM, Rutten H, Witmer AN, Koolwijk P, Partanen TA, et al. Polarized Vascular Endothelial Growth Factor Secretion by Human Retinal Pigment Epithelium and Localization of Vascular Endothelial Growth Factor Receptors on the Inner Choriocapillaris. Am J Pathol. 1999;155: 421–428. doi:10.1016/S0002-9440(10)65138-3

4. Kay P, Yang YC, Paraoan L. Directional protein secretion by the retinal pigment epithelium: roles in retinal health and the development of age-related macular degeneration. J Cell Mol Med. Wiley-Blackwell; 2013;17: 833–43. doi:10.1111/jcmm.12070

5. Sparrow JR, Hicks D, Hamel CP. The retinal pigment epithelium in health and disease. Curr Mol Med. NIH Public Access; 2010;10: 802–23. Available: http://www.ncbi.nlm.nih.gov/pubmed/21091424

6. Bonilha VL. Age and disease-related structural changes in the retinal pigment epithelium. Clin Ophthalmol. Dove Press; 2008;2: 413–24. Available: http://www.ncbi.nlm.nih.gov/pubmed/19668732

7. Al-Hussaini H, Schneiders M, Lundh P, Jeffery G. Drusen are associated with local and distant disruptions to human retinal pigment epithelium cells. Exp Eye Res. 2009;88: 610–612. doi:10.1016/j.exer.2008.09.021

8. Jager RD, Mieler WF, Miller JW. Age-Related Macular Degeneration. N Engl J Med. Massachusetts Medical Society ; 2008;358: 2606–2617. doi:10.1056/NEJMra0801537

9. Garcia-Layana A, Cabrera-López F, García-Arumí J, Arias-Barquet L, Ruiz-Moreno JM. Early and intermediate age-related macular degeneration: update and clinical review. Clin Interv Aging. 2017;Volume 12: 1579–1587. doi:10.2147/CIA.S142685

10. Kaszubski P, Ami B, Saade C, Smith RT, Ben Ami T, Saade C, et al. Geographic Atrophy and Choroidal Neovascularization in the Same Eye: A Review. Ophthalmic Res. 2016;55: 185–193. doi:10.1159/000443209

11. Klein R, Peto T, Bird A, Vannewkirk MR. The epidemiology of age-related macular degeneration. Am J Ophthalmol. Elsevier; 2004;137: 486–495.

doi:10.1016/J.AJO.2003.11.069

12. Nivison-Smith L, Milston R, Madigan M, Kalloniatis M. Age-Related Macular Degeneration. Optom Vis Sci. 2014;91: 832–848. doi:10.1097/OPX.0000000000000281

13. Bird AC, Bressler NM, Bressler SB, Chisholm IH, Coscas G, Davis MD, et al. An international classification and grading system for age-related maculopathy and age-related macular degeneration. The International ARM Epidemiological Study Group. Surv Ophthalmol. 39: 367–74. Available: http://www.ncbi.nlm.nih.gov/pubmed/7604360

14. Fleckenstein M, Mitchell P, Freund KB, Sadda S, Holz FG, Brittain C, et al. The Progression of Geographic Atrophy Secondary to Age-Related Macular Degeneration. Ophthalmology. Elsevier; 2018;125: 369–390. doi:10.1016/J.OPHTHA.2017.08.038

15. Rudnicka AR, Kapetanakis V V., Jarrar Z, Wathern AK, Wormald R, Fletcher AE, et al. Incidence of Late-Stage Age-Related Macular Degeneration in American Whites: Systematic Review and Meta-analysis. Am J Ophthalmol. Elsevier; 2015;160: 85-93.e3. doi:10.1016/J.AJO.2015.04.003

16. Grunwald JE, Pistilli M, Daniel E, Ying G-S, Pan W, Jaffe GJ, et al. Incidence and Growth of Geographic Atrophy during 5 Years of Comparison of Age-Related Macular Degeneration Treatments Trials. Ophthalmology. NIH Public Access; 2017;124: 97–104. doi:10.1016/j.ophtha.2016.09.012

17. Bird AC. Therapeutic targets in age-related macular disease. J Clin Invest. American Society for Clinical Investigation; 2010;120: 3033–41. doi:10.1172/JCI42437

18. Bird AC, Phillips RL, Hageman GS. Geographic atrophy: a histopathological assessment. JAMA Ophthalmol. NIH Public Access; 2014;132: 338–45. doi:10.1001/jamaophthalmol.2013.5799

19. Ding J-D, Johnson L V, Herrmann R, Farsiu S, Smith SG, Groelle M, et al. Anti-amyloid therapy protects against retinal pigmented epithelium damage and vision loss in a model of age-related macular degeneration. Proc Natl Acad Sci U S A. National Academy of Sciences; 2011;108: E279-87. doi:10.1073/pnas.1100901108

20. Daniel E, Toth CA, Grunwald JE, Jaffe GJ, Martin DF, Fine SL, et al. Risk of scar in the comparison of age-related macular degeneration treatments trials. Ophthalmology. NIH Public Access; 2014;121: 656–66. doi:10.1016/j.ophtha.2013.10.019

21. Frank RN, Amin RH, Eliott D, Puklin JE, Abrams GW. Basic fibroblast growth factor and vascular endothelial growth factor are present in epiretinal and choroidal neovascular membranes. Am J Ophthalmol. 1996;122: 393–403. Available: http://www.ncbi.nlm.nih.gov/pubmed/8794712

22. Lopez PF, Sippy BD, Lambert HM, Thach AB, Hinton DR. Transdifferentiated retinal pigment epithelial cells are immunoreactive for vascular endothelial growth factor in surgically excised age-related macular degeneration-related choroidal neovascular membranes. Invest Ophthalmol Vis Sci. 1996;37: 855–68. Available: http://www.ncbi.nlm.nih.gov/pubmed/8603870

23. Nita M, Grzybowski A. The Role of the Reactive Oxygen Species and Oxidative Stress in the Pathomechanism of the Age-Related Ocular Diseases and Other Pathologies of the Anterior and Posterior Eye Segments in Adults. Oxid Med Cell Longev. Hindawi Limited; 2016;2016: 3164734. doi:10.1155/2016/3164734

24. Khandhadia S, Lotery A. Oxidation and age-related macular degeneration: insights from molecular biology. Expert Rev Mol Med. 2010;12: e34. doi:10.1017/S146239941000164X

25. Hanus J, Anderson C, Wang S. RPE necroptosis in response to oxidative stress and in AMD. Ageing Res Rev. 2015;24: 286–298. doi:10.1016/j.arr.2015.09.002

26. Jarrett SG, Boulton ME. Consequences of oxidative stress in age-related macular degeneration. Mol Aspects Med. Pergamon; 2012;33: 399–417. doi:10.1016/J.MAM.2012.03.009

27. Sparrow JR, Boulton M. RPE lipofuscin and its role in retinal pathobiology. Exp Eye Res. 2005;80: 595–606. doi:10.1016/j.exer.2005.01.007

28. Radeke MJ, Radeke CM, Shih Y-H, Hu J, Bok D, Johnson L V., et al. Restoration of mesenchymal retinal pigmented epithelial cells by TGFβ pathway inhibitors: implications for age-related macular degeneration. Genome Med. BioMed Central; 2015;7: 58. doi:10.1186/s13073-015-0183-x

29. Ashburn FS, Pilkerton AR, Rao NA, Marak GE. The effects of iodate and iodoacetate on the retinal adhesion. Invest Ophthalmol Vis Sci. 1980;19: 1427–32. Available: http://www.ncbi.nlm.nih.gov/pubmed/7440100

30. Greene WA, Burke TA, Por ED, Kaini RR, Wang H-C. Secretion Profile of Induced Pluripotent Stem Cell-Derived Retinal Pigment Epithelium During Wound Healing. Investig Opthalmology Vis Sci. 2016;57: 4428. doi:10.1167/iovs.16-19192

31. Kamei M, Lewis JM, Hayashi A, Sakagami K, Ohji M, Tano Y. A new wound healing model of retinal pigment epithelial cells in sheet culture. Curr Eye Res. 1996;15: 714–8. Available: http://www.ncbi.nlm.nih.gov/pubmed/8670778

32. Hanus J, Zhang H, Wang Z, Liu Q, Zhou Q, Wang S. Induction of necrotic cell death by oxidative stress in retinal pigment epithelial cells. Cell Death Dis. Nature Publishing Group; 2013;4: e965–e965. doi:10.1038/cddis.2013.478

33. Hu J, Bok D. A cell culture medium that supports the differentiation of human retinal pigment epithelium into functionally polarized monolayers. Mol Vis. 2001;7: 14–9. Available: http://www.ncbi.nlm.nih.gov/pubmed/11182021

34. Hu J, Bok D. Culture of highly differentiated human retinal pigment epithelium for analysis of the polarized uptake, processing, and secretion of retinoids. Methods Mol Biol. 2010;652: 55–73. doi:10.1007/978-1-60327-325-1_2

35. Maminishkis A, Chen S, Jalickee S, Banzon T, Shi G, Wang FE, et al. Confluent monolayers of cultured human fetal retinal pigment epithelium exhibit morphology and physiology of native tissue. Invest Ophthalmol Vis Sci. 2006;47: 3612–24. doi:10.1167/iovs.05-1622

36. Kim D, Pertea G, Trapnell C, Pimentel H, Kelley R, Salzberg SL. TopHat2: accurate alignment of transcriptomes in the presence of insertions, deletions and gene fusions. Genome Biol. BioMed Central; 2013;14: R36. doi:10.1186/gb-2013-14-4-r36

37. Robinson MD, Oshlack A. A scaling normalization method for differential expression analysis of RNA-seq data. Genome Biol. BioMed Central; 2010;11: R25. doi:10.1186/gb-2010-11-3-r25

38. McCarthy DJ, Chen Y, Smyth GK. Differential expression analysis of multifactor RNA-Seq experiments with respect to biological variation. Nucleic Acids Res. 2012;40: 4288–4297. doi:10.1093/nar/gks042

39. Keese CR, Wegener J, Walker SR, Giaever I. Electrical wound-healing assay for cells in vitro. 2003; Available: http://www.pnas.org/content/pnas/101/6/1554.full.pdf

40. Peitzman ER, Zaidman NA, Maniak PJ, O'Grady SM. Agonist binding to β-adrenergic receptors on human airway epithelial cells inhibits migration and wound repair. Am J Physiol Physiol. American Physiological Society Bethesda, MD; 2015;309: C847–C855. doi:10.1152/ajpcell.00159.2015

41. Giaever I, Keese CR. A morphological biosensor for mammalian cells. Nature. Nature Publishing Group; 1993. pp. 591–592. doi:10.1038/366591a0

42. Kim S, Ramasamy S, Bennet D. Drug and bioactive molecule screening based on a bioelectrical impedance cell culture platform. Int J Nanomedicine. Dove Medical Press Ltd.; 2014;9: 5789. doi:10.2147/IJN.S71128

43. Keese CR, Wegener J, Walker SR, Giaever I. Electrical wound-healing assay for cells in vitro. Proc Natl Acad Sci U S A. National Academy of Sciences; 2004;101: 1554–1559. doi:10.1073/pnas.0307588100

44. Chen Y, Hu Y, Lu K, Flannery JG, Ma J-X. Very low density lipoprotein receptor, a

negative regulator of the wnt signaling pathway and choroidal neovascularization. J Biol Chem. American Society for Biochemistry and Molecular Biology; 2007;282: 34420–8. doi:10.1074/jbc.M611289200

45. Qiu F, Liu Z, Zhou Y, He J, Gong S, Bai X, et al. Decreased Circulating Levels of Dickkopf-1 in Patients with Exudative Age-related Macular Degeneration. Sci Rep. Nature Publishing Group; 2017;7: 1263. doi:10.1038/s41598-017-01119-2

46. Travis GH, Golczak M, Moise AR, Palczewski K. Diseases Caused by Defects in the Visual Cycle: Retinoids as Potential Therapeutic Agents. Annu Rev Pharmacol Toxicol. Annual Reviews; 2007;47: 469–512. doi:10.1146/annurev.pharmtox.47.120505.105225

47. Plafker SM, O'Mealey GB, Szweda LI. Mechanisms for countering oxidative stress and damage in retinal pigment epithelium. Int Rev Cell Mol Biol. NIH Public Access; 2012;298: 135–77. doi:10.1016/B978-0-12-394309-5.00004-3

48. Newman AM, Gallo NB, Hancox LS, Miller NJ, Radeke CM, Maloney MA, et al. Systems-level analysis of age-related macular degeneration reveals global biomarkers and phenotype-specific functional networks. Genome Med. BioMed Central; 2012;4: 16. doi:10.1186/gm315

49. Bhatia SK, Rashid A, Chrenek MA, Zhang Q, Bruce BB, Klein M, et al. Analysis of RPE morphometry in human eyes. Mol Vis. Emory University; 2016;22: 898–916. Available: http://www.ncbi.nlm.nih.gov/pubmed/27555739

50. Johnson L V, Forest DL, Banna CD, Radeke CM, Maloney MA, Hu J, et al. Cell culture model that mimics drusen formation and triggers complement activation associated with age-related macular degeneration. Proc Natl Acad Sci U S A. National Academy of Sciences; 2011;108: 18277–82. doi:10.1073/pnas.1109703108

51. Anderson DH, Mullins RF, Hageman GS, Johnson L V. A role for local inflammation in the formation of drusen in the aging eye. Am J Ophthalmol. Elsevier; 2002;134: 411–431. doi:10.1016/S0002-9394(02)01624-0

52. Friedman AH, Beckerman B, Gold DH, Walsh JB, Gartner S. Drusen of the optic disc. Surv Ophthalmol. Elsevier; 1977;21: 375–390. doi:10.1016/0039-6257(77)90041-8

53. Wang L, Clark ME, Crossman DK, Kojima K, Messinger JD, Mobley JA, et al. Abundant Lipid and Protein Components of Drusen. Koch K-W, editor. PLoS One. Public Library of Science; 2010;5: e10329. doi:10.1371/journal.pone.0010329

54. Penfold PL, Madigan MC, Gillies MC, Provis JM. Immunological and aetiological aspects of macular degeneration. Prog Retin Eye Res. 2001;20: 385–414. doi:10.1016/s1350-9462(00)00025-2

55. Sennlaub F, Auvynet C, Calippe B, Lavalette S, Poupel L, Hu SJ, et al. CCR2(+) monocytes infiltrate atrophic lesions in age-related macular disease and mediate photoreceptor degeneration in experimental subretinal inflammation in Cx3cr1 deficient mice. EMBO Mol Med. Wiley-Blackwell; 2013;5: 1775–93. doi:10.1002/emmm.201302692

56. Levy O, Calippe B, Lavalette S, Hu SJ, Raoul W, Dominguez E, et al. Apolipoprotein E promotes subretinal mononuclear phagocyte survival and chronic inflammation in age-related macular degeneration. EMBO Mol Med. 2015;7: 211–226. doi:10.15252/emmm.201404524

57. Kutty RK, Samuel W, Boyce K, Cherukuri A, Duncan T, Jaworski C, et al. Proinflammatory cytokines decrease the expression of genes critical for RPE function. Mol Vis. 2016;22: 1156–1168. Available: http://www.ncbi.nlm.nih.gov/pubmed/27733811

58. Yang Y, Liu F, Tang M, Yuan M, Hu A, Zhan Z, et al. Macrophage polarization in experimental and clinical choroidal neovascularization. Sci Rep. Nature Publishing Group; 2016;6: 30933. doi:10.1038/srep30933

59. Yang D, Elner SG, Chen X, Field MG, Petty HR, Elner VM. MCP-1-activated monocytes induce apoptosis in human retinal pigment epithelium. Invest Ophthalmol Vis Sci. Association for Research in Vision and Ophthalmology; 2011;52: 6026–34. doi:10.1167/iovs.10-7023

60. Jonas JB, Tao Y, Neumaier M, Findeisen P. Monocyte Chemoattractant Protein 1, Intercellular Adhesion Molecule 1, and Vascular Cell Adhesion Molecule 1 in Exudative Age-Related Macular Degeneration. Arch Ophthalmol. American Medical Association; 2010;128: 1281. doi:10.1001/archophthalmol.2010.227

61. Luhmann UFO, Robbie S, Munro PMG, Barker SE, Duran Y, Luong V, et al. The drusenlike phenotype in aging Ccl2-knockout mice is caused by an accelerated accumulation of swollen autofluorescent subretinal macrophages. Invest Ophthalmol Vis Sci. Europe PMC Funders; 2009;50: 5934–43. doi:10.1167/iovs.09-3462

62. Tsutsumi C, Sonoda K-H, Egashira K, Qiao H, Hisatomi T, Nakao S, et al. The critical role of ocular-infiltrating macrophages in the development of choroidal neovascularization. J Leukoc Biol. Wiley-Blackwell; 2003;74: 25–32. doi:10.1189/jlb.0902436

63. Dunaief JL, Dentchev T, Ying G-S, Milam AH. The Role of Apoptosis in Age-Related Macular Degeneration. Arch Ophthalmol. American Medical Association; 2002;120: 1435. doi:10.1001/archopht.120.11.1435

64. Elmore S. Apoptosis: a review of programmed cell death. Toxicol Pathol. NIH Public Access; 2007;35: 495–516. doi:10.1080/01926230701320337

65. Kim Y, Tarallo V, Kerur N, Yasuma T, Gelfand BD, Bastos-Carvalho A, et al. DICER1/Alu RNA dysmetabolism induces Caspase-8-mediated cell death in age-related macular degeneration. Proc Natl Acad Sci U S A. 2014;111: 16082–7. doi:10.1073/pnas.1403814111

66. Tarallo V, Hirano Y, Gelfand BD, Dridi S, Kerur N, Kim Y, et al. DICER1 Loss and Alu RNA Induce Age-Related Macular Degeneration via the NLRP3 Inflammasome and MyD88. Cell. 2012;149: 847–859. doi:10.1016/j.cell.2012.03.036

67. Chua HL, Serov Y, Brahmi Z. Regulation of FasL expression in natural killer cells. Hum Immunol. Hum Immunol; 2004;65: 317–327. doi:10.1016/j.humimm.2004.01.004

68. Hahne M, Renno T, Schroeter M, Irmler M, French L, Bornand T, et al. Activated B cells express functional Fas ligand. Eur J Immunol. Eur J Immunol; 1996;26: 721–724. doi:10.1002/eji.1830260332

69. Kaplan HJ, Leibole MA, Tezel T, Ferguson TA. Fas ligand (CD95 ligand) controls angiogenesis beneath the retina. Nat Med. Nat Med; 1999;5: 292–297. doi:10.1038/6509

70. Matsumoto H, Murakami Y, Kataoka K, Notomi S, Mantopoulos D, Trichonas G, et al. Membrane-bound and soluble Fas ligands have opposite functions in photoreceptor cell death following separation from the retinal pigment epithelium. Cell Death Dis. Nature Publishing Group; 2015;6: e1986–e1986. doi:10.1038/cddis.2015.334

71. Hirano Y, Yasuma T, Mizutani T, Fowler BJ, Tarallo V, Yasuma R, et al. IL-18 is not therapeutic for neovascular age-related macular degeneration. Nature Medicine. Nature Publishing Group; 2014. pp. 1372–1375. doi:10.1038/nm.3671

72. Longbottom R, Fruttiger M, Douglas RH, Martinez-Barbera JP, Greenwood J, Moss SE. Genetic ablation of retinal pigment epithelial cells reveals the adaptive response of the epithelium and impact on photoreceptors. Proc Natl Acad Sci U S A. National Academy of Sciences; 2009;106: 18728–33. doi:10.1073/pnas.0902593106

73. Leschey KH, Hackett SF, Singer JH, Campochiaro PA. Growth factor responsiveness of human retinal pigment epithelial cells. Invest Ophthalmol Vis Sci. 1990;31: 839–46. Available: http://www.ncbi.nlm.nih.gov/pubmed/2186011

74. Cassidy L, Barry P, Shaw C, Duffy J, Kennedy S. Platelet derived growth factor and fibroblast growth factor basic levels in the vitreous of patients with vitreoretinal disorders. Br J Ophthalmol. 1998;82: 181–5. Available: http://www.ncbi.nlm.nih.gov/pubmed/9613386

75. Casaroli-Marano RP, Pagan R, Vilaró S. Epithelial-mesenchymal transition in

proliferative vitreoretinopathy: intermediate filament protein expression in retinal pigment epithelial cells. Invest Ophthalmol Vis Sci. 1999;40: 2062–72. Available: http://www.ncbi.nlm.nih.gov/pubmed/10440262

76. Wang C, Cao G-F, Jiang Q, Yao J. TNF-α promotes human retinal pigment epithelial (RPE) cell migration by inducing matrix metallopeptidase 9 (MMP-9) expression through activation of Akt/mTORC1 signaling. Biochem Biophys Res Commun. 2012;425: 33–38. doi:10.1016/j.bbrc.2012.07.044

77. Jin M, He S, Wörpel V, Ryan SJ, Hinton DR. Promotion of adhesion and migration of RPE cells to provisional extracellular matrices by TNF-alpha. Invest Ophthalmol Vis Sci. 2000;41: 4324–32. Available: http://www.ncbi.nlm.nih.gov/pubmed/11095634

78. Farazdaghi M, Ebrahimi K. Role of the choroid in age-related macular degeneration: A current review. Journal of Ophthalmic and Vision Research. Wolters Kluwer Medknow Publications; 2019. pp. 78–87. doi:10.4103/jovr.jovr_125_18

79. Seddon JM, McLeod DS, Bhutto IA, Villalonga MB, Silver RE, Wenick AS, et al. Histopathological insights into choroidal vascular loss in clinically documented cases of age-related macular degeneration. JAMA Ophthalmol. American Medical Association; 2016;134: 1272–1280. doi:10.1001/jamaophthalmol.2016.3519

80. Lambert NG, ElShelmani H, Singh MK, Mansergh FC, Wride MA, Padilla M, et al. Risk factors and biomarkers of age-related macular degeneration. Prog Retin Eye Res. NIH Public Access; 2016;54: 64–102. doi:10.1016/j.preteyeres.2016.04.003

81. Fisher CR, Ferrington DA. Perspective on AMD Pathobiology: A Bioenergetic Crisis in the RPE. Invest Ophthalmol Vis Sci. Association for Research in Vision and Ophthalmology; 2018;59: AMD41–AMD47. doi:10.1167/iovs.18-24289

Chapter III: Identification of Y-27632 as a Potential Treatment for AMD using a Novel Wound Healing Platform

A. Introduction

Retinal pigmented epithelial (RPE) cells form a tightly packed, cuboidal, and highly pigmented monolayer at the base of the retina. Although RPE cells are not directly responsible for vision, they play a critical role in sustaining the health of overlaying light-sensitive photoreceptors. RPE cells have several vital functions in maintaining retinal health, including maintenance of the blood-retinal barrier (BRB), re-isomerization of all-*trans*-retinal, transport of nutrients, removal of waste from the overlying photoreceptors, and absorption of stray light [1–3]. With a long list of critical functions for the neural retina's maintenance, it is no surprise that the degeneration of this single layer of cells can result in dysfunction of the neural retina and ultimate loss of vision.

RPE degeneration is a central feature of age-related macular degeneration (AMD), a blinding disease that affects nearly 11 million people in the United States and almost 196 million people worldwide [4]. Early stages of AMD can be identified by the presence of sub-RPE deposits called drusen, which are thought to be sites of inflammation and pigmentary abnormalities [5]. As the disease progresses, the number and size of drusen increases, leading to two clinically distinct late stages of AMD known as choroidal neovascularization (CNV) and geographic atrophy (GA). In CNV, blood vessels infiltrate the retina through the BRB. This may lead to leakage of blood into the retina causing RPE damage and loss of vision if not treated promptly.

While VEGF inhibitors to prevent new blood vessel growth can be used to delay the progression of CNV, no commercial treatment exists to treat or slow the progression of GA [6]. Geographic atrophy is characterized by a growing area of RPE atrophy over the macular region, increasing at a rate of 1.8 mm^2/year [7]. RPE atrophy leads to degeneration of the overlying photoreceptors and ultimate loss of central vision. Although the exact mechanism of RPE cell death leading to atrophic areas is still a topic of debate, there is no denying the ultimate failure of the surviving RPE to repair regions of atrophy adequately.

In vitro methods have been developed to study the innate ability of RPE to regenerate in culture, including mechanical or chemical ablation, enzymatic disassociation, and, more recently, localized wounding using electrical current [8–11]. Although each of these methods has advantages for studying wound repair, no wounding model has succeeded at mimicking the phenotype of late-stage GA. Therefore, we developed a system which induces large, localized wounds in a mature RPE monolayer that remaining RPE fails to adequately repair. We can use this system to screen for therapeutics that aid in the ability of bystander RPE to repair large wounds.

B. Results

RPE monolayers are unable to repair large wounds

Apoptosis is thought to play a role in the progression of GA as apoptotic RPE have been noted surrounding growing regions of RPE atrophy [12,13]. Thus, the ability of bystander RPE to respond and repair large areas of RPE apoptotic cell death is of interest. Hence, to better mimic GA *in vitro*, we established a new cell culture model employing RPE

expressing a recombinant inducible Caspase-9 gene (iCaspase9) and a custom plating device to trigger apoptosis and generate large well-defined areas of RPE atrophy.

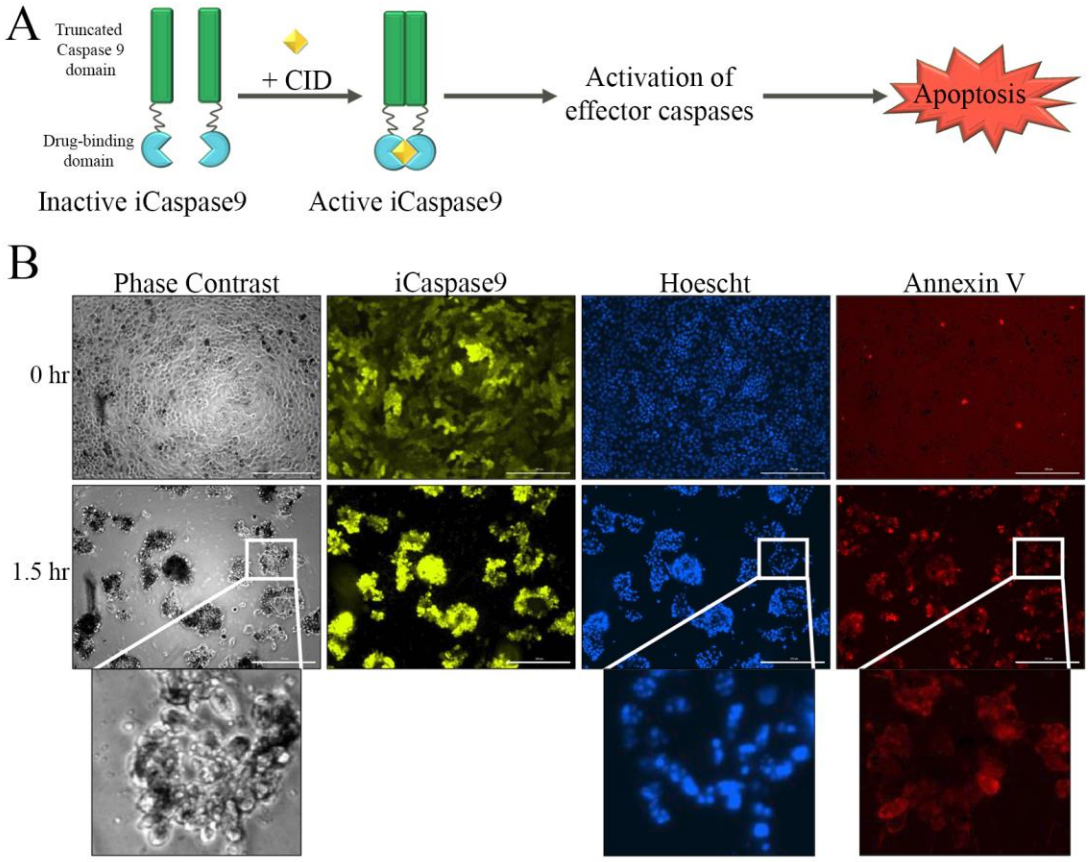

Figure 3-1. Inducible Caspase9 iPS-RPE undergo apoptosis with addition of the chemical inducer of dimerization. (A) The inducible Caspase 9 (iCaspase9) construct consists of a truncated Caspase 9 catalytic domain (green) linked to a high-affinity drug binding domain (blue). Without the presence of the chemical inducer of dimerization (CID; yellow), iCaspase9 do not dimerize. Upon addition of the CID, dimerization of iCaspase9 occurs triggering the activation of effector caspases, such as Caspase 3, causing the induction of apoptosis. Figure modified from Gargett *et al.*, 2014. (B) Differentiated RPE cells containing the iCaspase9 construct induce apoptosis after addition of the CID. Hallmark characteristics of apoptosis such as membrane blebbing (phase contrast), nuclei fragmentation (Hoechst), and phospholipid flipping (Annexin V) are visible 1.5 hours after addition 25 nM CID. Scale bars are 200 µm.

To establish RPE cell lines that express an inducible Caspase-9, minimally passaged stem cell-derived RPE were transduced with a replication deficient retrovirus construct, pMSCV-F-del-iCasp9.IRES.GFP. The construct allows for constitutive expression of a recombinant fusion protein, iCaspase9, comprised of a small molecule drug binding domain

linked to the Caspase-9 catalytic subunit, as well as a recombinant green fluorescent protein (GFP) that allows for the identification of transduced cells (Fig 3-1A) [14,15]. One month following viral transduction, iCaspase9-RPE cells were then isolated based on the expression of GFP using fluorescence activated cell sorting (FACS). To verify that RPE cells expressing iCaspase9 could be triggered to undergo apoptosis, iCaspase9-RPE cells were cultured for one month to allow for cuboidal morphology and pigmentation to develop and the cells were treated with the chemical inducer of dimerization (CID; AP20187). The CID is a dimeric ligand with high affinity to the iCaspase9 small molecule binding domain. Binding of the CID promotes the dimerization of iCaspase9, consequent induction of Caspase-9 protease activity, and subsequent apoptotic cell death (Fig 3-1A). Within 90 minutes of addition of the CID, iCaspase9-RPE showed hallmarks of apoptosis including plasma membrane blebbing, nuclei fragmentation, and externalization of phosphatidylserine (Fig 3-1 B) [16–19]. Importantly, apoptosis was only evident when the chemical inducer of dimerization (CID) was supplemented to the media.

Having determined that iCaspase9-RPE can be triggered to undergo apoptosis using the CID, we then proceeded to develop a device that facilitates the generation of macula sized regions of RPE atrophy. In this system, a custom stainless-steel plating device is used to restrict the plating of iCaspase9 RPE to a 4 mm diameter region in the center of a 24-well microplate well and control RPE expressing mCherry to surrounding regions (Fig 3-2A). Twenty-four hours after the cells are plated and have attached to the substrate, the plating device is removed, and the cells are allowed differentiate in culture for four weeks. Once the RPE have matured, the CID is then added to the media for 48-hours. Apoptosis of the

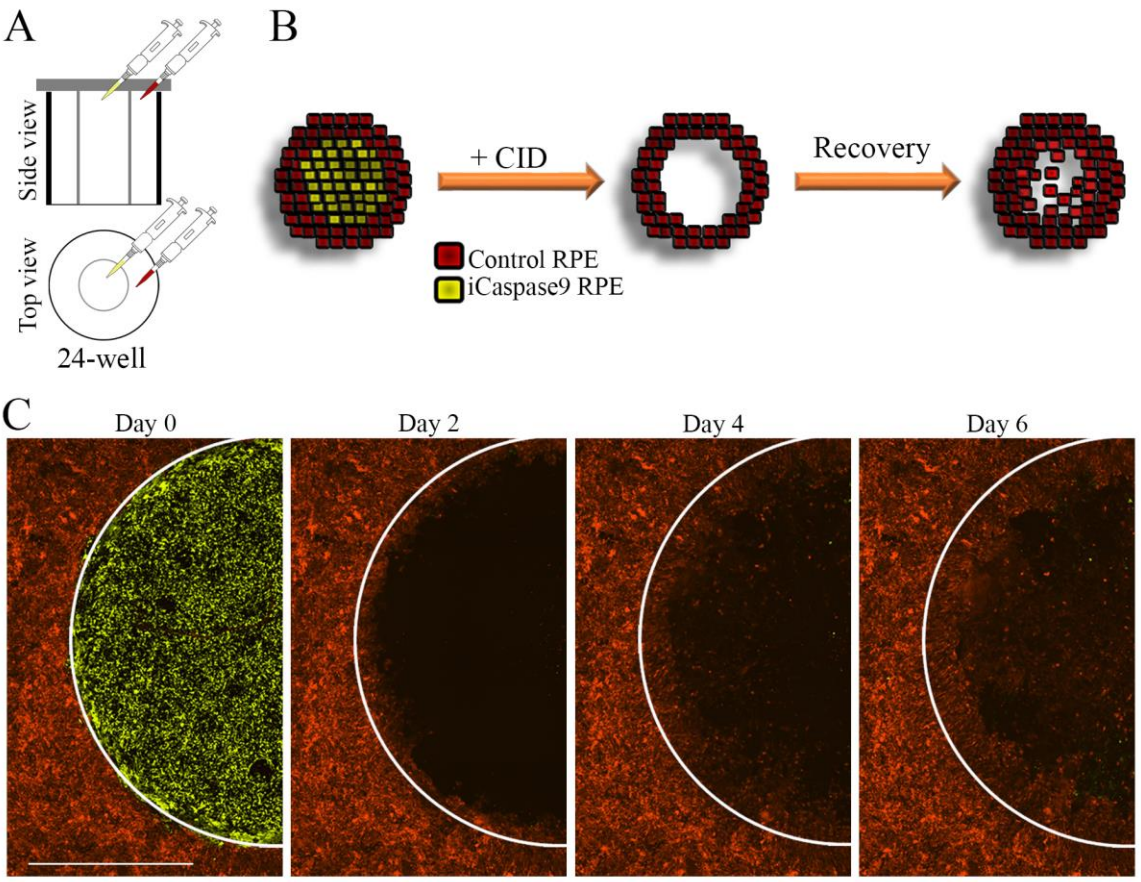

Figure 3-2. Generation of macula sized apoptotic lesion in RPE monolayer. (A) Using a specialized plating device (grey), iCaspase9-RPE (yellow) are plated in a macula sized pattern in the center of the well, surrounded by control RPE (red). (B) Experimental overview of large lesion wounding method. iCaspase9 RPE (yellow) are plated in the center of the well surrounded by control RPE cells (red). After the addition of the CID the iCaspase9 cells die off, leaving a large, centralized wound. The bystander cells attempt to repair the large lesion during the four-week recovery time. (C) RPE cells are plated as stated above and differentiated in culture for one month. Following addition of the CID, iCaspase9 RPE die off and leave a large, centralized wound. Surviving bystander RPE respond to the wound and attempt to repair the lesioned area. White half circular represents original wounded area. Scale bar is 2 mm.

iCaspase9 RPE generates a roughly 13 mm^2 wound in the monolayer. Over the next four weeks, the cells are monitored as the surviving bystander RPE attempt to repair the large lesion (Fig 3-2B and C). One month after wounding, vehicle alone control (DMSO) RPE cells cannot repair the lesion adequately (Fig 3-3). Large holes and mesenchymal RPE are visible within the repaired area and confluent RPE with correct morphology encompass only about 70% of the affected region (Fig 3-3).

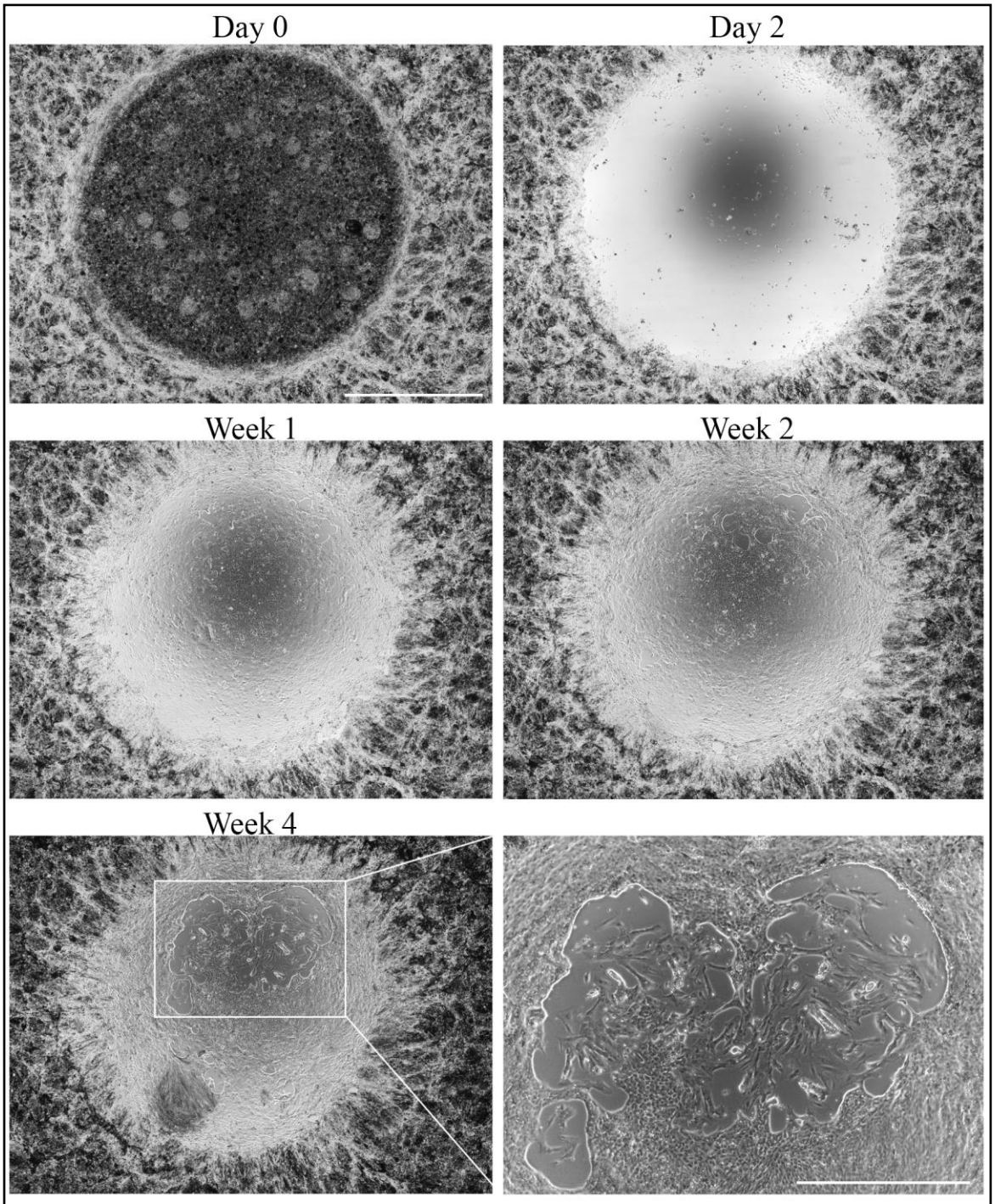

Figure 3-3. RPE cells cannot efficiently repair large lesion four weeks post wounding. Phase contrast images of a representative control well prior to and post wound induction. RPE fill in a majority of the wounded area 1-week post wounding but confluency is not maintained. Holes and mesenchymal RPE cells are seen in the repaired area 4-weeks post wounding. Images taken as a 4 x 4 montage at 4x. Scale bar for stitched images are 2 mm. Scale bar for enlarged image (bottom right) is 1 mm.

RepSox and Y-27632 improve the ability of bystander RPE to repair large lesions

RPE cells failed to mount a wound response productive enough to repair the large centralized apoptotic lesion in the monolayer, leaving large areas of RPE atrophy, reminiscent of GA (Fig 3-3). We next investigated whether therapeutic intervention may improve the innate ability of surviving RPE to repair the large lesion. The loss of epithelial morphology of control RPE in the center of the repaired area led us to search for therapeutics that may be able to suppress epithelial-to-mesenchymal transition (EMT). Both RepSox, an activin-like kinase 5 (ALK5) inhibitor, and Y-26632, a Rho-dependent protein kinase (ROCK) inhibitor, have both been shown to extend the passage of RPE *in vitro* by suppressing EMT while retaining the ability to re-differentiate back into functional RPE [8,20]. In addition, surviving RPE cells were treated with the glycogen synthase kinase 3 (GSK3) inhibitor CHIR-99021 (CHIR), previously found to promote RPE differentiation [21].

Treatment wither either RepSox or Y-27632 improved the ability of RPE to repair the large lesion, while CHIR hindered repair (Fig 3-4). Treatment with RepSox increased confluency of RPE over the damaged region to roughly 90%, while treatment with Y-27632 resulted in nearly 100% confluency (Fig 3-5). Treatment with CHIR had the opposite effect, hindering RPE wound repair resulting in only 20% confluency over the wounded area. In addition, treatment with Y-27632 resulted in the best RPE morphology compared to any other treatment (Fig 3-5A).

Although CHIR appeared to prevent RPE wounding healing it had a positive effect on promoting pigmentation in RPE surrounding the lesion (Fig 3-6A). Pigmentation is perhaps

one of the most striking phenotypes of RPE cells. It is thought to absorb light to improve visual acuity and to protect the retina by protecting against oxidative damage [2,3,22,23].

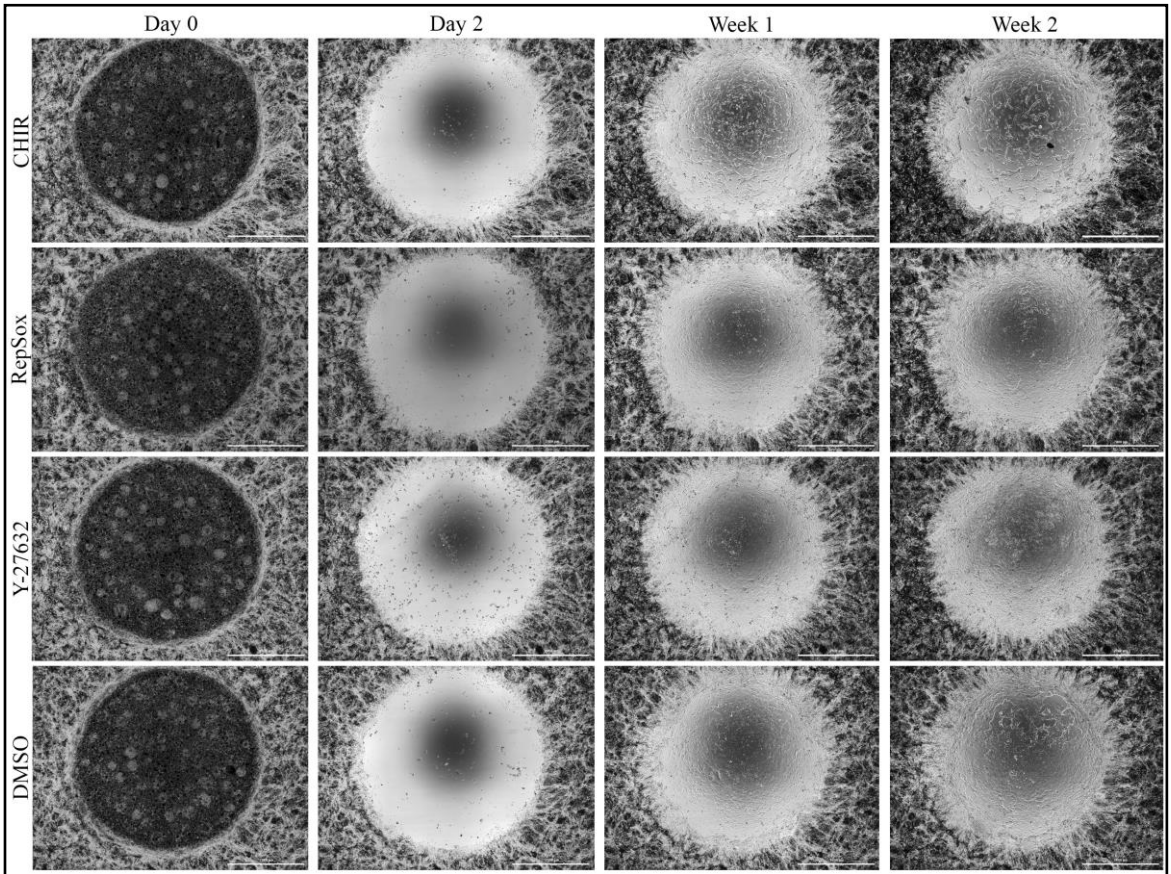

Figure 3-4. Treatment of RPE cells with Y-27632 or RepSox improve RPE confluency two weeks post wounding. Phase contrast images of a representative well from each drug treatment. CHIR treatment increases pigmentation outside the lesion, but RPE cells fail to repair the wounded area, leaving large holes across the lesion. Treatment with RepSox or Y-27632 increases ability of RPE to maintain confluency after two weeks of recovery. Control RPE (DMSO) are not able to maintain confluency of RPE after two weeks recovery. Images taken as a 4 x 4 montage at 4x. Scale bars are 2 mm.

Pigmentation of an RPE monolayer can be quantified using optical absorption. We found our RPE cultures to absorb maximally at 510 nm, although other groups use wavelengths between 475 nm and 550 nm to quantify pigmentation [24,25]. Absorbance readings were acquired on RPE outside (upper depiction Fig 3-6E) and within (upper depiction Fig 3-6F) the repaired area using a 5 x 5 spot read array. Treatment with either CHIR or Y-27632 increased pigmentation in RPE cells distal to the wound region, while RepSox had no

significant effect compared to the DMSO control (Fig 3-6E). Within the wounded area, none of the treatments significantly (p-value ≤ 0.05) increased pigmentation over the control,

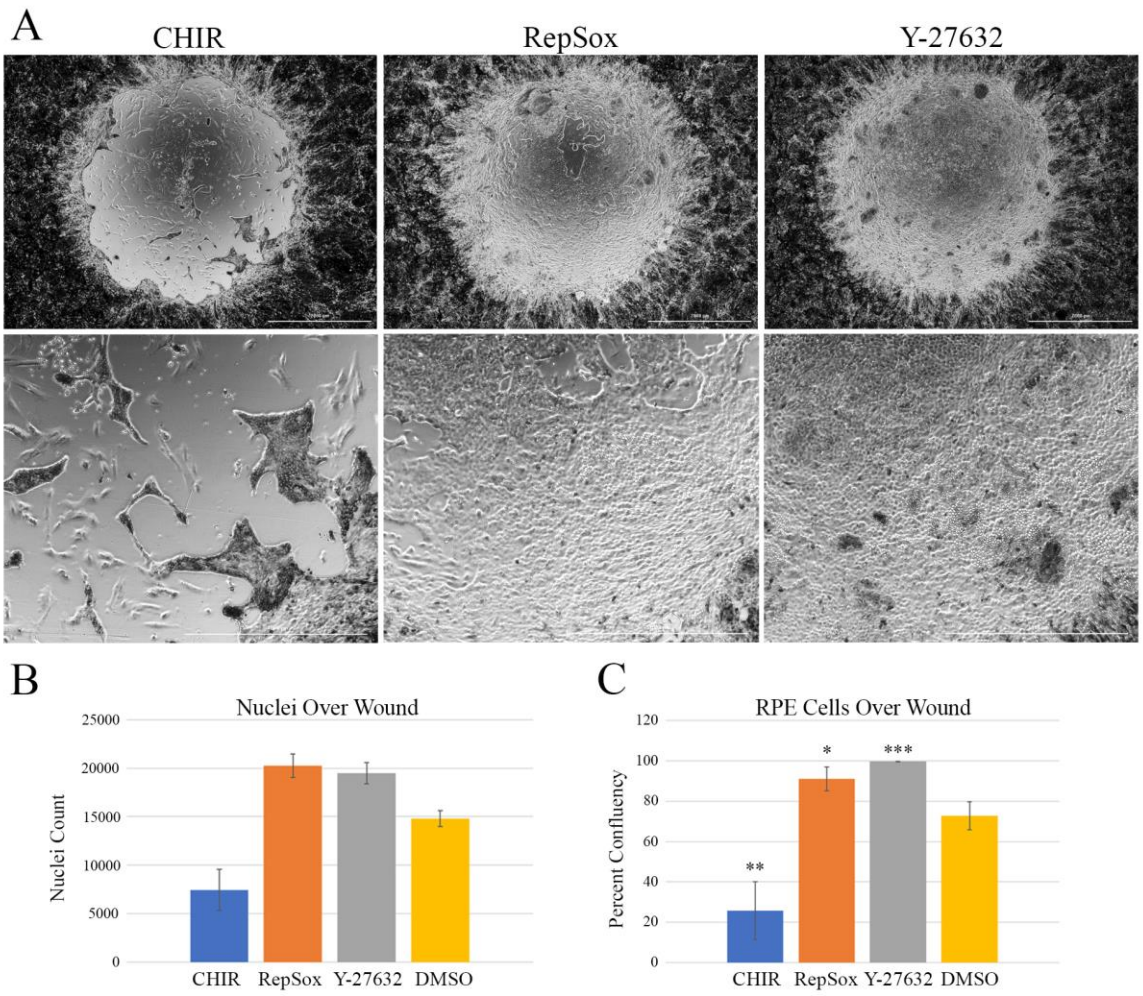

Figure 3-5. Treatment of RPE cells with RepSox or Y-27632 maintain RPE confluency and morphology four weeks post wounding. (A) Phase contrast images of RPE treated with CHIR, RepSox, or Y-27632 after four weeks of recovery. Enlarged images near the center of the lesion show detailed RPE morphology. Scale bars are 2 mm (top row) and 1 mm (bottom row). (B) Nuclei count for CHIR (blue), RepSox (orange), Y-27632 (grey), and DMSO (yellow) treated cells over the lesioned area four weeks after wounding. n=2 error bars are range. (C) Percent of RPE cell confluency over the lesioned area four weeks after wounding. CHIR (blue) significantly reduced RPE confluency, while RepSox (orange) and Y-27632 (grey) significantly increases RPE confluency compared to the DMSO control (yellow). n=4 error bars are standard deviation. * p-value ≤ 0.05, ** p-value ≤ 0.01, *** p-value 0.001, **** p-value ≤ 0.0001.

however, treatment with Y-27632 approaches significance with a p-value of 0.12 (Fig 3-6F). In addition, treatment with Y-27632 resulted in much more uniform RPE with light

pigmentation across the entire repaired area (Fig 3-6C). It is possible that a longer recovery time may allow for a more significant increase in pigmentation over pigmentation over the DMSO control.

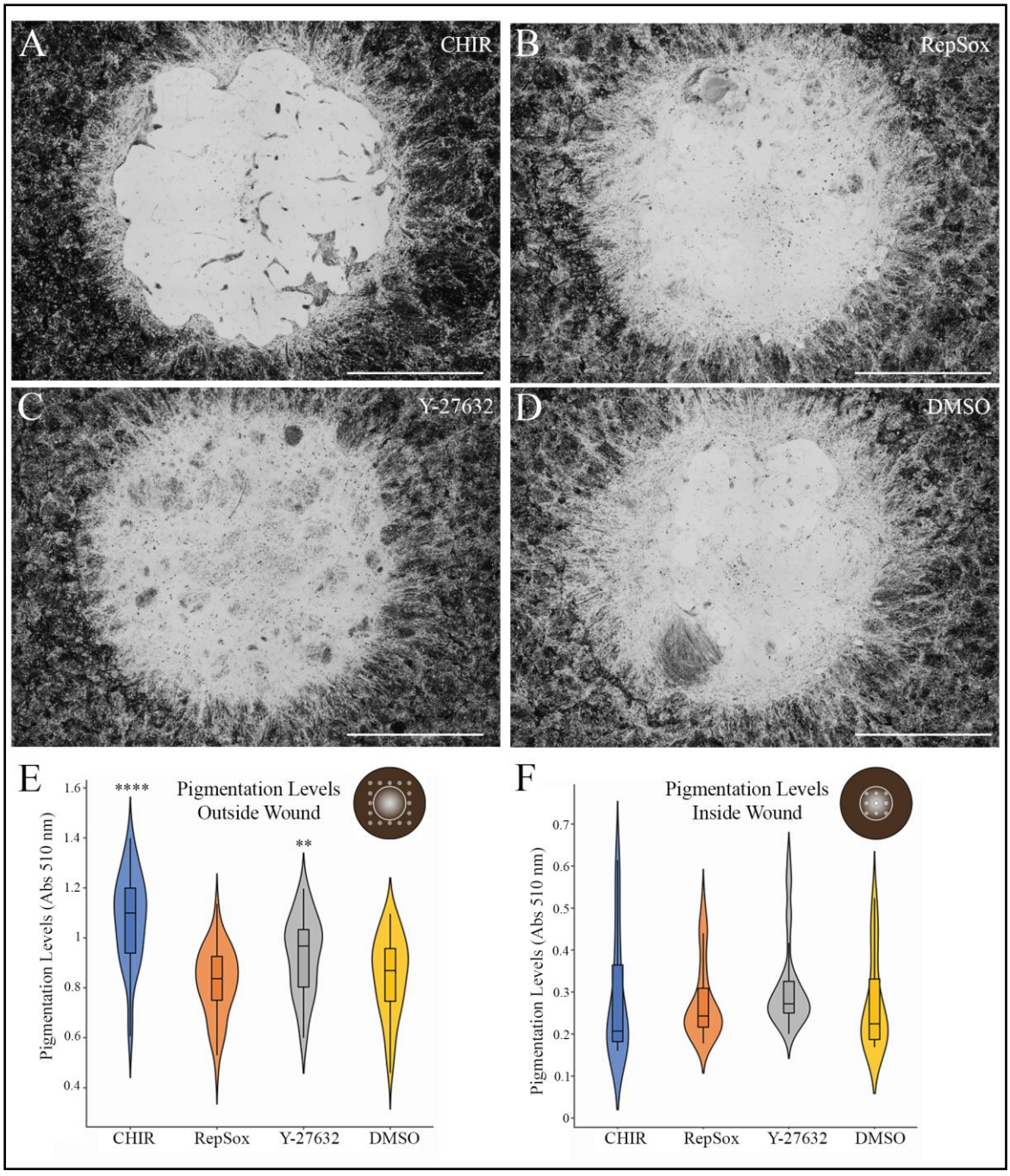

Figure 3-6. Effect of CHIR, RepSox, and Y-27632 on RPE confluency and pigmentation four weeks post wounding. (A-D) Bright-field images four weeks post wound induction. Wells were treated with CHIR (A), RepSox (B), Y-27632 (C), or DMSO (D). Images taken as a 4 x 4 montage at 4x. Scale bars are 2 mm. (E) A violin plow showing pigmentation levels in RPE cells outside the lesioned area four weeks after wounding with drug treatment. CHIR (blue) and Y-27632 (grey) significantly increases pigmentation of RPE cells outside of the lesioned area compared to the DMSO control (yellow). RepSox (orange) had no significant change in pigmentation levels outside the lesioned area. Pigmentation spot reads shown as small circles in cartoon depiction, lesioned area represented inside large white circle. n=4, eighteen spot reads for each sample. (F) A violin plow showing pigmentation levels in RPE cells inside the lesioned area four weeks after wounding with drug treatment. No compound had a statistically significant change in pigmentation levels over the lesioned area four weeks after wounding than the DMSO control. However, Y-27632 is approaching significance, with a P-value of 0.12 compared to the control. Cartoon depiction shows pigmentation spot reads inside wounded area. n=4, nine reads for each sample. ** p-value ≤ 0.01, **** p-value ≤ 0.0001.

Y-27632 improves RPE65 expression and photoreceptor phagocytosis

To gain a better idea of what other effects extensive wound repair and treatment with compounds have on RPE function, we used immunocytochemistry to assess the expression of RPE65, a key enzyme in the visual cycle. RepSox had no effect on RPE65 expression on cells distal or within the lesion and CHIR treated RPE showed reduced RPE65 expression in the distal area (Fig 3-7). The increased levels of pigmentation resulting from CHIR treatment may interfere with the ability to quantify RPE65 expression using immunofluorescence, therefore the expression should be confirmed using quantitative PCR. Treatment with Y-27632 increased RPE65 expression in RPE cells both outside and inside the lesioned area (Fig 3-7).

Another critical function of RPE is the phagocytosis of photoreceptor outer segments (POS). This process was tested *in vitro* by supplementing media with fluorescently labeled photoreceptor outer segments. The use of a serum-free RPE medium for our experiments required the addition of two co-factors, MFG-E8 and Protein S, for more efficient

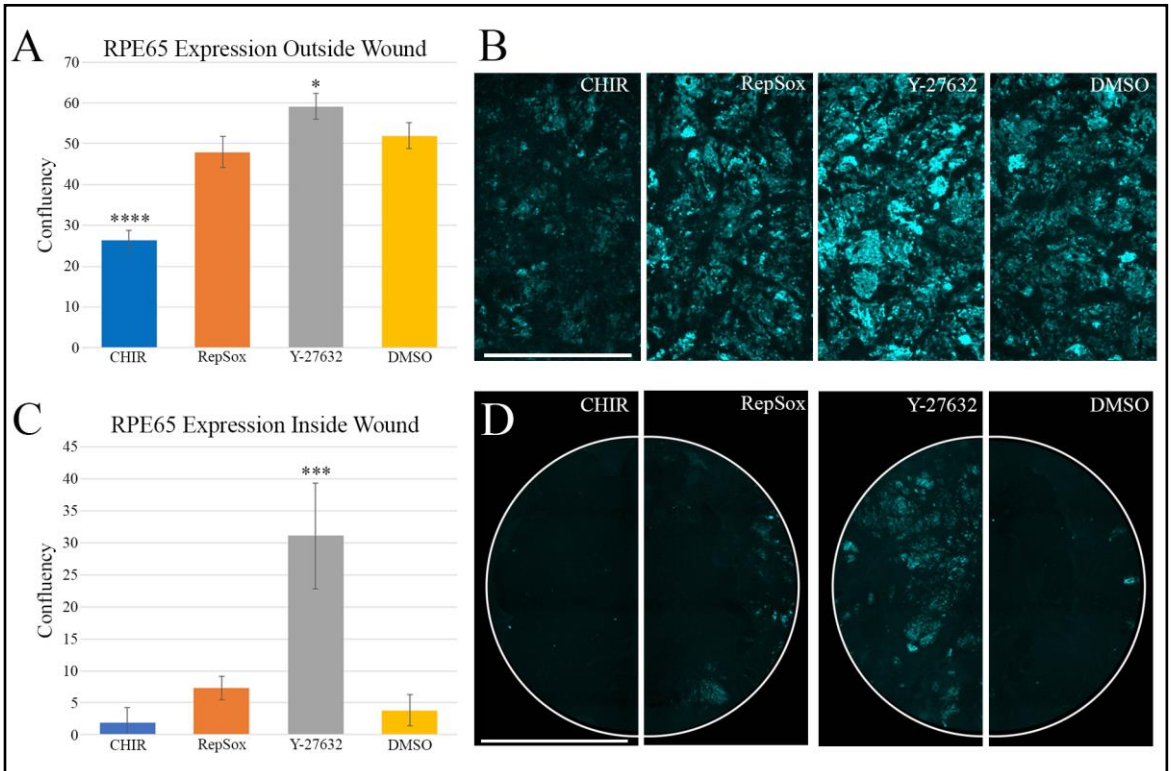

Figure 3-7. Expression of RPE65 over repaired area four weeks post wounding. (A) Confluency of RPE expressing RPE65 outside of the lesioned area. CHIR (blue) significantly reduces RPE65 expression, while Y-27632 (grey) significantly increases RPE65 confluency compared to the DMSO control (yellow). RepSox (orange) has no significant effect on RPE65 expression outside the wounded area. n=4 error bars are standard deviation. (B) Immunocytochemistry showing RPE65 expression (blue) in RPE cells outside the lesioned area. Scale bar is 2 mm. (C) Confluency of RPE cells expressing RPE65 inside of the lesioned area. Y-27632 (grey) significantly increases RPE65 confluency compared to the DMSO control (yellow). CHIR (blue) and RepSox (orange) showed no significant effect on RPE65 expression inside the repaired area. A 4 mm diameter plug was used to assess RPE65 expression over the lesion. n=4 error bars are standard deviation. (D) Immunocytochemistry showing RPE65 expression (blue) in RPE cells inside the lesioned area (white half circle). Scale bar is 2 mm. * p-value ≤ 0.05, *** p-value 0.001, **** p-value ≤ 0.0001.

phagocytosis (Fig 3-8A) [26,27]. Roughly 5% of the RPE were able to phagocytose FITC labeled POS without the supplementation of co-factors (Fig 3-8B). When MFG-E8 and Protein S were supplemented to media during the phagocytosis assay, nearly 30% of the RPE were able to phagocytose POS, seen by the shift in the scatterplots in Fig 3-8C. Roughly 15% of RPE cells differentiated in the presence of Y-27632 phagocytosed POS without the presence of co-factors, a nearly three-fold increase over control RPE. When co-factors were added, the number of RPE with engulfed POS increased to over 40% (Fig 3-6B). These

results suggest that not only can the ROCK inhibitor Y-27632 improve the ability of RPE to wound repair effectively, but it also appears to promote other critical functions of RPE including the visual cycle and POS phagocytosis.

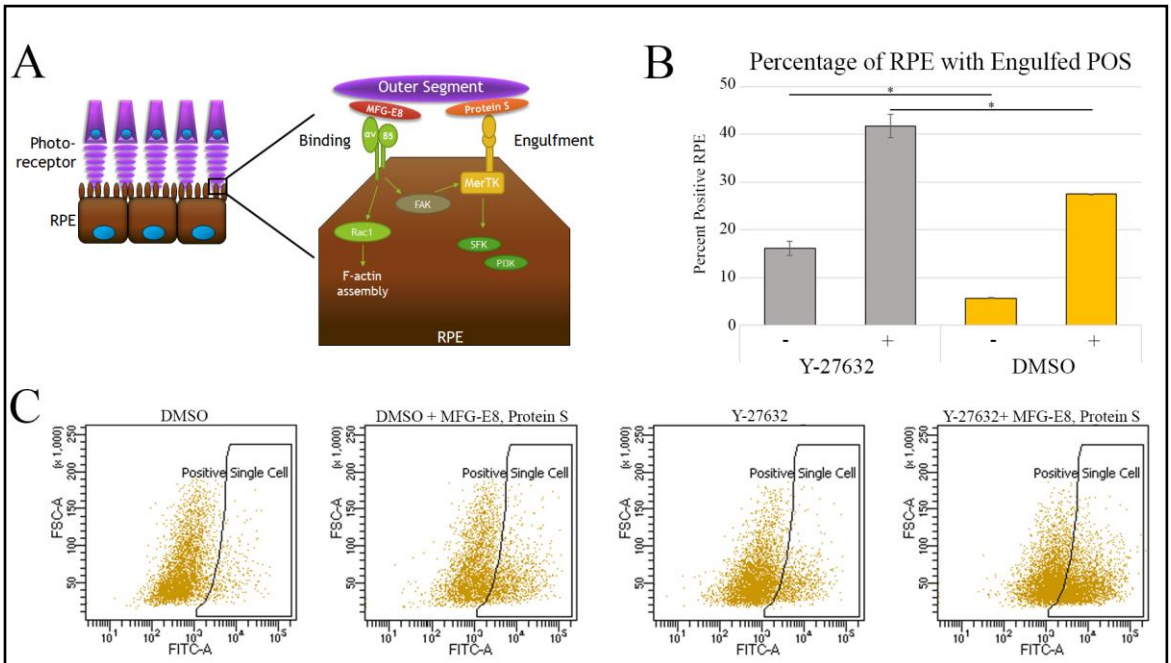

Figure 3-8. RPE cells differentiated with Y-27632 improve RPE cell phagocytosis of photoreceptor outer segments. (A) Overview of proteins involved in photoreceptor outer segment (POS) phagocytosis. Modified from Mazzoni *et al.*, 2014. (B) Percentage of RPE cells containing at least one fluorescent POS. RPE were differentiated in media supplemented with Y-27623 (grey) or DMSO (Yellow). Phagocytosis assay was performed in the presence (+) or absence (-) of the co-factors MFG-E8 and Protein S. n=2 error bars are range. * p-value ≤ 0.05. (C) Flow cytometry scatter plots showing the ability of RPE cells differentiated in the presence of DMSO or Y-27632 to phagocytose POS. RPE cells differentiated with DMSO or Y-27632 were both able to bind and engulf FITC-labeled POS with the addition of co-factors MFG-E8 and Protein S as seen by the shift increase in population within the positive single cell gate.

C. Discussion

In this study, we devised a cell culture model with key features of GA and used this model to investigate the ability of human iPS-derived RPE to repair large focal lesions in a mature monolayer. RPE cells in culture have some repair and proliferative capacity after wounding. In contrast, in GA this reparative capacity is absent or substantially reduced, resulting in atrophic areas which enlarge over time [28,29]. Like the case in GA, we found that mature cultured RPE monolayers were incapable of faithfully repairing macular size

wounds (~13mm^2). While the RPE reached near confluence in the wound region after one week, the cells failed to acquire a prototypical RPE phenotype (Fig 3-3). Over time, atrophic areas within the wound region developed and the cells developed distinct mesenchymal RPE morphology. These phenotypes along with the reduction in pigmentation over the monolayer are reminiscent of phenotypes seen in atrophic areas in GA [28,30]. Having established a cell culture model with phenotypic similarities to GA, we then used this model to determine if small molecules that have been previously identified as facilitators of RPE repair could improve the capacity of RPE to repair regions of atrophy.

Activation of Wnt/β-catenin signaling, via supplementation with the GSK-3β inhibitor CHIR-99021, has been shown to improve RPE cell differentiation and promote proliferation in some cell types [31–33]. However, in contrast to our expectations, instead of facilitating large wound repair, CHIR treatment severely hindered the ability of RPE to repair the wound. Significantly fewer RPE cells were able to migrate or proliferate to heal the large, induced lesion and those cells that did enter the wound region failed to maintain correct RPE morphology (Fig 3-5). Interestingly though, we saw a significant increase in pigmentation levels in RPE outside the lesioned area (Fig 3-6). Fisetin, a dietary flavonoid found in fruits and vegetables, was recently shown to promote pigmentation in melanoma cells by inhibiting GSK-3β and promoting β-catenin activity, which increased expression of MITF and tyrosinase [34]. Wnt/β-catenin signaling is required for RPE differentiation in the developing mouse eye but is tightly controlled [35,36]. Although promoting Wnt/β-catenin signaling by treating with CHIR has a positive effect on RPE pigmentation, constant activation may be unfavorable for wound repair.

Persistent wound response driven by prolonged activation of the TGFβ pathway, resulting in irreversible EMT, has been implicated in AMD pathogenesis [8]. We therefore utilized the TGFBR1/ALK5 inhibitor RepSox and the ROCK inhibitor Y-27632, previously shown to reduce TGF-β1 induced Smad2/3 phosphorylation, to improve RPE wound repair [8,20,37,38]. Treatment of RPE with either RepSox or Y-27632 improved the ability of RPE to repair the large lesion. As seen in Fig 3-5, treatment with RepSox resulted in a few holes over the monolayer, but the morphology of RPE was more uniform than the DMSO control. Treatment with Y-27632 resulted in the best-looking monolayer, with little to no holes and uniform morphology across the repaired area. RPE coverage of the lesioned area significantly increased with treatment with RepSox or Y-27632, with Y-27632 approaching nearly 100% confluency (Fig 3-5C).

Interestingly, it appears Y-27632 increased the ability of iCaspase9-RPE to adhere to the wounded area compared to the control as seen by the increase in number of cells in the wounded area two days post wound induction (Fig 3-4). Previous studies on cultured corneal endothelial cells showed reduced apoptosis and increased adhesion with ROCK inhibitor treatment [39]. The combination of these effects may be seen here. Future experiments delaying the treatment of Y-27632 will be important to see if bystander RPE surrounding the wound can still adequately repair without the suggested increased viability and adhesion of residual iCaspase9-RPE in the center of the lesion.

Pigmentation is a defining feature of RPE which absorbs light and protects the cell from oxidative damage [2]. RepSox treatment resulted in no significant changes in pigmentation levels versus untreated cells, while treatment with Y-27632 significantly increased pigmentation in cells surrounding the lesion, a phenotype noted previously in

epidermal cells (Fig 3-6) [40]. Treatment with Y-27632 also resulted in increased pigmentation levels within the wound repaired area compared to the control. By eye, RPE over the lesioned area are far more pigmented and uniform when treated with Y-27632 than control RPE, but the p-value for our data is greater than 0.05 (Fig 3-6). It is possible that nine spot reads over the wounded area cannot detect the increase in pigmentation at four weeks and increasing the number of spot reads could help reduce the variability of the reads. It is also possible that four weeks is not long enough to see a statistically significant difference. A more extended recovery period may help emphasize the ability of Y-27632 to increase melanogenesis in RPE.

Assessing the expression of RPE65 in RPE cells outside and within the wounded area allowed us to assess the functionality of the visual cycle resulting from prolonged inhibition of TGF-β or ROCK signaling. Treatment with RepSox had no significant effect on RPE65 expression outside or within the lesioned area (Fig 3-7). The morphology of RPE in the wound recovered area appeared more uniform than the control, suggesting with a longer recovery time, RPE65 expression could eventually result in significantly higher expression than controls over this area. Treatment with Y-27632 increased the expression of RPE65 both outside and inside the wounded area, with nearly a six-fold increase in the expression of RPE65 in cells over the lesioned area compared to the control.

RPE65 is most well-known for its critical enzymatic role in the visual cycle, converting all-*trans*-retinyl ester into 11-*cis*-retinol [41,42]. Recently, however, it has been implicated in playing a role in the biosynthesis of *meso*-zeaxanthin, one of only three carotenoids present in the macula [43,44]. Unlike the other two macular carotenoids, lutein and zeaxanthin, which are readily found in foods in Western diets, *meso*-zeaxanthin is found

in only a few food items such as some types of fish skin and turtle fat [45,46]. Recent work has shown that lutein is converted to *meso*-zeaxanthin, and RPE65 is the enzyme thought to be responsible for this conversion [43,47,48]. Interestingly, due to these macular pigment carotenoids' protective role against damaging reactive oxygen species (ROS), the supplementation of macular carotenoids to patients with early AMD may slow the progression of the disease [49–52]. Future work may investigate the ability of Y-27632 treated RPE to upregulate the production of *meso*-zeaxanthin, potentially protecting the cell from damage associated with AMD.

In addition to playing a key role in the visual cycle, RPE cells also promote the health of overlaying photoreceptors by phagocytosing spent outer segments. Defects in RPE phagocytosis have been implicated in retinal degeneration, highlighting the importance of this function [53,54]. RPE phagocytosis is known to decline with age, however this ability is significantly lower patients with AMD compared to equally aged controls, which may contribute to RPE dysfunction [55]. Interestingly, we found that RPE cells differentiated in the presence of Y-27632 were able to significantly increase the ability of RPE to phagocytose FITC-labeled POS (Fig 3-8). This improvement is likely due to a previous observation in our lab in which the differentiation of RPE plated at low-density was improved with Y-27632 treatment (results not shown). Future work should assess the phagocytic ability of RPE over the wound repaired area as well as the ability to breakdown POS.

Increases in oxidative stress and immune response are thought to play important roles in driving the progression of AMD [56]. Previous work in other cell types have shown that ROCK inhibitors may provide protection against damage caused by oxidative stress or immune response. The inhibition of ROCK signaling in retinal vasculature for example,

resulted in a decreased ability of leukocytes to adhere by reducing the expression of intracellular adhesion molecule-1 (ICAM-1) [57,58]. More importantly, macrophage polarization, which was shown to increase due to aging, could be mitigated using ROCK2 inhibitors [59]. Activated macrophages have been noted around the periphery of atrophic areas in GA and are thought to contribute to the disease's progression [60,61]. ROCK inhibitors have been shown to protect Müller cells from oxidative stress and hypoxia, both of which are known risk factors that increase AMD progression [56,62]. Based on these previous findings, treatment with Y-27632 may also prove beneficial for the treatment of GA by slowing immune activity and protecting against oxidative damage.

In conclusion, we developed a model system to generate large wounds to a differentiated RPE monolayer, similar to GA, which can be used to screen therapeutics. The size of the wound can be easily modified by designing plating devices with larger or smaller plugs. We were able to generate a large, localized lesion, which untreated RPE were unable to repair adequately. We identified Y-27632 as an agent to significantly improve the ability of bystander RPE to productively repair large regions of atrophy. By combining this method with other disease-related stressors implicated in AMD, such as oxidative stress, amyloid-β, or age, we may find therapeutics best suited to treat AMD and ultimately slow the progression of the disease.

D. Materials and Methods

Retrovirus production

GP2-293 (Takara) cells were seeded at $1x10^7$ in T-150 flasks and grown until reaching 80-90% confluence. Flasks were transfected with 40.5 µg retroviral plasmid,

pMSCV-F-del Casp9.IRES.GFP (iCaspase9, Addgene #15567) or mCherry control pMSCV-IRES-mCherry (control, Addgene #52114), 40.5 µg envelope plasmid (pVSVG, Takara), 24.3 µg Xfect polymer (Takara) and 1.503 mL Xfect reaction buffer. Cells were incubated overnight, and the media was discarded. Medium between 24-72 hours was collected daily, combined with 1/3 volume of Retro-X concentrator (Takara), and incubated at 4º for 1-2 days. To prepare concentrated virus, tubes were centrifuged for 45 minutes at 1500 x g and 4ºC in a swinging bucket. The supernatant was slowly removed and discarded. The pellet was gently resuspended in 1/100th volume using phosphate buffer saline (PBS). Concentrated viral particles were then aliquoted and stored at -80ºC until needed.

Cell culture

Primary human fetal RPE cells were obtained by a previously described method [8,63] and passaged until mesenchymal, roughly 3 passages. Cells were then reprogramed using ReproRNA^{TM}-OKSGM (STEMCELL Technologies) using manufacturer instructions. Cells were passaged until tight colonies formed. Successful induced pluripotent stem cells (iPS) were purified using Anti-TRA-1-60 microbeads (Milteyni Biotec) using manufacturer instructions. iPS lines were checked for major karyotypic abnormalities using the hPSC Genetic Analysis Kit (STEMCELL Technologies) using manufacturer instructions before further experimental use. Successfully reprogrammed iPS lines were differentiated into RPE cells using our unpublished method. Pigmented RPE cells were frozen in mFreSR (STEMCELL Technologies) and stored in liquid nitrogen until needed.

Passage 1 RPE cells were thawed and plated at 10,000 cells/cm^2 in Matrigel (Corning) coated T-25 flasks in RPE medium containing 2 µM Thiazovivin (Fisher Scientific) and incubated overnight. Fresh medium containing retroviral particles (no more

than 10% total volume) and 10 µg/mL polybrene (Millipore Sigma) was added the next morning and incubated overnight. Media was discarded and fresh medium was added and changed every 2-3 days for 28 days. Differentiated RPE were disassociated using 0.025% trypsin EDTA (Lonza) and sorted using fluorescence-activated cell sorting (FACS) to isolate pigmented RPE cells containing either iCaspase9/GFP or mCherry. Positive cells were plated at 20,000 cells/cm^2 on Matrigel coated dishes and allowed to recover for 2-3 days. RPE cells containing either iCaspase9 or control constructs were lifted and frozen at passage 3. iCaspase9-RPE were plated at 80,000 cells/cm^2 on Matrigel coated dishes with Thiazovivin for 24 hours and let differentiate for 2-3 months before use in the final assay. Aged iCaspase9-RPE showed more consistent apoptosis in the final assay compared to younger iCaspase9-RPE. Control cells were plated at 500,000 cells in a T-75 with Thiazovivin for 24 hours and then let recover and divide for 3 days before use in the final assay.

The stainless-steel plating device was designed using Solidworks and CNC machined using stainless steel 304 with default finish (Fig 3-9). The plating device was carefully placed on top of Matrigel coated lummox 24-well dishes (Sarstedt) so that each tube formed a tight seal with the bottom of the dish. Aged iCaspase9-RPE were lifted and plated in the center at 200,000 cells/cm^2 and control RPE were plated at 100,000 cells/cm^2 in RPE medium containing Thiazovivin. The dish was gently rocked to disperse control cells in the outer ring and left at room temperature for one hour before moving to the incubator. After 24 hours, the plating device was gently lifted, and medium was replaced with RPE medium containing 2 ng/mL basic fibroblast growth factor (FGF) and 0.1% DMSO. Medium was changed every 2-3 days and FGF and DMSO were removed after one week. Cells were let differentiate for at least one month before starting the apoptosis assay with CID.

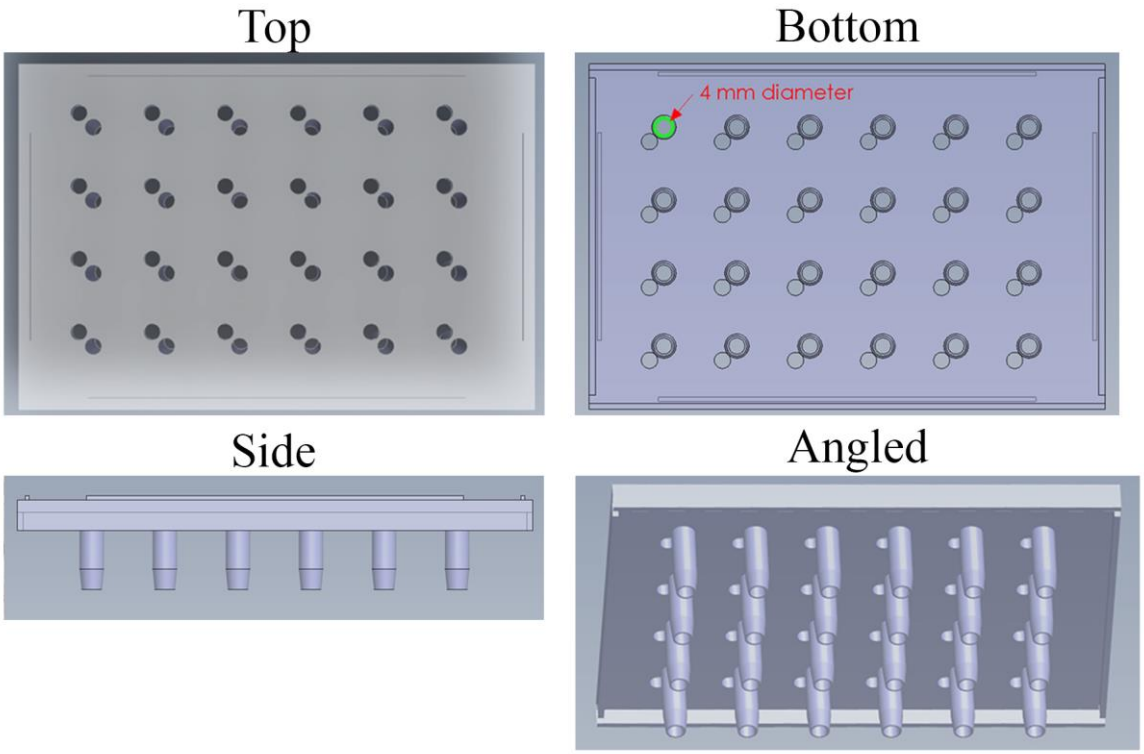

Figure 3-9. Plating device. Top, bottom, side, and angled view of steel plating lid. Holes are used to plate cells inside and outside the restricted center area. The 4 mm diameter tube is colored green and used to restrict the plating of iCaspase9 cells to only the inner circle. Lids can be modified to make larger or smaller holes. Images not to scale.

Wounding assay

Differentiated control and iCaspase9 RPE were given 25 nM CID (AP20187, B/B Homodimerizer, Clontech) in RPE medium to induce apoptosis in iCaspase9 RPE. CHIR-99021 (3 µM, ApexBio Technology), RepSox (100 nM, Cayman Chemical), Y-27632 (10 µM, STEMCELL Technologies), or DMSO (1 µl/mL, Fisher Scientific) was supplemented to medium with CID. The CID was removed after 48 hours, and cells were fed RPE medium with small molecules every 2-3 days for four weeks.

Imaging

Cells were imaged prior to induction and 2 days post, and then weekly for four weeks using the Cytation5 (BioTek). Images were taken in a 4x4 montage at 4x and stitched using the Gen5 software. Absorbance readings were taken using 5x5 spot read array at 510 nm.

Cell labeling

After four weeks of recovery, RPE cells were rinsed with PBS and fixed with 4% formaldehyde in PBS for 15 minutes at room temperature. Samples were blocked overnight using 5% normal donkey serum in PBS containing 0.1% Tween 20. RPE65 primary antibody (1:250 Abcam ab231782) and Alexa Fluor 647 donkey anti-rabbit secondary antibody (1:1000 Life Technologies) were incubated at room temperature for 1 hour. Nuclei were labeled by staining with Hoechst 33342 using a 1:2000 dilution in PBS, incubated on cells for 10 minutes at room temperature. Cells were imaged using a 6x6 montage at 4x and quantified using the Gen5 Image+ software.

Phagocytosis assay

iPS-RPE cells were differentiated in Matrigel coated 48-well dishes in the presence of Y-27632 or DMSO. Photoreceptor outer segments were purchased from Invision Bioresources and labeled with FITC using a previously published protocol [64] and stored in aliquots of $1x10^6$ POS at -80ºC until needed. POS were thawed quickly at 37ºC and spun for 5’ at 2,4000 x g at room temperature. One POS aliquot was used for two 48-wells. The POS pellet was resuspended in a minimum volume of RPE medium. MFG-E8 (120 nM R&D Systems) was added to POS and then added to cells, POS alone was used for control wells. Cells were incubated in the dark at room temperature for 2 hours. Excess POS were

aspirated, and wells were gently washed three times with medium with 4 minutes agitation on a rocker. Protein S (1 ug/mL, R&D Systems), or medium alone, was added to wells and incubated at 37ºC for 3 hours. Cells were gently rinsed with PBS and lifted using 150 ul trypsin (Lonza). After the cells lifted, 150 ul trypsin neutralization solution was added, and cells were gently disassociated by pipetting. Cells were filtered with a 35 µm cell strainer (Falcon) and stored covered on ice. Flow cytometry was used to assess POS containing RPE. RPE without POS and POS alone were used to set gates.

E. References

1. Boulton M, Dayhaw-Barker P. The role of the retinal pigment epithelium: Topographical variation and ageing changes. Eye. 2001;15: 384–389. doi:10.1038/eye.2001.141
2. Sparrow JR, Hicks D, Hamel CP. The retinal pigment epithelium in health and disease. Curr Mol Med. 2010;10: 802–23. Available: http://www.ncbi.nlm.nih.gov/pubmed/21091424
3. Simó R, Villarroel M, Corraliza L, Hernández C, Garcia-Ramírez M. The retinal pigment epithelium: something more than a constituent of the blood-retinal barrier--implications for the pathogenesis of diabetic retinopathy. J Biomed Biotechnol. 2010;2010: 190724. doi:10.1155/2010/190724
4. Age-Related Macular Degeneration: Facts & Figures | BrightFocus Foundation. [cited 25 Sep 2018]. Available: https://www.brightfocus.org/macular/article/age-related-macular-facts-figures
5. Garcia-Layana A, Cabrera-López F, García-Arumí J, Arias-Barquet L, Ruiz-Moreno JM. Early and intermediate age-related macular degeneration: update and clinical review. Clin Interv Aging. 2017;Volume 12: 1579–1587. doi:10.2147/CIA.S142685
6. Kovach JL, Schwartz SG, Flynn HW, Scott IU. Anti-VEGF treatment strategies for wet AMD. Journal of Ophthalmology. Hindawi Limited; 2012. doi:10.1155/2012/786870
7. Fleckenstein M, Mitchell P, Freund KB, Sadda SV, Holz FG, Brittain C, et al. The Progression of Geographic Atrophy Secondary to Age-Related Macular Degeneration. Ophthalmology Mar 1, 2018 pp. 369–390. Available: https://www.sciencedirect.com/science/article/pii/S0161642017309685
8. Radeke MJ, Radeke CM, Shih Y-H, Hu J, Bok D, Johnson L V., et al. Restoration of mesenchymal retinal pigmented epithelial cells by TGFβ pathway inhibitors:

implications for age-related macular degeneration. Genome Med. 2015;7: 58. doi:10.1186/s13073-015-0183-x

9. Hulkower KI, Herber RL. Cell Migration and Invasion Assays as Tools for Drug Discovery. Pharmaceutics. 2011;3: 107–124. doi:10.3390/pharmaceutics3010107

10. Storm T, Wilson I, Campbell R, Bolinches-Amorós A, Russell AJ, Davies SG, et al. A Semiautomated, Phenotypic, in Vitro Scratch Assay for Assessing Retinal Pigment Epithelial Cell Wound Healing. J Ocul Pharmacol Ther. 2020;36: 257–266. doi:10.1089/jop.2019.0116

11. Bailey-Steinitz LJ, Shih Y-H, Radeke MJ, Coffey PJ. An in vitro model of chronic wounding and its implication for age-related macular degeneration. Lewin AS, editor. PLoS One. 2020;15: e0236298. doi:10.1371/journal.pone.0236298

12. Dunaief JL, Dentchev T, Ying G-S, Milam AH. The Role of Apoptosis in Age-Related Macular Degeneration. Arch Ophthalmol. 2002;120: 1435. doi:10.1001/archopht.120.11.1435

13. Kaneko H, Dridi S, Tarallo V, Gelfand BD, Fowler BJ, Cho WG, et al. DICER1 deficit induces Alu RNA toxicity in age-related macular degeneration. Nature. 2011;471: 325–330. doi:10.1038/nature09830

14. Straathof KC, Pulè MA, Yotnda P, Dotti G, Vanin EF, Brenner MK, et al. An inducible caspase 9 safety switch for T-cell therapy. Blood. 2005;105: 4247–54. doi:10.1182/blood-2004-11-4564

15. Gargett T, Brown MP. The inducible caspase-9 suicide gene system as a “safety switch” to limit on-target, off-tumor toxicities of chimeric antigen receptor T-cells. Front Pharmacol. 2014;5. doi:10.3389/fphar.2014.00235

16. Kerr JFR, Wyllie AH, Currie AR. Apoptosis: A basic biological phenomenon with wide-ranging implications in tissue kinetics. Br J Cancer. 1972;26: 239–257. doi:10.1038/bjc.1972.33

17. Messam CA, Pittman RN. Asynchrony and commitment to die during apoptosis. Exp Cell Res. 1998;238: 389–398. doi:10.1006/excr.1997.3845

18. Solary E, Bertrand R, Kohn KW, Pommier Y. Differential induction of apoptosis in undifferentiated and differentiated HL-60 cells by DNA topoisomerase I and II inhibitors. Blood. 1993;81: 1359–1368. doi:10.1182/blood.v81.5.1359.1359

19. Saraste A, Pulkki K. Morphologic and biochemical hallmarks of apoptosis. Cardiovasc Res. 2000;45: 528–537. doi:10.1016/S0008-6363(99)00384-3

20. Croze RH, Buchholz DE, Radeke MJ, Thi WJ, Hu Q, Coffey PJ, et al. ROCK Inhibition Extends Passage of Pluripotent Stem Cell-Derived Retinal Pigmented Epithelium. Stem Cells Transl Med. 2014;3: 1066–1078. doi:10.5966/sctm.2014-0079

21. Regent F, Morizur L, Lesueur L, Habeler W, Plancheron A, Ben M’Barek K, et al. Automation of human pluripotent stem cell differentiation toward retinal pigment epithelial cells for large-scale productions. Sci Rep. 2019;9. doi:10.1038/s41598-019-

47123-6

22. Beatty S, Boulton M, Henson D, Koh HH, Murray IJ. Macular pigment and age related macular degeneration. Br J Ophthalmol. 1999;83: 867–877. doi:10.1136/bjo.83.7.867

23. Beatty S, Koh HH, Phil M, Henson D, Boulton M. The role of oxidative stress in the pathogenesis of age-related macular degeneration. Surv Ophthalmol. 2000;45: 115–134. doi:10.1016/S0039-6257(00)00140-5

24. Rambhatla L, Chiu C-P, Glickman RD, Rowe-Rendleman C. In Vitro Differentiation Capacity of Telomerase Immortalized Human RPE Cells | IOVS | ARVO Journals. Investig Ophthalmol Vis Sci. 2002;43: 1622–1630. Available: https://iovs.arvojournals.org/article.aspx?articleid=2123105

25. Hu DN, McCormick SA, Orlow SJ, Rosemblat S, Lin AY, Wo K. Melanogenesis by human uveal melanocytes in vitro. | IOVS | ARVO Journals. Investig Ophthalmol Vis Sci. 1995;36: 931–938. Available: https://iovs.arvojournals.org/article.aspx?articleid=2161420

26. Mazzoni F, Safa H, Finnemann SC. Understanding photoreceptor outer segment phagocytosis: use and utility of RPE cells in culture. Exp Eye Res. 2014;126: 51–60. doi:10.1016/j.exer.2014.01.010

27. Nandrot EF, Anand M, Almeida D, Atabai K, Sheppard D, Finnemann SC. Essential role for MFG-E8 as ligand for αvβ5 integrin in diurnal retinal phagocytosis. Proc Natl Acad Sci U S A. 2007;104: 12005–12010. doi:10.1073/pnas.0704756104

28. Bird AC, Bressler NM, Bressler SB, Chisholm IH, Coscas G, Davis MD, et al. An international classification and grading system for age-related maculopathy and age-related macular degeneration. Surv Ophthalmol. 1995;39: 367–374. doi:10.1016/S0039-6257(05)80092-X

29. Sacconi R, Corbelli E, Querques L, Bandello F, Querques G. A Review of Current and Future Management of Geographic Atrophy. Ophthalmology and Therapy. Springer Healthcare; 2017. pp. 69–77. doi:10.1007/s40123-017-0086-6

30. Zanzottera EC, Ach T, Huisingh C, Messinger JD, Spaide RF, Curcio CA. Visualizing retinal pigment epithelium phenotypes in the transition to geographic atrophy in age-related macular degeneration. Retina. 2016;36 Suppl 1: S12–S25. doi:10.1097/IAE.0000000000001276

31. Wang S, Ye L, Li M, Liu J, Jiang C, Hong H, et al. GSK-3β Inhibitor CHIR-99021 Promotes Proliferation Through Upregulating β-Catenin in Neonatal Atrial Human Cardiomyocytes. J Cardiovasc Pharmacol. 2016;68: 425–432. doi:10.1097/FJC.0000000000000429

32. Li C, Zhang S, Lu Y, Zhang Y, Wang E, Cui Z. The Roles of Notch3 on the Cell Proliferation and Apoptosis Induced by CHIR99021 in NSCLC Cell Lines: A Functional Link between Wnt and Notch Signaling Pathways. Chellappan SP, editor. PLoS One. 2013;8: e84659. doi:10.1371/journal.pone.0084659

33. Leach LL, Buchholz DE, Nadar VP, Buchholz DE, Lowenstein SE, Clegg DO. Canonical/β-catenin wnt pathway activation improves retinal pigmented epithelium derivation from human embryonic stem cells. Investig Ophthalmol Vis Sci. 2015;56: 1002–1013. doi:10.1167/iovs.14-15835

34. Molagoda IMN, Karunarathne WAHM, Park SR, Choi YH, Park EK, Jin CY, et al. GSK-3β-targeting fisetin promotes melanogenesis in B16F10 melanoma cells and zebrafish larvae through β-catenin activation. Int J Mol Sci. 2020;21: 312. doi:10.3390/ijms21010312

35. Westenskow P, Piccolo S, Fuhrmann S. β-catenin controls differentiation of the retinal pigment epithelium in the mouse optic cup by regulating Mitf and Otx2 expression. Development. 2009;136: 2505–2510. doi:10.1242/dev.032136

36. Fujimura N. WNT/β-catenin signaling in vertebrate eye development. Frontiers in Cell and Developmental Biology. Frontiers Media S.A.; 2016. p. 138. doi:10.3389/fcell.2016.00138

37. Xu T, Wu M, Feng J, Lin X, Gu Z. RhoA/Rho kinase signaling regulates transforming growth factor-β1-induced chondrogenesis and actin organization of synovium-derived mesenchymal stem cells through interaction with the Smad pathway. Int J Mol Med. 2012;30: 1119–1125. doi:10.3892/ijmm.2012.1107

38. Zhu J, Nguyen D, Hong O, Zhang XH, Chen XM, Zhang K. Inhibition of RhoA/Rho-kinase pathway suppresses the expression of extracellular matrix induced by CTGF or TGF-β in ARPE-19. Int J Ophthalmol. 2013;6: 8–14. doi:10.3980/j.issn.2222-3959.2013.01.02

39. Okumura N, Ueno M, Koizumi N, Sakamoto Y, Hirata K, Hamuro J, et al. Enhancement on primate corneal endothelial cell survival in vitro by a rock inhibitor. Investig Ophthalmol Vis Sci. 2009;50: 3680–3687. doi:10.1167/iovs.08-2634

40. Mi J, Feng Y, Wen J, Su Y, Xu L, Zu T, et al. A ROCK inhibitor promotes keratinocyte survival and paracrine secretion, enhancing establishment of primary human melanocytes and melanocyte–keratinocyte co-cultures. Pigment Cell Melanoma Res. 2020;33: 16–29. doi:10.1111/pcmr.12816

41. Cai X, Conley SM, Naash MI. RPE65: Role in the visual cycle, human retinal disease, and gene therapy. Ophthalmic Genetics. NIH Public Access; 2009. pp. 57–62. doi:10.1080/13816810802626399

42. Jin M, Li S, Moghrabi WN, Sun H, Travis GH. Rpe65 is the retinoid isomerase in bovine retinal pigment epithelium. Cell. 2005;122: 449–459. doi:10.1016/j.cell.2005.06.042

43. Shyam R, Gorusupudi A, Nelson K, Horvath MP, Bernstein PS. RPE65 has an additional function as the lutein to meso-zeaxanthin isomerase in the vertebrate eye. Proc Natl Acad Sci U S A. 2017;114: 10882–10887. doi:10.1073/pnas.1706332114

44. Bernstein PS, Li B, Vachali PP, Gorusupudi A, Shyam R, Henriksen BS, et al. Lutein, zeaxanthin, and meso-zeaxanthin: The basic and clinical science underlying

carotenoid-based nutritional interventions against ocular disease. Progress in Retinal and Eye Research. Elsevier Ltd; 2016. pp. 34–66. doi:10.1016/j.preteyeres.2015.10.003

45. M Nolan J. Verification of Meso-Zeaxanthin in Fish. J Food Process Technol. 2014;05. doi:10.4172/2157-7110.1000335

46. Maoka T, Arai A, Shimizu M, Matsuno T. The first isolation of enantiomeric and Meso-zeaxanthin in nature. Comp Biochem Physiol -- Part B Biochem. 1986;83: 121–124. doi:10.1016/0305-0491(86)90341-X

47. Johnson EJ, Neuringer M, Russell RM, Schalch W, Snodderly DM. Nutritional manipulation of primate retinas, III: Effects of lutein or zeaxanthin supplementation on adipose tissue and retina of xanthophyll-free monkeys. Investig Ophthalmol Vis Sci. 2005;46: 692–702. doi:10.1167/iovs.02-1192

48. Bhosale P, Serban B, Da YZ, Bernstein PS. Identification and metabolic transformations of carotenoids in ocular tissues of the Japanese quail Coturnix japonica. Biochemistry. 2007;46: 9050–9057. doi:10.1021/bi700558f

49. Stahl W. Biological activities of natural and synthetic carotenoids: induction of gap junctional communication and singlet oxygen quenching. Carcinogenesis. 1997;18: 89–92. doi:10.1093/carcin/18.1.89

50. Bernstein PS, Khachik F, Carvalho LS, Muir GJ, Zhao DY, Katz NB. Identification and quantitation of carotenoids and their metabolites in the tissues of the human eye. Exp Eye Res. 2001;72: 215–223. doi:10.1006/exer.2000.0954

51. Bartlett H, Howells O, Eperjesi F. The role of macular pigment assessment in clinical practice: a review. Clin Exp Optom. 2010;93: 300–308. doi:10.1111/j.1444-0938.2010.00499.x

52. Ma L, Liu R, Du JH, Liu T, Wu SS, Liu XH. Lutein, zeaxanthin and meso-zeaxanthin supplementation associated with macular pigment optical density. Nutrients. 2016;8. doi:10.3390/nu8070426

53. Bok D, Hall MO. The role of the pigment epithelium in the etiology of inherited retinal dystrophy in the rat. J Cell Biol. 1971;49: 664–682. doi:10.1083/jcb.49.3.664

54. Gal A, Li Y, Thompson DA, Weir J, Orth U, Jacobson SG, et al. Mutations in MERTK, the human orthologue of the RCS rat retinal dystrophy gene, cause retinitis pigmentosa. Nat Genet. 2000;26: 270–271. doi:10.1038/81555

55. Inana G, Murat C, An W, Yao X, Harris IR, Cao J. RPE phagocytic function declines in age-related macular degeneration and is rescued by human umbilical tissue derived cells. J Transl Med. 2018;16. doi:10.1186/s12967-018-1434-6

56. Langford-Smith A, Keenan TDL, Clark SJ, Bishop PN, Day AJ. The Role of Complement in Age-Related Macular Degeneration: Heparan Sulphate, a ZIP Code for Complement Factor H? J Innate Immun. 2014;6: 407–416. doi:10.1159/000356513

57. Arita R, Hata Y, Nakao S, Kita T, Miura M, Kawahara S, et al. Rho kinase inhibition

by fasudil ameliorates diabetes-induced microvascular damage. Diabetes. 2009;58: 215–226. doi:10.2337/db08-0762

58. Arita R, Hata Y, Ishibashi T. ROCK as a Therapeutic Target of Diabetic Retinopathy. J Ophthalmol. 2010;2010: 1–9. doi:10.1155/2010/175163

59. Zandi S, Nakao S, Chun KH, Fiorina P, Sun D, Arita R, et al. ROCK-Isoform-Specific Polarization of Macrophages Associated with Age-Related Macular Degeneration. Cell Rep. 2015;10: 1173–1186. doi:10.1016/j.celrep.2015.01.050

60. Yang D, Elner SG, Chen X, Field MG, Petty HR, Elner VM. MCP-1-activated monocytes induce apoptosis in human retinal pigment epithelium. Invest Ophthalmol Vis Sci. 2011;52: 6026–34. doi:10.1167/iovs.10-7023

61. Jonas JB, Tao Y, Neumaier M, Findeisen P. Monocyte Chemoattractant Protein 1, Intercellular Adhesion Molecule 1, and Vascular Cell Adhesion Molecule 1 in Exudative Age-Related Macular Degeneration. Arch Ophthalmol. 2010;128: 1281. doi:10.1001/archophthalmol.2010.227

62. Zhang X, Feng Z, Wang X. The ROCK pathway inhibitor Y-27632 mitigates hypoxia and oxidative stress-induced injury to retinal Müller cells. Neural Regen Res. 2018;13: 549. doi:10.4103/1673-5374.228761

63. Hu J, Bok D. A cell culture medium that supports the differentiation of human retinal pigment epithelium into functionally polarized monolayers. Mol Vis. 2001;7: 14–9. Available: http://www.ncbi.nlm.nih.gov/pubmed/11182021

64. Carr A-J, Vugler AA, Hikita ST, Lawrence JM, Gias C, Chen LL, et al. Protective Effects of Human iPS-Derived Retinal Pigment Epithelium Cell Transplantation in the Retinal Dystrophic Rat. Koch K-W, editor. PLoS One. 2009;4: e8152. doi:10.1371/journal.pone.0008152

Chapter IV: Effects of Aging on RPE Transcriptome and Potential for AMD Pathogenesis

A. Introduction

Age-related macular degeneration (AMD) is a potentially blinding disease with complex etiology affecting millions of people worldwide. Characterized by death and degeneration of the retina, advanced stages of AMD can result in the irreversible loss of central vision. RPE degeneration is a common feature of advanced stages of AMD, which is described as wet or dry depending on the presence or absence of neovascularization. Early stages of the disease are identified by the presence of drusen, inflammatory deposits located in between the retinal pigmented epithelial (RPE) cells, and Brüch's membrane [1]. As the drusen begin to accumulate in size and number, the RPE cells start to lose their ability to function and their characteristic epithelial morphology, often undergoing an epithelial-to-mesenchymal transition (EMT), a common response to wounding [2–5]. With the progression of the disease, RPE cells enter a chronic state of wounding, regardless of the presence or absence of a stimulus, resulting in the permanent loss of pigmentation and ultimate death [3,6]. RPE are essential in maintaining the health of the overlaying neural retina by providing nutrients, removing waste, and completing the visual cycle, among other functions [7–9]. Degeneration of this single layer of cells can result in the death of overlaying photoreceptors and ultimate blindness [10].

Over the past decades, scientists have discovered many genetic and environmental factors that increase the likelihood of AMD development. Genetic risk variants include genes involved in the complement system, while environmental risks include smoking, hypertension, and high body mass index [11–18]. Age, however, is by far the most

substantial factor associated with AMD, with people over the age of 75 having significantly higher frequencies of AMD than younger people [17].

The RPE monolayer, Brüch's membrane, and the choriocapillaris together form the blood-retinal barrier (BRB) which regulates the movement of water, ions, and proteins into and out of the vascular choroid [19–21]. Brüch's membrane is a five-layered acellular structure located between the RPE and vascular choroid. It serves as a point of attachment for the RPE and choriocapillaris and acts as a molecular sieve, regulating the exchange of solutes between the RPE and choroid [19,22–25]. Brüch's membrane is composed of collagens, laminins, fibronectin, and heparan sulfate proteoglycans (HSPGs) produced and remodeled by the overlying RPE and underlying choroidal cells [22,26–28].

Many age-related changes occur in Brüch's membrane over an individual's lifetime, including lipid accumulation, reduction in HSPGs, collagen cross-linking, calcification of the elastic layer, and increase in thickness. These age-related changes may affect the structural and functional properties of the membrane. The accumulation of lipids and increased thickness may decrease elasticity and permeability, increasing the likelihood of drusen formation. Collagen cross-linking also decreases elasticity while affecting permeability, likely reducing the ability to turnover components of the membrane. Calcification may make the membrane more brittle, which increases the likelihood of breakage and potential for wet AMD [22,29].

Like Brüch's membrane, the RPE monolayer also undergoes several age-related changes such as loss of melanin granules and accumulation of lipofuscin and basal deposits [30]. In this study, we used a transcriptomic approach to investigate age-related changes in RPE cells *in vitro*. In addition, we investigated changes in the ability of aged RPE to recover

from wounding. Finally, we discuss our findings and how they may relate to the pathology of AMD.

B. Results

Aged RPE have a reduced ability to restore pigmentation following injury

Aging, which can ultimately lead to the dysfunction and degeneration of the RPE monolayer, is the most significant risk factor for the development and progression of AMD, which ultimately leads to the dysfunction and degeneration of the RPE monolayer. However, how aging influences RPE gene expression over time is not fully understood. Therefore, we sought to investigate whether the effects of cellular aging in a controlled environment could be observed in cultured RPE. In addition, because apoptotic RPE have been observed around the regions of RPE atrophy, we also investigated whether age impacts the ability of bystander RPE to recover from apoptotic cell death and disruption of the monolayer [31,32].

To model the effects of cellular aging on RPE phenotype and wound repair *in vitro*, we devised a system where differentiated cultured RPE are allowed to age in culture for up to 12 months where wounds can be created at various times of aging. RPE expressing iCaspase9 (GFP) and RPE expressing a control construct (mCherry) were mixed in equal numbers and plated in 24-well cultureware, allowed to differentiate, and maintained in culture for up to 12 months. Cultures of 100% mCherry control RPE plated at equal total density served as aged controls. At 1, 3, 6, or 12 months of age in culture, widespread wounds were created by treating the cells with the chemical inducer of dimerization (CID,

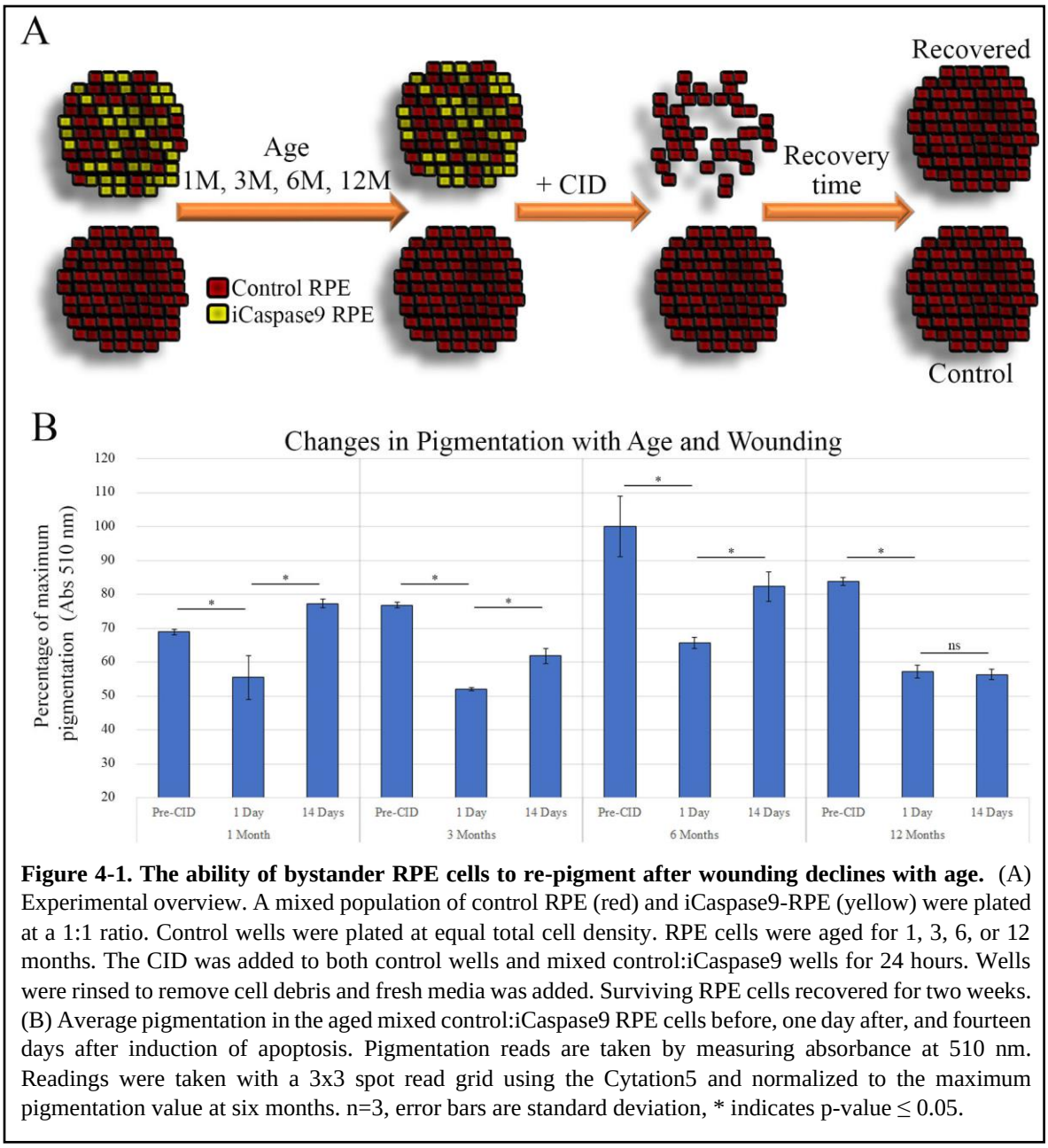

Figure 4-1. The ability of bystander RPE cells to re-pigment after wounding declines with age. (A) Experimental overview. A mixed population of control RPE (red) and iCaspase9-RPE (yellow) were plated at a 1:1 ratio. Control wells were plated at equal total cell density. RPE cells were aged for 1, 3, 6, or 12 months. The CID was added to both control wells and mixed control:iCaspase9 wells for 24 hours. Wells were rinsed to remove cell debris and fresh media was added. Surviving RPE cells recovered for two weeks. (B) Average pigmentation in the aged mixed control:iCaspase9 RPE cells before, one day after, and fourteen days after induction of apoptosis. Pigmentation reads are taken by measuring absorbance at 510 nm. Readings were taken with a 3x3 spot read grid using the Cytation5 and normalized to the maximum pigmentation value at six months. n=3, error bars are standard deviation, * indicates p-value ≤ 0.05.

AP20187) for 24 hours and cultures were allowed to recover for up to 14 days (Fig 4-1A). Because we could trigger apoptosis in only the iCaspase9-RPE, we were able to analyze potential age-related changes that occurred after injury and disruption to the monolayer.

Pigmentation is a defining feature of RPE cells. It plays a protective role by absorbing stray light to prevent photooxidation associated damage [31,32]. Changes in pigmentation are known to occur with age, with melanin content bring reduced 2.5-fold by the age of 90 [33].

To analyze whether any age-related changes in pigmentation could be observed in cultured RPE, we assessed the pigmentation levels of the cultures using optical absorbance. Pigmentation readings were acquired at three time points: before apoptotic induction, one day post-induction, and 14 days post-induction.

RPE cells in our culture conditions reached maximal pigmentation around 6-months, followed by a slight decrease in pigmentation over the following months (Fig 4-1B). Interestingly, there appears to be an age-dependent reduction in the ability of RPE to re-pigment following wounding. One day post wounding, a significant decrease in the pigmentation levels was seen in all samples containing iCaspase9-RPE, corresponding to the induction of RPE cell death. Young 1-month-old RPE recovered and surpassed original pigmentation levels within the two weeks recovery. Three- and six-month-old RPE also recovered after wounding, but to a lesser degree than younger RPE. In contrast, pigmentation did not recover at all in aged 12-month-old RPE within the same time limit (Fig 4-1B). This suggests age may be affecting the ability of RPE to re-pigment following injury.

Transcriptome analysis of aged and recovered RPE

To understand the effects of age and wound repair on RPE gene expression, we carried out transcriptome profiling and analysis of aged control and wound recovered RPE using AmpliSeq. Two weeks following CID supplementation wound recovered and control RPE cells were dissociated into single cells. To avoid potential artifacts due to the presence of residual iCaspase9-RPE, transcriptome profiles were generated using only surviving mCherry cells, which were isolated using florescence-activated cell sorting (FACS).

Multidimensional scaling (MDS) analysis revealed that aging cells in culture impacts the gene expression profiles of both control and wound recovered RPE. While both young 1-

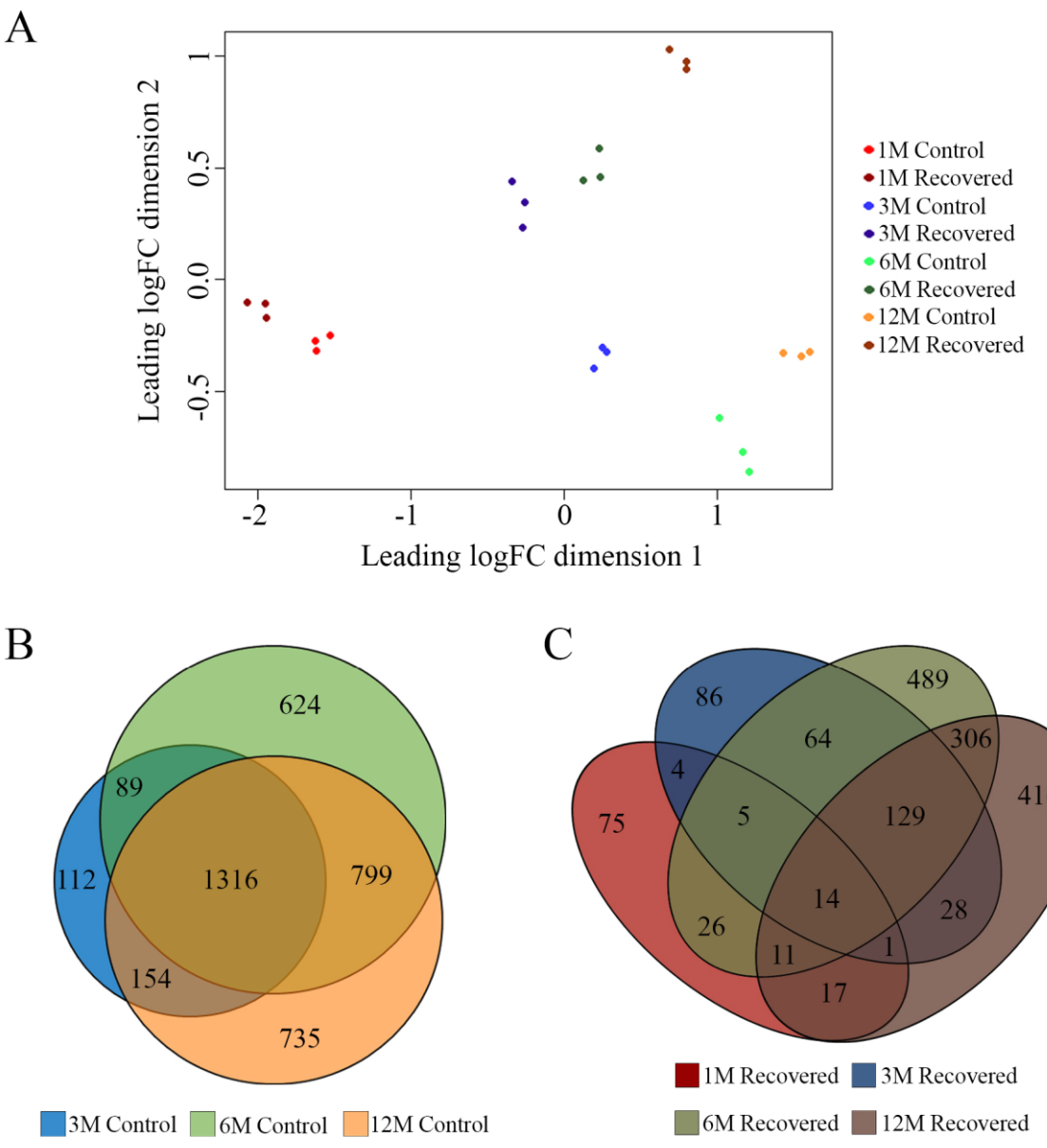

Figure 4-2. Age has a significant impact on transcriptome profile of RPE. (A) MDS plot of aged control and wound recovered RPE. Recovered cells were plated at a 1:1 ratio of control:iCaspase9 cells. Control and recovered cells were aged for 1, 3, 6, or 12 months before addition of CID to the media. Control and recovered cells recovered from CID for two weeks before sequencing. Each point is one replicate, three replicates per condition. (B) Venn diagram comparing control cells aged for 3 (blue), 6 (green), or 12 months (orange) to RPE cells aged for 1 month. A total of 3,843 genes were differentially expressed (FDR $\leq$ 0.05 and $\geq$ 2-fold change) compared to the 1-month aged control. (C) Venn diagram comparing the 1,671 differentially expressed genes in bystander RPE cells recovering from wounding compared to equally aged controls.

month old control and wound recovered RPE cluster tightly together, as the cells age, the distance between young and aged RPE increased sequentially (Fig 4-2A). In addition, increased aging time in culture also affected the ability of wound recovered RPE to return to an unwounded state, as seen by the increase in the distance between recovered cells and equally aged controls. These results suggest age plays a role in progressively modulating RPE gene expression, and the ability of RPE cells to promptly restore gene expression after wounding may decline with age.

Nearly 4,000 genes in total were differentially expressed (with $\geq$ 2-fold change and FDR $\leq$ 0.05) due to age alone (Fig 4-2B). After only three months in culture, over 1,600 genes were differentially expressed compared to the young 1-month control. The number of differentially expressed genes (DEGs) increased with age and by 12-months in culture, over 20% of the transcriptome (> 3,000 genes) were differentially expressed compared to the young 1-month old RPE.

Similarly, we saw an increase in the number of DEGs between wound recovered RPE compared to equally aged controls. Young cultures recovering from wounding were able to restore gene expression profiles quickly, with only 153 genes being differentially expressed after two weeks compared to the 1-month control (Fig 4-2C). The ability of RPE to restore the transcriptome profile appears to decline with age, as aged 1-year-old wound recovered RPE differentially expressed nearly 1,000 genes compared to aged controls. Fourteen DEGs were in common between all wound recovered cells, regardless of age. Some upregulated genes of interest include *CSMD2* and *BDKRB1*, both of which are associated with inflammation, *NPTX2*, which is associated with the genetic disease neuropathy, ataxia and

Retinitis Pigmentosa (NARP), and *ID1*, which may be involved in cell growth and senescence [34–38].

A total of 4,208 unique genes were differentially expressed due to aging or wound repair. Using k-means clustering, the DEGs were clustered into 8 clusters based on the

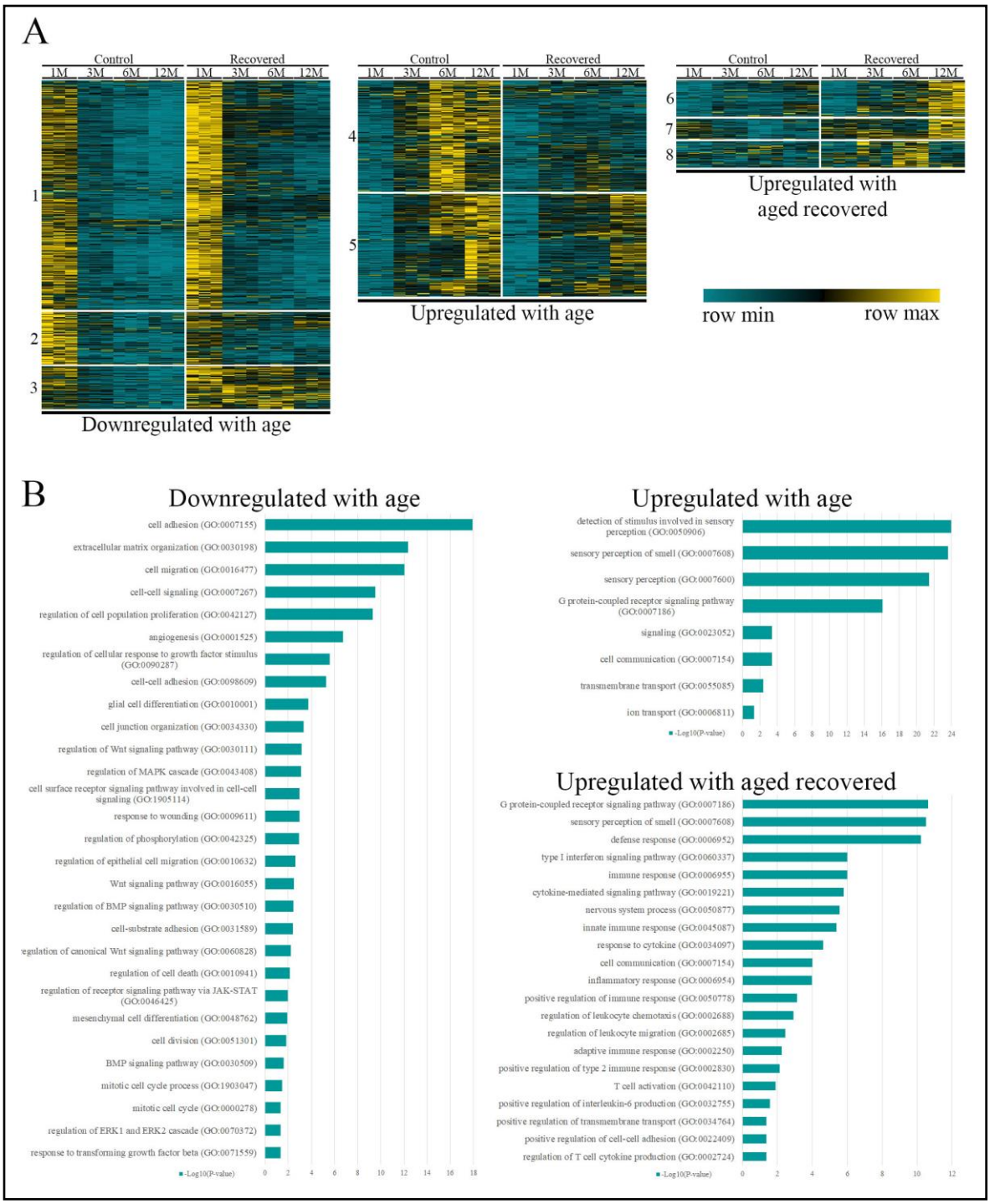

Figure 4-3. Heatmap reveals distinct age related and wound repair changes. (A) K-means clustering of 4,208 genes differentially expressed by aging or wound recovery. Genes were separated into eight distinct clusters using one minus Pearson correlation and 1,000 maximum iterations. Color scale indicates maximum (yellow) and minimum (blue) for each row. Clusters 1-3 downregulate expression with age, while clusters 4 and 5 upregulate expression with age. Clusters 6-8 show minimal change due to age alone but show upregulation in aged cells recovering from wounding. Data is TMM normalized and three replicates for each condition. (B) Enriched gene ontology terms in groups downregulated with age, upregulated with age, and genes upregulated in aged recovered RPE cells. Bar graph represents significance using $-\log_{10}$(P-value). P-valves are corrected for multiple testing using Benjamini-Hochberg procedure. Gene ontology analysis was completed using STRING using the 14,361 detected genes in our dataset as the background.

expression pattern (Fig 4-3A). The eight clusters were grouped into three distinct groups based on the heatmap expressions. Clusters 1-3 showed downregulation with age, clusters 4 and 5 showed upregulation with age, and clusters 6-8 are grouped together as they upregulate expression in aged RPE following wound repair (Fig 4-3A).

Aged RPE reduce expression of cell cycle and cell migration genes and increase expression of genes involved in sensory perception

We next employed gene ontology (GO) analysis to get a better understanding of the genes contained within these three groups (Fig 4-3B). The group with age-dependent reduced expression is enriched for genes involved in cell adhesion, cell migration, cell cycle, and pathways such as Wnt, BMP, JAK-STAT, and ERK1/ERK2 signaling. Genes required for proper cell division such as *CDK6*, *CDK14*, *CDC7* and *CDT1* all showed reduced levels in aged cells regardless of wounding (Fig 4-4B). This suggests that it may be harder for aged RPE cells to successfully proceed through the cell cycle.

In addition to decreased expression of cell cycle genes, genes involved in cell migration and extracellular matrix (ECM) organization also decreased with age. Some interesting genes within these GO groups include *ITGA5*, *CDH2* (N-cadherin), *FGF10*, and *VEGFC* (Fig 4-4D). The use of a neutralizing antibody against ITGA5 in ARPE-19 has been shown to cause a significant decrease in cell proliferation and migration, while FGF10 has been shown to

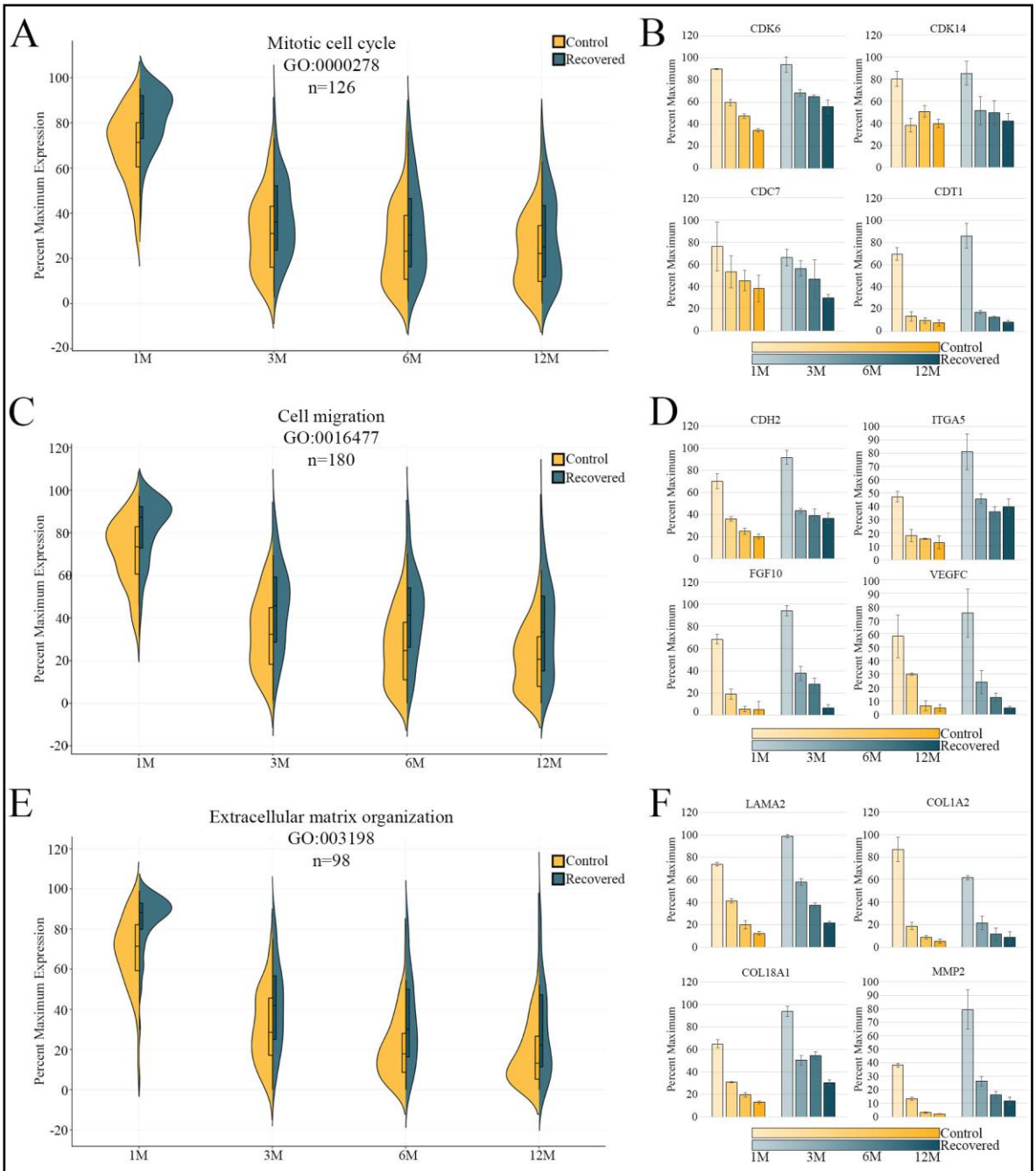

Figure 4-4. Genes involved in cell cycle, migration, wound healing, and extracellular matrix organization are downregulated with age. (A, C, D) Violin plots showing percent maximum expression of genes involved in mitotic cell cycle (GO:0000278), cell migration (GO:0016477) and extracellular matric organization (GO:003198) after wounding after 1, 3, 6, or 12 months (blue). RPE cultures without iCaspase9 cells served as controls (yellow). n = number of DEGs contained within the gene ontology (GO) group. (B, D, F) Percent of maximum expression levels of interesting DEGs contained within each GO group. Color scales indicate length of aging. n = 3, error bars indicate standard deviation.

promote EMT, migration, and can also increase N-cadherin expression, the dominant cadherin in RPE cell culture [39–41]. Among other functions, the ECM plays a role in regulating cell

migration, and disruption of the ECM may cause decreased migratory ability of the overlaying cells. RPE cells secrete proteins such as laminins, collagens, and matrix metalloproteinases (MMPs) to maintain the integrity of the underlying Brüch's membrane [42,43]. Here we saw a reduction in expression of genes involved in production of laminin components, collagen components, and *MMP2* with age (Fig 4-4F).

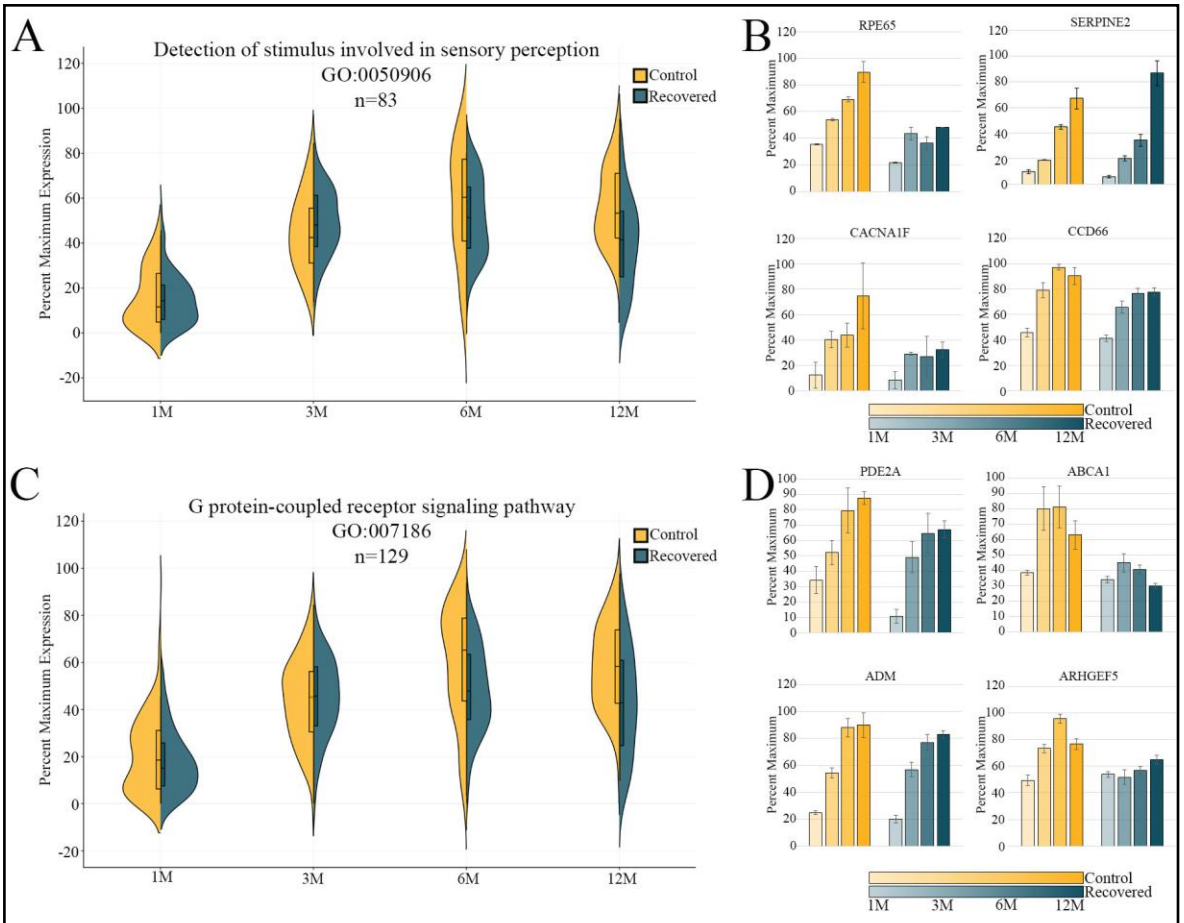

Figure 4-5. Expression of genes involved in detection of stimulus involved in sensory perception and G protein-coupled receptor signaling pathway upregulate with age. (A, C) Violin plots showing percent maximum expression of genes involved in detection of stimulus involved in sensory perception (GO:0050906) and G protein-coupled receptor signaling pathway (GO:0071865) after wounding after 1, 3, 6, or 12 months (blue). RPE cultures without iCaspase9 cells served as controls. n = number of DEGs contained within the GO group. (B, D) Percent of maximum expression levels of interesting DEGs contained within each GO group. Color scales indicate length of aging. n = 3, error bars indicate standard deviation.

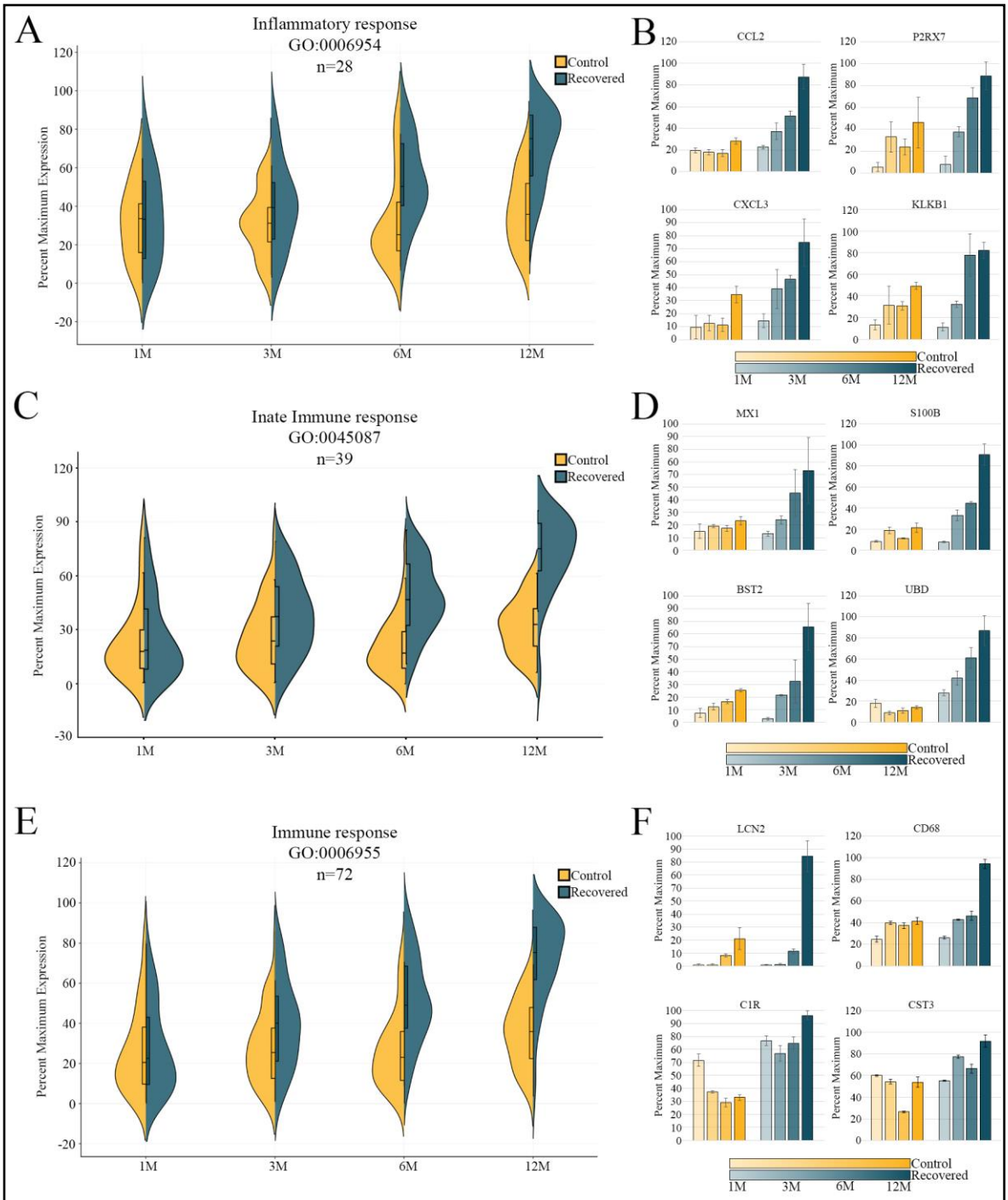

Figure 4-6. Upregulation in inflammatory response and immune response genes following wounding. (A, C) Violin plots showing percent maximum expression of genes involved in detection of stimulus involved in inflammatory response (GO:0006954), innate immune response (GO:0045087), and immune response (GO:0006955) after wounding after 1, 3, 6, or 12 months (blue). RPE cultures without iCaspase9 cells served as controls (yellow). n = number of DEGs contained within the GO group. (B, D) Expression of interesting genes from each GO group with expression normalized to percent of maximum. Color scales indicate length of aging. n = 3, error bars indicate standard deviation.

An enrichment in genes involved in sensory perception, G protein-coupled receptor

signaling, cell communication and transport were found to show an age-dependent upregulation (Fig 4-3B). Within the detection of stimulus involved in sensory perception (GO:0050906) GO group, a few genes are of particular interest including *RPE65*, *SERPINE2*, *CACNA1F* and *CCDC66*. RPE65, a key enzyme involved in the visual cycle, and CCDC66, a microtubule-associated protein localized to the primary cilium of RPE, are both critical proteins needed for RPE function. Disruption of either of these genes can lead to blinding disorders [44,45]. Protease nexin-1 (*PN-1*), the protein product of the SERPINE2 gene, is interesting due to its role as a potential cell survival factor and neuroprotectant [46]. *CACNA1F*, a calcium channel subunit, can cause night blindness when mutated [47]. Except for SERPINE2 at the 12M time-point, the expression of these genes declined following wound repair, suggesting a prolonged downregulation following repair in aged RPE. We saw a similar trend of genes involved in G protein-coupled receptor signaling (Fig 4-5C). Genes of interest include PDE2A, a regulator of secondary messengers such as cAMP and cGMP, the transmembrane transporter ABCA1, and the Rho GTPase ARHGEF5.

Aged RPE show increased inflammatory response following wounding

Perhaps most interesting is the enrichment of inflammatory genes in wound recovered aged RPE. This group showed a dramatic and progressive upregulation following wound repair in aged samples (Fig 4-6). This group is enriched in genes involved in inflammatory response, immune response, type I interferon signaling, cytokine-mediated signaling, leukocyte migration, and cell communication. CCL2 and CXCL3 are of interest due to their role in macrophage and neutrophil attraction respectively [48–50]. LCN2, a secreted

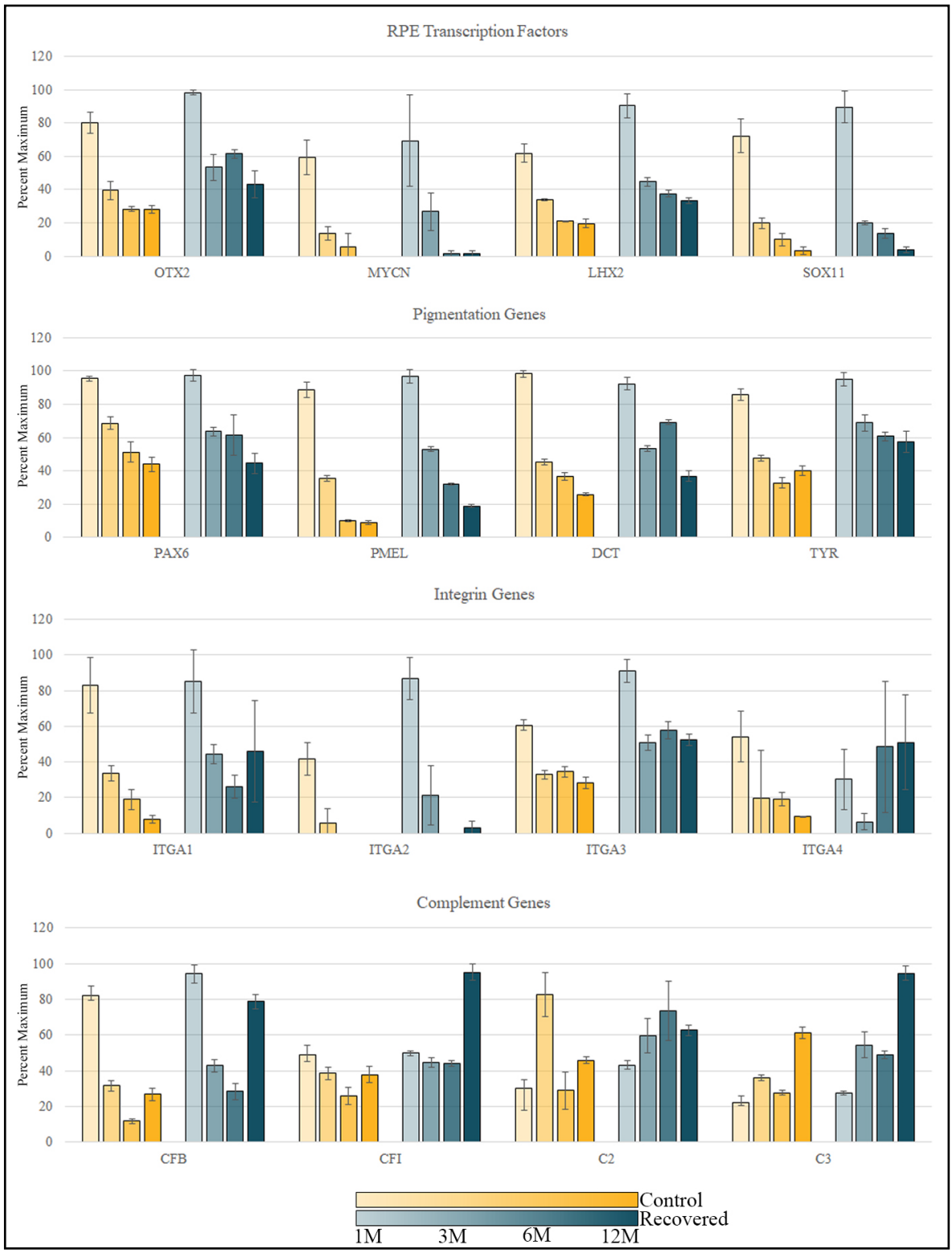

adipokine, has recently been implicated in ocular diseases including retinal degeneration [51,52]. KLKB1, a glycoprotein which can activate inflammation, and C2 and C3, key

Figure 4-7. Expression levels of select RPE transcription factors, pigmentation genes, integrin components, and complement genes. Expression levels normalized to maximum expression. Color scales indicate aging length before wounding (blue). Unwounded cells served as controls (yellow). n=3, error bars indicate standard deviation.

proteins in complement activation, remain upregulated two weeks post wound repair (Fig 4-7). Together this data suggests an interesting overactivation or prolonged activation of inflammatory and immune response following wound repair in aged RPE.

Reduction in expression of RPE transcription factors and pigmentation genes following aged wound repair

We then took a closer look at specific genes with key functions in RPE such as differentiation and pigmentation. Transcription factors such as OTX2, MYCN, LHX2, SOX11 are all known to be important in RPE differentiation and function [53–60]. Interestingly OTX2 and MYCN have been shown previously to extend the passage of RPE cells when exogenously expressed [61]. In our experiments, we saw an age-dependent reduction in expression, however, wounded aged RPE failed to upregulate expression to the same levels as young RPE cells (Fig 4-7). Genes involved in pigmentation also followed the same expression trend.

Age-dependent reduction in Brüch's membrane associated genes

Brüch's membrane is a five-layered acellular structure which requires secretion of proteins from the overlaying RPE and underlaying choriocapillaris for proper function. We investigated the expression of genes in aged RPE which have known functions in Brüch's membrane. We observed a reduction in expression of many collagen components, including collagen I, IV, and XVIII and laminin subunits in aged RPE (Fig 4-4, 4-8). RPE cells express integrins to adhere to the basement membrane and link extracellular matrix proteins to the

cytoskeleton [25,62]. Interestingly, we saw an age-dependent reduction in the expression of several integrin genes including integrins α1-4 (Fig 4-7). Although there is an increase in expression following wound repair, the expression levels do not reach expression levels of young RPE.

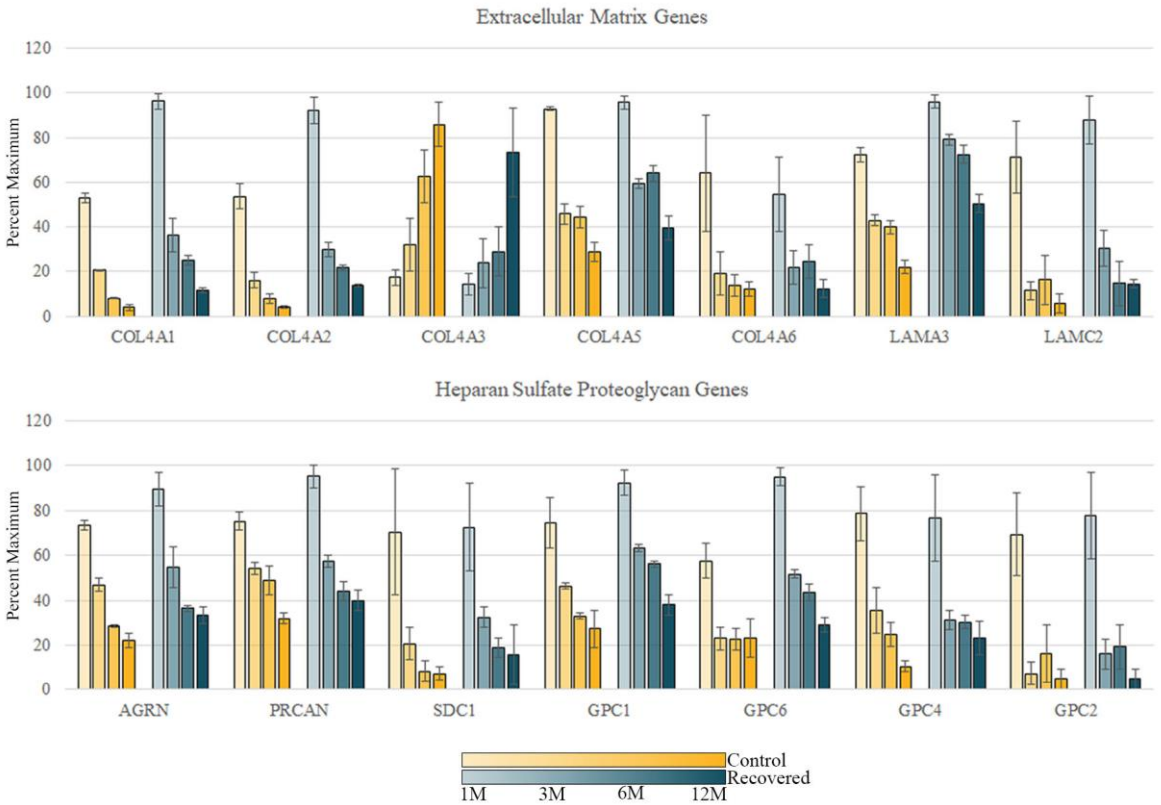

Figure 4-8. Expression of select Brüch's membrane associated genes. Expression levels normalized to maximum expression. Color scales indicate aging length before wounding (blue). Unwounded cells served as controls (yellow). n=3, error bars indicate standard deviation.

Several age-related changes occur in Brüch's membrane, including the reduction in HSPG proteins [63]. It is unknown if these changes occur from increased breakdown of HSPG core proteins or decreased synthesis. We found no age-related changes in the enzyme heparinase-1 involved in the breakdown of HSPGs. Interestingly, we found reduced expression of eight of the thirteen HSPG core proteins in aged RPE. These genes include agrin (*AGRN*), perlecan (*PRCAN*), collagen type XVIII (*COL18A1*), syndecan 1 (*SDC1*), and glypicans (*GPC*) 1, 2, 4, and 6 (Figs 4-4F, 4-8) [63–65]. This result suggests that the

reduction in HSPGs seen in aged Brüch's membrane could be the result of reduced synthesis of HSPG core proteins in aged RPE.

C. Discussion

In this study we investigated age-related changes in RPE monolayers. In addition, we investigated how aging affects the capacity of RPE to repair following wounding events. We report that the transcriptome of differentiated RPE monolayers is modulated after aging in culture. We observed a reduced ability of aged cultured RPE to promote the expression of cell migration, cell proliferation, and adhesion genes. Interestingly, in contrast to young RPE, aged RPE show increased expression of inflammatory genes following wounding. In addition, we found significant change in expression in genes involved in maintaining the integrity of Brüch's membrane.

Age is the number one factor contributing to the onset and progression of AMD. Several age-related changes are known to occur in the RPE cell monolayer as well as the underlaying Brüch's membrane. Pigmentation abnormalities, accumulation of lipofuscin, formation of drusen, shortening of microvilli, and increasing disorganization of the basal infoldings are just a few of the known age-related changes which occur in RPE [30,66]. Pigmentation is a defining feature of RPE cells and provides protection from damage associated with reactive radical species [8,67]. Previous research has reported reduced pigmentation levels in aged RPE, which may ultimately increase photo-oxidative stress in the cell [33]. In our study, we found reduced levels of pigmentation following wounding of the monolayer. As the surviving RPE proliferated to fill the wounded area, melanin granules are likely split between the cells, reducing the overall pigmentation of the culture. Young RPE

can increase pigmentation levels following wounding, however this ability is seemingly absent in aged RPE (Fig 4-1B).

Genes involved in melanogenesis such as *PAX6*, *PMEL*, *DCT*, and *TYR* all showed reduced levels of expression with increased age (Fig 4-7). Following wounding, the expression of *PMEL* and *TYR* increased slightly over aged controls, but never reached the levels of young RPE, suggesting aged RPE may have an overall reduced ability to re-pigment, or perhaps may take a longer time-period to re-pigment. Wnt signaling can stimulate melanogenesis through the expression of MITF and TYR [68]. Our GO analysis revealed an age-dependent reduction in the expression of genes involved in Wnt signaling along with genes involved in the regulation of Wnt signaling (Fig 4-3B).

Reduced RPE cell density, like pigmentation, has also been observed in aged eyes [69]. Like the age-dependent modulation of pigmentation genes, we also observed a dramatic reduction in expression of genes involved in cell proliferation and migration (Fig 4-4). The proliferative and migratory ability of RPE plays a key role in the success of RPE wound repair and both are required to properly repair lesions in RPE monolayers. Although results from our previous work show that the initiation of the cell cycle is not required to heal small lesions, it ultimately results in a reduction in cell density over the lesioned area (Fig 2-3) [70].

Advanced stages of AMD show a reduction in RPE cell density as seen by enlarged RPE cells near drusen [71]. Drusen are suggested to be sites of inflammation which can result in ultimate RPE dysfunction and death [1,72]. These enlarged cells could perhaps be the result of an age-dependent reduction in the ability to trigger cell proliferation to heal drusen associated cell death. Interestingly, aged RPE fail to increase expression of cell cycle

genes to levels of young RPE following injury (Fig 4-4A). The reduced levels of mitotic genes may suggest a reduction in the ability of aged RPE to proliferate in order to repair wounds in the monolayer, resulting in enlarged RPE following injury. As our data is only composed of a single time point, it is possible that aged RPE can upregulate expression of these genes to a level similar to young RPE at an earlier time point. Alternatively, it is possible that aged RPE do not need to express cell proliferation or cell cycle genes at the same levels as young RPE to have an adequate effect. Future work assessing the proliferative ability of aged RPE after injury by supplementing media with a modified nucleoside such as EdU (5-ethynyl-2'-doexyuridine), could help to confirm these findings.

Previous studies have shown the age of RPE influences the ability to adhere and migrate, where younger RPE attach and migrate faster than older RPE cells [73,74]. Attachment of RPE to the basement membrane is mediated by the basal expression of integrins, which link extracellular matrix proteins to the cytoskeleton [25,62]. Integrins, composed of an α and β subunit, play a key role in the ability of a cell to adhere to the basement membrane and thus affect the ability for the cell to proliferate and migrate, among other functions [25,75,76]. RPE have been shown to express a number of α subunits including integrin α1-6 which can combine with integrin β1 to bind to a number of matrix proteins [25]. The inhibition of integrin α1, for instance, significantly decreases the ability of RPE to bind to laminin, and inhibition of integrin α1 and 2 decreases the ability of RPE to bind to collagen [25]. Interestingly, blocking any α 1-6 integrins in RPE reduced the ability of RPE to bind to aged Brüch's membrane. In our study, we saw a significant age-dependent reduction in integrin α subunit expression of *ITGA1, ITGA2*, *ITGA3*, and *ITGA5*, suggesting a potential for reduced attachment ability of aged RPE to Brüch's membrane (Fig 4-7).

Brüch's membrane anchors both the RPE monolayer and the choriocapillaris and undergoes several age-dependent changes such as membrane thickening, decreased elasticity, reduced HSPGs, and calcification [63,77–79]. The top layer of Brüch's membrane, serving as the RPE cell basement membrane, is composed of fibronectin, collagen types I, III, IV, and XVIII, laminins 1, 5, 10, and 11 and HSPGs [23,80–82]. RPE in culture have been shown previously to preferentially bind to laminin 5, composed of α3β3γ2 chains [23]. Although *LAMB3* (β3 subunit) was expressed at very low levels in our experiments, the expression of *LAMA3* (α3 subunit) and *LAMC2* (γ2 subunit) were both significantly reduced the following aging. Collagen type VI has been shown to be a major form of collagen in the RPE basement membrane, composed of collagen IV subunits α1-5 [83,84]. Although we found an increase in expression in one collagen IV subunit, *COL4A3,* we also observed an age-dependent decrease in *COL4A1*, *COL4A2*, *COL4A5,* and *COL4A6* expression.

Collagen XVIII (COL18A1) has been shown to be important for retinal function, as knockout mice show increased accumulation of sub-RPE deposits, abnormal RPE, and ultimately suffer from retinal degeneration [85,86]. Interestingly, collagen XVIII has properties of both collagen and a proteoglycan. Proteolytic cleavage of COL18A1 results in the production of endostatin, a potent inhibitor of angiogenesis [87,88]. Reduced endostatin levels have been reported in the RPE basal lamina of Brüch's membrane in eyes with AMD [89]. Our experiments showed a significant reduction in the expression of *COL18A1* transcripts as a function of age (Fig4-4F). Decreased expression of collagen XVIII could result in an age-related increase in sub-RPE deposits. The combined decrease in expression of the angiogenesis inhibitor endostatin and age-dependent increase in calcification of

Brüch's membrane may make the membrane vulnerable to infiltration of new blood vessels associated with wet AMD.

The reduction in expression of collagen, laminin, and integrin components in RPE cells suggests aging plays a major role in the ability of RPE to maintain and adhere to matrix components, particularly those in Brüch's membrane. These findings may explain why aged RPE cell transplants into the fovea of AMD patients do not adhere well to Brüch's membrane [25,90]. Reduced expression of integrins may be compounding the ability of aged RPE to heal wounds, as integrins are required for both proliferation and migration. Degeneration of the BRB can result not only in the infiltration of blood vessels but also results in the breaching of immune privilege status in the eye, which can lead to infiltration of immune cells such as macrophages and dendritic cells [91].

Although activity of resident immune cells in the retina, such as microglia, are required for maintenance of retinal homeostasis, over activation or chronic activation of immune cells is associated with AMD pathogenesis [92]. The identification of dendritic cells and activated macrophages near sites of laser induced injury and drusen strengthens the hypothesis that chronic local inflammation plays a significant role in AMD pathogenesis [93,94]. The chemoattractant CCL2 has been implicated in AMD pathogenesis as it can recruit and activate mononuclear phagocytes such as macrophages and dendritic cells, causing RPE degeneration [95,96]. Interestingly, we saw a dramatic upregulation of *CCL2* expression following injury in aged RPE (Fig 4-6B). This implies that aging can cause an intrinsic change in RPE which results in overexpression or prolonged expression of inflammatory response genes. To distinguish between these outcomes, future work may assess CCL2 secretion at additional time points.

Sub-RPE deposits such as drusen have been identified as sites of complement activation and inflammation [1,93,97,98]. The complement system has been implicated in AMD pathology, supported by the finding of increased complement activity in AMD eyes and increased genetic risk in people with mutations in genes involved in the complement cascade [12,99,100]. Interestingly, it was shown that CFH binds to HSPGs in Brüch's membrane, acting as a negative complement regulator [101,102]. However, the age-dependent reduction in the amounts of HSPG in Brüch's membrane supports the idea of increased complement activity with age. In addition, the Y402H CFH mutant has been shown to have a reduced ability to bind HSPG resulting in higher complement activity in Brüch's membrane [102]. The reduction in expression of HSPG core protein genes in aged RPE aligns with the reduction in HSPGs seen in aged Brüch's membrane (Fig 4-8). We found no significant change in the expression of CFH in our system. However, reduced production of HSPG proteins from aged RPE may ultimately lead to increased complement activity, as seen in AMD.

In conclusion, we have developed a simple system to help analyze cellular aging in RPE. Our results suggest age has a significant impact on RPE gene expression and may affect the ability of RPE to repair wounds. Aged RPE have a decreased potential to express cell proliferation, migration, and ECM associated genes. This suggests a reduced ability of aged RPE to proliferate or migrate and a reduced ability to synthesize structural and adhesion proteins needed to maintain the attachment to and integrity of Brüch's membrane. In addition, we saw an increased or prolonged immunological response in aged RPE after wound repair. Levels of inflammatory and immune response genes remain significantly elevated after wound repair in aged RPE compared to young RPE. Many of these age-related

changes are reminiscent of phenotypes seen in AMD. This simple system may be used to deepen our understanding of age-related changes in RPE and how they may contribute to AMD pathology.

D. Materials and Methods

Retrovirus production and Cell Culture taken from Chapter III

Retrovirus production

GP2-293 (Takara) cells were seeded in T-150 flasks at $1x10^7$ and grown to 80-90% confluence. Flasks were transfected with 40.5 µg retroviral plasmid, pMSCV-F-del Casp9.IRES.GFP (iCaspase9, Addgene #15567) or mCherry control pMSCV-IRES-mCherry (control, Addgene #52114), 40.5 µg envelope plasmid (pVSVG, Takara), and 24.3 µg Xfect polymer (Takara) in 1.503 mL Xfect reaction buffer. After an overnight incubation, the transfection media was discarded, and fresh medium was added. The medium between 24-72 hours was collected, combined with 1/3 volume of Retro-X concentrator (Takara), and incubated at 4º for 1-2 days. To prepare concentrated virus, tubes were centrifuged for 45 minutes at 1500 g and 4ºC in a swinging bucket rotor. The supernatant was slowly removed and discarded. The pellet was gently resuspended in $1/100^{th}$ volume using phosphate-buffered saline (PBS). Concentrated viral particles were then aliquoted and stored at -80ºC until needed.

Cell culture

The primary human fetal line 110211, homozygous for the CFH 402H polymorphism, was obtained by a previously described method [3,103] and passaged until mesenchymal, roughly 3 passages. Cells were then reprogramed using ReproRNA^{TM}-OKSGM (STEMCELL

Technologies) according to the manufacturer's instructions. Once tight colonies became apparent, induced pluripotent stem cells (iPS) were purified using Anti-TRA-1-60 microbeads (Milteyni Biotec) according to methods of the manufacturer. iPS lines were checked for major karyotypic abnormalities using the hPSC Genetic Analysis Kit (STEMCELL Technologies) using manufacturer instructions before further experimental use. Successfully reprogrammed iPS lines were differentiated into RPE cells using our unpublished method. Pigmented RPE cells were frozen in mFreSR (STEMCELL Technologies) and stored in liquid nitrogen until needed.

Passage 1 RPE cells were thawed and plated at 10,000 cells/cm^2 in Matrigel (Corning) coated T-25 flasks in RPE medium containing 2 μM Thiazovivin (Fisher Scientific) and incubated overnight. Fresh medium containing retroviral particles (no more than 10% total volume) and 10 μg/mL polybrene (Millipore Sigma) was added the following morning and incubated overnight. The medium was discarded, and fresh medium was added and changed every 2-3 days for 28 days. Differentiated RPE were disassociated using 0.025% trypsin EDTA (Lonza) and sorted using fluorescence-activated cell sorting (FACS) to isolate pigmented RPE cells containing either iCaspase9/GFP or mCherry. Positive cells were plated at 20,000 cells/cm^2 on Matrigel coated dishes and allowed to recover for 2-3 days. Cells were then lifted using trypsin and frozen down in mFreSR (STEMCELL Technologies) for future use. Before use, cells were quickly resuspended in 10 mL medium and spun down at 500 g for 4 minutes to remove storage medium. Cells were plated at a total density of 80,000 cells/cm^2 in medium containing FGF and 1 μl/mL DMSO. After one week, FGF and DMSO were removed from the medium, and RPE were fed every 3-4 days.

Pigmentation was assessed using a 3 by 3 spot read grid at 510 nm using the Cytation5 (BioTek).

Wounding Assay

Cells were differentiated for 1, 3, 6, or 12 months before inducing apoptosis. Aged control and mixed iCaspase9/control RPE were given 25 nM CID (AP20187, B/B Homodimerizer, Clontech) in RPE medium to induce apoptosis in iCaspase9 RPE. After 24 hours, cells were rinsed with fresh RPE medium to remove dead cells. The medium was changed every 3-4 days. Fourteen days after wounding, cells were dissociated into single cells using trypsin (Lonza) followed by a 15 min treatment with Accumax (Innovative Cell Technologies). Cells were fixed for 15 minutes in 15 mL Falcon tubes on a rotator in 4 mL of 1% formaldehyde (Sigma Aldrich) in PBS. Cells were passed through 35 μm cell strainer (Falcon) and stored covered on ice. Cells with mCherry expression were collected using fluorescent activated cell sorting, spun down, and frozen at -80ºC overnight.

Transcriptomic analysis

RNA was extracted using the RecoverAll total nucleic acid isolation kit (Invitrogen) using manufacturer instructions. RNA was quantified using Qubit RNA HS assay kit (Invitrogen) using manufacturer instructions. A total of 10 ng of RNA was converted into cDNA using the SuperScript VILO cDNA Synthesis Kit (Invitrogen) using manufacturer instructions. The cDNA samples were barcoded using the IonCode 96-Well PCR Plate on the Ion Chef (Ion Torrent). Sequencing libraries were generated using the Ion AmpliSeq kit for Chef DL8 (Invitrogen) and the Ion AmpliSeq Transcriptome Human gene expression panel (Invitrogen) using 1 primer pool, 16 target amplification cycles, and 16 minutes anneal and

extension time on the Ion Chef. The final sequencing library was quantified using the Ion AmpliSeq Transcriptome Human Gene Expression Kit (Ion Torrent) using manufacturer instructions. Final sequencing libraries were diluted to a concentration of 50 pM and loaded onto Ion 520 Chip (Ion Torrent) using the Ion Chef system. The Chips were sequenced using the Ion S5 System (Ion Torrent) and sequences were aligned to the hg19 AmpliSeq Transcriptome ERCC v1 using the Torrent Suite Software. Analysis of expressed genes were performed in R using edgeR. Libraries were normalized using TMM-normalization factors (S4-1 Table). Genes with read counts per million ≥ 1 in three or more samples were selected for further statistical analysis using edgeR (S4-2 and 3 Tables).

Cluster analysis was carried out on TMM normalized expression on differentially expressed genes (DEGs; FDR≤ 0.05 and $-1 \geq \log_2 FC \geq 1$) due to aging (aged control vs. 1M control) or recovery (aged recovered vs. aged control) using Morpheus (https://software.broadinstitute.org/morpheus/). K-means clustering for 8 clusters using default parameters. Gene ontology (GO) analysis was conducted using STRING version 11.0 for each clustering group [104]. Violin plots were generated using Bio Vinci software version 3.0.9 (Bio Turing Inc., San Diego, CA, USA).

E. References

1. Anderson DH, Mullins RF, Hageman GS, Johnson L V. A role for local inflammation in the formation of drusen in the aging eye. Am J Ophthalmol. 2002;134: 411–431. doi:10.1016/S0002-9394(02)01624-0
2. Ghosh S, Shang P, Terasaki H, Stepicheva N, Hose S, Yazdankhah M, et al. A role for βA3/A1-crystallin in type 2 EMT of RPE cells occurring in dry age-related Macular degeneration. Investig Ophthalmol Vis Sci. 2018;59: AMD104–AMD113. doi:10.1167/iovs.18-24132
3. Radeke MJ, Radeke CM, Shih Y-H, Hu J, Bok D, Johnson L V., et al. Restoration of mesenchymal retinal pigmented epithelial cells by TGFβ pathway inhibitors: implications for age-related macular degeneration. Genome Med. 2015;7: 58. doi:10.1186/s13073-015-0183-x

4. Zanzottera EC, Ach T, Huisingh C, Messinger JD, Spaide RF, Curcio CA. Visualizing retinal pigment epithelium phenotypes in the transition to geographic atrophy in age-related macular degeneration. Retina. 2016;36 Suppl 1: S12–S25. doi:10.1097/IAE.0000000000001276

5. Guidry C, Medeiros NE, Curcio CA. Phenotypic variation of retinal pigment epithelium in age-related macular degeneration. Investig Ophthalmol Vis Sci. 2002;43: 267–273. Available: https://pubmed.ncbi.nlm.nih.gov/11773041/

6. Newman AM, Gallo NB, Hancox LS, Miller NJ, Radeke CM, Maloney MA, et al. Systems-level analysis of age-related macular degeneration reveals global biomarkers and phenotype-specific functional networks. Genome Med. 2012;4: 16. doi:10.1186/gm315

7. Volland S, Esteve-Rudd J, Hoo J, Yee C, Williams DS. A Comparison of Some Organizational Characteristics of the Mouse Central Retina and the Human Macula. Li T, editor. PLoS One. 2015;10: e0125631. doi:10.1371/journal.pone.0125631

8. Sparrow JR, Hicks D, Hamel CP. The retinal pigment epithelium in health and disease. Curr Mol Med. 2010;10: 802–23. Available: http://www.ncbi.nlm.nih.gov/pubmed/21091424

9. Young RW, Bok D. Participation of the retinal pigment epithelium in the rod outer segment renewal process. J Cell Biol. 1969;42: 392–403. doi:10.1083/jcb.42.2.392

10. Carido M, Zhu Y, Postel K, Benkner B, Cimalla P, Karl MO, et al. Characterization of a mouse model with complete RPE loss and its use for RPE cell transplantation. Invest Ophthalmol Vis Sci. 2014;55: 5431–5444. doi:10.1167/iovs.14-14325

11. Fritsche LG, Igl W, Bailey JNC, Grassmann F, Sengupta S, Bragg-Gresham JL, et al. A large genome-wide association study of age-related macular degeneration highlights contributions of rare and common variants. Nat Genet. 2016;48: 134–143. doi:10.1038/ng.3448

12. Fritsche LG, Chen W, Schu M, Yaspan BL, Yu Y, Thorleifsson G, et al. Seven new loci associated with age-related macular degeneration. Nat Genet. 2013;45: 433–9, 439e1-2. doi:10.1038/ng.2578

13. Lambert NG, ElShelmani H, Singh MK, Mansergh FC, Wride MA, Padilla M, et al. Risk factors and biomarkers of age-related macular degeneration. Prog Retin Eye Res. 2016;54: 64–102. doi:10.1016/j.preteyeres.2016.04.003

14. Pons M, Marin-Castaño ME. Nicotine increases the VEGF/PEDF ratio in retinal pigment Epithelium: A possible mechanism for CNV in passive smokers with AMD. Investig Ophthalmol Vis Sci. 2011;52: 3842–3853. doi:10.1167/iovs.10-6254

15. Evans JR, Fletcher AE, Wormald RPL. 28 000 Cases of age related macular degeneration causing visual loss in people aged 75 years and above in the United Kingdom may be attributable to smoking. Br J Ophthalmol. 2005;89: 550–553. doi:10.1136/bjo.2004.049726

16. Seddon JM, Cote J, Rosner B. Progression of Age-Related Macular Degeneration:

Association with Dietary Fat, Transunsaturated Fat, Nuts, and Fish Intake. Arch Ophthalmol. 2003;121: 1728–1737. doi:10.1001/archopht.121.12.1728

17. Klein R, Klein BEK, Linton KLP. Prevalence of Age-related Maculopathy: The Beaver Dam Eye Study. Ophthalmology. 1992;99: 933–943. doi:10.1016/S0161-6420(92)31871-8

18. Group AEDSR, Ardourel JE. Risk factors associated with age-related macular degeneration: A case-control study in the Age-Related Eye Disease Study: Age-Related Eye Disease Study report number 3. Ophthalmology. 2000;107: 2224–2232. doi:10.1016/S0161-6420(00)00409-7

19. Cunha-Vaz J, Bernardes R, Lobo C. Blood-retinal barrier. Eur J Ophthalmol. 2011;21: 3–9. doi:10.5301/EJO.2010.6049

20. Campbell M, Humphries P. The blood-retina barrier: tight junctions and barrier modulation - PubMed. Adv Exp Med Biol. 2012; 70–84. Available: https://pubmed.ncbi.nlm.nih.gov/23397619/

21. Cheng CY, editor. Advances in Experimental Medicine and Biology. 2013. Available: https://link.springer.com/bookseries/5584

22. Booij JC, Baas DC, Beisekeeva J, Gorgels TGMF, Bergen AAB. The dynamic nature of Bruch's membrane. Progress in Retinal and Eye Research. Prog Retin Eye Res; 2010. pp. 1–18. doi:10.1016/j.preteyeres.2009.08.003

23. Aisenbrey S, Zhang M, Bacher D, Yee J, Brunken WJ, Hunter DD. Retinal pigment epithelial cells synthesize laminins, including laminin 5, and adhere to them through α3- and α6-containing integrins. Investig Ophthalmol Vis Sci. 2006;47: 5537–5544. doi:10.1167/iovs.05-1590

24. Zarbin MA. Analysis of retinal pigment epithelium integrin expression and adhesion to aged submacular human Bruch's membrane. Transactions of the American Ophthalmological Society. American Ophthalmological Society; 2003. pp. 499–520. Available: /pmc/articles/PMC1359002/?report=abstract

25. Gullapalli VK, Sugino IK, Zarbin MA. Culture-induced increase in alpha integrin subunit expression in retinal pigment epithelium is important for improved resurfacing of aged human Bruch's membrane. Exp Eye Res. 2008;86: 189–200. doi:10.1016/j.exer.2007.10.009

26. van Soest SS, de Wit GMJ, Essing AHW, ten Brink JB, Kamphuis W, de Jong PTVM, et al. Comparison of human RPE gene expression in macula and periphery highlights potential topographic differences in Bruch's membrane. Mol Vis. 2007;13: 1608–1617. Available: https://europepmc.org/article/med/17893662

27. Hewitt AT, Nakazawa K, Newsome DA. Analysis of newly synthesized Bruch's membrane proteoglycans. | IOVS | ARVO Journals. Investig Ophthalmol Vis Sci. 1989;30: 478–486. Available: https://iovs.arvojournals.org/article.aspx?articleid=2160505

28. Curcio CA, Johnson M. Structure, Function, and Pathology of Bruch's Membrane.

Retina Fifth Edition. Elsevier Inc.; 2012. pp. 465–481. doi:10.1016/B978-1-4557-0737-9.00020-5

29. Spraul CW, Lang GE, Grossniklaus HE, Lang GK. Histologic and morphometric analysis of the choroid, Bruch's membrane, and retinal pigment epithelium in postmortem eyes with age-related macular degeneration and histologic examination of surgically excised choroidal neovascular membranes. Surv Ophthalmol. 1999;44: S10–S32. doi:10.1016/S0039-6257(99)00086-7

30. Gu X, Neric NJ, Crabb JS, Crabb JW, Bhattacharya SK, Rayborn ME, et al. Age-related changes in the retinal pigment epithelium (RPE). PLoS One. 2012;7: e38673. doi:10.1371/journal.pone.0038673

31. Sarna T. New trends in photobiology. Properties and function of the ocular melanin - a photobiophysical view. Journal of Photochemistry and Photobiology, B: Biology. Elsevier; 1992. pp. 215–258. doi:10.1016/1011-1344(92)85027-R

32. Kollias N, Sayre RM, Zeise L, Chedekel MR. New trends in photobiology. Photoprotection by melanin. Journal of Photochemistry and Photobiology, B: Biology. Elsevier; 1991. pp. 135–160. doi:10.1016/1011-1344(91)80147-A

33. Sarna T, Burke JM, Korytowski W, Rózanowska M, Skumatz CMB, Zaręba A, et al. Loss of melanin from human RPE with aging: Possible role of melanin photooxidation. Exp Eye Res. 2003;76: 89–98. doi:10.1016/S0014-4835(02)00247-6

34. Kraus DM, Elliott GS, Chute H, Horan T, Pfenninger KH, Sanford SD, et al. CSMD1 Is a Novel Multiple Domain Complement-Regulatory Protein Highly Expressed in the Central Nervous System and Epithelial Tissues. J Immunol. 2006;176: 4419–4430. doi:10.4049/jimmunol.176.7.4419

35. Matus CE, Ehrenfeld P, Pavicic F, González CB, Concha M, Bhoola KD, et al. Activation of the human keratinocyte B1 bradykinin receptor induces expression and secretion of metalloproteases 2 and 9 by transactivation of epidermal growth factor receptor. Exp Dermatol. 2016;25: 694–700. doi:10.1111/exd.13038

36. Othman R, Berbari S, Vaucher E, Couture R. Differential expression of kinin receptors in human wet and dry age-related macular degeneration retinae. Pharmaceuticals. 2020;13: 1–20. doi:10.3390/ph13060130

37. Wang S, Liu Y, Liu Y, Li C, Wan Q, Yang L, et al. Reversed Senescence of Retinal Pigment Epithelial Cell by Coculture With Embryonic Stem Cell via the TGFβ and PI3K Pathways. Front Cell Dev Biol. 2020;8: 588050. doi:10.3389/fcell.2020.588050

38. Zebedee Z, Hara E. Id proteins in cell cycle control and cellular senescence. Oncogene. 2001;20: 8317–8325. doi:10.1038/sj.onc.1205092

39. Kaida M, Cao F, Skumatz CMB, Irving PE, Burke JM. Time at confluence for human RPE cells: Effects on the adherens junction and in vitro wound closure. Investigative ophthalmology and visual science Sep, 2000. Available: https://pubmed.ncbi.nlm.nih.gov/10967086/

40. Abolhassani A, Riazi GH, Azizi E, Amanpour S, Muhammadnejad S, Haddadi M, et

al. FGF10: Type III epithelial mesenchymal transition and invasion in breast cancer cell lines. J Cancer. 2014;5: 537–547. doi:10.7150/jca.7797

41. Chen Z, Chen C, Gong W, Li J, Xing Y. Integrin-α₅ Mediates Epidermal Growth Factor-Induced Retinal Pigment Epithelial Cell Proliferation and Migration. Pathobiology. 2010;77: 88–95. doi:10.1159/000278290

42. Nita M, Strzałka-Mrozik B, Grzybowski A, Mazurek U, Romaniuk W. Age-related macular degeneration and changes in the extracellular matrix. Medical Science Monitor. International Scientific Literature Inc.; 2014. pp. 1003–1016. doi:10.12659/MSM.889887

43. García-Onrubia L, Valentín-Bravo FJ, Coco-Martin RM, González-Sarmiento R, Pastor JC, Usategui-Martín R, et al. Matrix metalloproteinases in age-related macular degeneration (Amd). International Journal of Molecular Sciences. MDPI AG; 2020. pp. 1–32. doi:10.3390/ijms21165934

44. Cai X, Conley SM, Naash MI. RPE65: Role in the visual cycle, human retinal disease, and gene therapy. Ophthalmic Genetics. NIH Public Access; 2009. pp. 57–62. doi:10.1080/13816810802626399

45. Conkar D, Culfa E, Odabasi E, Rauniyar N, Yates JR, Firat-Karalar EN. The centriolar satellite protein CCDC66 interacts with CEP290 and functions in cilium formation and trafficking. J Cell Sci. 2017;130: 1450–1462. doi:10.1242/jcs.196832

46. Winokur PN, Subramanian P, Bullock JL, Arocas V, Becerra SP. Comparison of two neurotrophic serpins reveals a small fragment with cell survival activity. Mol Vis. 2017;23: 372–384. Available: http://www.molvis.org/molvis/v23/372

47. Mansergh F, Orton NC, Vessey JP, Lalonde MR, Stell WK, Tremblay F, et al. Mutation of the calcium channel gene Cacna1f disrupts calcium signaling, synaptic transmission and cellular organization in mouse retina. Hum Mol Genet. 2005;14: 3035–3046. doi:10.1093/hmg/ddi336

48. Raoul W, Auvynet C, Camelo S, Guillonneau X, Feumi C, Combadière C, et al. CCL2/CCR2 and CX3CL1/CX3CR1 chemokine axes and their possible involvement in age-related macular degeneration. Journal of Neuroinflammation BioMed Central; Dec 2, 2010 p. 87. doi:10.1186/1742-2094-7-87

49. Ambati J, Anand A, Fernandez S, Sakurai E, Lynn BC, Kuziel WA, et al. An animal model of age-related macular degeneration in senescent Ccl-2- or Ccr-2-deficient mice. Nat Med. 2003;9: 1390–1397. doi:10.1038/nm950

50. Ghosh S, Padmanabhan A, Vaidya T, Watson AM, Bhutto IA, Hose S, et al. Neutrophils homing into the retina trigger pathology in early age-related macular degeneration. Commun Biol. 2019;2: 1–17. doi:10.1038/s42003-019-0588-y

51. Ghosh S, Stepicheva N, Yazdankhah M, Shang P, Watson AM, Hose S, et al. The role of lipocalin-2 in age-related macular degeneration (AMD). Cellular and Molecular Life Sciences. Springer; 2020. pp. 835–851. doi:10.1007/s00018-019-03423-8

52. Parmar T, Parmar VM, Arai E, Sahu B, Perusek L, Maeda A. Acute stress responses

are early molecular events of retinal degeneration in Abca4-/-Rdh8-/- mice after light exposure. Investig Ophthalmol Vis Sci. 2016;57: 3257–3267. doi:10.1167/iovs.15-18993

53. Martinez-Morales JR, Signore M, Acampora D, Simeone A, Bovolenta P. Otx genes are required for tissue specification in the developing eye. Development. 2001;128.

54. Béby F, Housset M, Fossat N, Le Greneur C, Flamant F, Godement P, et al. Otx2 gene deletion in adult mouse retina induces rapid RPE dystrophy and slow photoreceptor degeneration. PLoS One. 2010;5: 1–8. doi:10.1371/journal.pone.0011673

55. Housset M, Samuel A, Ettaiche M, Bemelmans A, Béby F, Billon N, et al. Loss of Otx2 in the adult retina disrupts retinal pigment epithelium function, causing photoreceptor degeneration. J Neurosci. 2013;33: 9890–9904. doi:10.1523/JNEUROSCI.1099-13.2013

56. Martins RAP, Zindy F, Donovan S, Zhang J, Pounds S, Wey A, et al. N-myc coordinates retinal growth with eye size during mouse development. Genes Dev. 2008;22: 179–193. doi:10.1101/gad.1608008

57. Ashery-Padan R. Roles of LIM homeodomain 2 (Lhx2) in the differentiation of mammalian retinal pigmented epithelium. Acta Ophthalmol. 2019;97: j.1755-3768.2019.8119. doi:10.1111/j.1755-3768.2019.8119

58. Masuda T, Wahlin K, Wan J, Hu J, Maruotti J, Yang X, et al. Transcription factor sox9 plays a key role in the regulation of visual cycle gene expression in the retinal pigment epithelium. J Biol Chem. 2014;289: 12908–12921. doi:10.1074/jbc.M114.556738

59. Pillai-Kastoori L, Wen W, Wilson SG, Strachan E, Lo-Castro A, Fichera M, et al. Sox11 Is Required to Maintain Proper Levels of Hedgehog Signaling during Vertebrate Ocular Morphogenesis. Barsh GS, editor. PLoS Genet. 2014;10: e1004491. doi:10.1371/journal.pgen.1004491

60. Choudhary P, Booth H, Gutteridge A, Surmacz B, Louca I, Steer J, et al. Directing Differentiation of Pluripotent Stem Cells Toward Retinal Pigment Epithelium Lineage. Stem Cells Transl Med. 2017;6: 490–501. doi:10.5966/sctm.2016-0088

61. Shih YH, Radeke MJ, Radeke CM, Coffey PJ. Restoration of mesenchymal RPE by transcription factor-mediated reprogramming. Investig Ophthalmol Vis Sci. 2017;58: 430–441. doi:10.1167/iovs.16-20018

62. Van der Flier A, Sonnenberg A. Function and interactions of integrins. Cell Tissue Res. 2001;305: 285–298. doi:10.1007/s004410100417

63. Keenan TDL, Pickford CE, Holley RJ, Clark SJ, Lin W, Dowsey AW, et al. Age-dependent changes in heparan sulfate in human Bruch's membrane: Implications for age-related macular degeneration. Investig Ophthalmol Vis Sci. 2014;55: 5370–5379. doi:10.1167/iovs.14-14126

64. Keenan TDL, Clark SJ, Unwin RD, Ridge LA, Day AJ, Bishop PN. Mapping the differential distribution of proteoglycan core proteins in the adult human retina,

choroid, and sclera. Investig Ophthalmol Vis Sci. 2012;53: 7528–7538. doi:10.1167/iovs.12-10797

65. Iozzo R V. Series Introduction: Heparan sulfate proteoglycans: intricate molecules with intriguing functions. J Clin Invest. 2001;108: 165–167. doi:10.1172/jci13560

66. Bonilha VL. Age and disease-related structural changes in the retinal pigment epithelium. Clin Ophthalmol. 2008;2: 413–424. doi:10.2147/opth.s2151

67. Simon JD, Hong L, Peles DN. Insights into melanosomes and melanin from some interesting spatial and temporal properties. J Phys Chem B. 2008;112: 13201–13217. doi:10.1021/jp804248h

68. Molagoda IMN, Karunarathne WAHM, Park SR, Choi YH, Park EK, Jin CY, et al. GSK-3β-targeting fisetin promotes melanogenesis in B16F10 melanoma cells and zebrafish larvae through β-catenin activation. Int J Mol Sci. 2020;21: 312. doi:10.3390/ijms21010312

69. Bhatia SK, Rashid A, Chrenek MA, Zhang Q, Bruce BB, Klein M, et al. Analysis of RPE morphometry in human eyes. Mol Vis. 2016;22: 898–916. Available: http://www.ncbi.nlm.nih.gov/pubmed/27555739

70. Bailey-Steinitz LJ, Shih Y-H, Radeke MJ, Coffey PJ. An in vitro model of chronic wounding and its implication for age-related macular degeneration. Lewin AS, editor. PLoS One. 2020;15: e0236298. doi:10.1371/journal.pone.0236298

71. Al-Hussaini H, Schneiders M, Lundh P, Jeffery G. Drusen are associated with local and distant disruptions to human retinal pigment epithelium cells. Exp Eye Res. 2009;88: 610–612. doi:10.1016/j.exer.2008.09.021

72. Johnson L V, Forest DL, Banna CD, Radeke CM, Maloney MA, Hu J, et al. Cell culture model that mimics drusen formation and triggers complement activation associated with age-related macular degeneration. Proc Natl Acad Sci U S A. 2011;108: 18277–82. doi:10.1073/pnas.1109703108

73. Abu Khamidakh AE, Rodriguez-Martinez A, Kaarniranta K, Kallioniemi A, Skottman H, Hyttinen J, et al. Wound healing of human embryonic stem cell-derived retinal pigment epithelial cells is affected by maturation stage. Biomed Eng Online. 2018;17: 102. doi:10.1186/s12938-018-0535-z

74. Schwartz SD, Hubschman JP, Heilwell G, Franco-Cardenas V, Pan CK, Ostrick RM, et al. Embryonic stem cell trials for macular degeneration: A preliminary report. Lancet. 2012;379: 713–720. doi:10.1016/S0140-6736(12)60028-2

75. Zamir E, Geiger B. Molecular complexity and dynamics of cell-matrix adhesions | Journal of Cell Science. J Cell Sci. 2001;114: 3583–3590. Available: https://jcs.biologists.org/content/114/20/3583.short

76. Hynes RO. Integrins: Bidirectional, allosteric signaling machines. Cell. 2002;110: 673–687. doi:10.1016/S0092-8674(02)00971-6

77. Chirco KR, Sohn EH, Stone EM, Tucker BA, Mullins RF. Structural and molecular

changes in the aging choroid: Implications for age-related macular degeneration. Eye (Basingstoke). Nature Publishing Group; 2017. pp. 10–25. doi:10.1038/eye.2016.216

78. Fernandez-Bueno I, Rodriguez de la Rua E, Hileeto D, Parrado ML, Regueiro-Purriños M, Sala-Puigdollers A, et al. Histology and immunochemistry evaluation of autologous translocation of retinal pigment epithelium-choroid graft in porcine eyes. Acta Ophthalmol. 2013;91: e125-32. doi:10.1111/aos.12001

79. Zarbin MA. Current Concepts in the Pathogenesis of Age-Related Macular Degeneration. Arch Ophthalmol. 2004;122: 598. doi:10.1001/archopht.122.4.598

80. Afshari FT, Fawcett JW. Improving RPE adhesion to Bruch's membrane. Eye. Nature Publishing Group; 2009. pp. 1890–1893. doi:10.1038/eye.2008.411

81. Turksen K, Aubin JE, Sodek J, Kalnins VI. Localization of laminin, type IV collagen, fibronectin, and heparan sulfate proteoglycan in chick retinal pigment epithelium basement membrane during embryonic development. J Histochem Cytochem. 1985;33: 665–671. doi:10.1177/33.7.3159787

82. Campochiaro PA, Jerdon JA, Glaser BM. The extracellular matrix of human retinal pigment epithelial cells in vivo and its synthesis in vitro. | IOVS | ARVO Journals. Investig Ophthalmol Vis Sci. 1986;27: 1615–1621. Available: https://iovs.arvojournals.org/article.aspx?articleid=2177434

83. Chen L, Miyamura N, Ninomiya Y, Handa JT. Distribution of the collagen IV isoforms in human Bruch's membrane. Br J Ophthalmol. 2003;87: 212–215. doi:10.1136/bjo.87.2.212

84. Sado Y, Kagawa M, Naito I, Ueki Y, Seki T, Momota R, et al. Organization and Expression of Basement Membrane Collagen IV Genes and Their Roles in Human Disorders. J Biochem. 1998;123: 767–776. doi:10.1093/oxfordjournals.jbchem.a022003

85. Marneros AG, Keene DR, Hansen U, Fukai N, Moulton K, Goletz PL, et al. Collagen XVIII/endostatin is essential for vision and retinal pigment epithelial function. EMBO J. 2004;23: 89–99. doi:10.1038/sj.emboj.7600014

86. Fukai N, Eklund L, Marneros AG, Oh SP, Keene DR, Tamarkin L, et al. Lack of collagen XVIII/endostatin results in eye abnormalities. EMBO J. 2002;21: 1535–1544. doi:10.1093/emboj/21.7.1535

87. O'Reilly MS, Boehm T, Shing Y, Fukai N, Vasios G, Lane WS, et al. Endostatin: An endogenous inhibitor of angiogenesis and tumor growth. Cell. 1997;88: 277–285. doi:10.1016/S0092-8674(00)81848-6

88. Marneros AG, Olsen BR. Physiological role of collagen XVIII and endostatin. FASEB J. 2005;19: 716–728. doi:10.1096/fj.04-2134rev

89. Bhutto IA, Kim SY, McLeod DS, Merges C, Fukai N, Olsen BR, et al. Localization of collagen XVIII and the endostatin portion of collagen XVIII in aged human control eyes and eyes with age-related macular degeneration. Investig Ophthalmol Vis Sci. 2004;45: 1544–1552. doi:10.1167/iovs.03-0862

90. Del Priore L V., Kaplan HJ, Tezel TH, Hayashi N, Berger AS, Green WR. Retinal pigment epithelial cell transplantation after subfoveal membranectomy in age-related macular degeneration: Clinicopathologic correlation. Am J Ophthalmol. 2001;131: 472–480. doi:10.1016/S0002-9394(00)00850-3

91. Ambati J, Atkinson JP, Gelfand BD. Immunology of age-related macular degeneration. Nature Reviews Immunology. NIH Public Access; 2013. pp. 438–451. doi:10.1038/nri3459

92. Rathnasamy G, Foulds WS, Ling E-A, Kaur C. Retinal microglia – A key player in healthy and diseased retina. Prog Neurobiol. 2019;173: 18–40. doi:10.1016/J.PNEUROBIO.2018.05.006

93. Hageman GS, Luthert PJ, Victor Chong NHH, Johnson L V., Anderson DH, Mullins RF. An Integrated Hypothesis That Considers Drusen as Biomarkers of Immune-Mediated Processes at the RPE-Bruch's Membrane Interface in Aging and Age-Related Macular Degeneration. Prog Retin Eye Res. 2001;20: 705–732. doi:10.1016/S1350-9462(01)00010-6

94. Eter N, Engel DR, Meyer L, Helb H-M, Roth F, Maurer J, et al. In Vivo Visualization of Dendritic Cells, Macrophages, and Microglial Cells Responding to Laser-Induced Damage in the Fundus of the Eye. Investig Opthalmology Vis Sci. 2008;49: 3649. doi:10.1167/iovs.07-1322

95. Kutty RK, Samuel W, Boyce K, Cherukuri A, Duncan T, Jaworski C, et al. Proinflammatory cytokines decrease the expression of genes critical for RPE function. Mol Vis. 2016;22: 1156–1168. Available: http://www.ncbi.nlm.nih.gov/pubmed/27733811

96. Yang Y, Liu F, Tang M, Yuan M, Hu A, Zhan Z, et al. Macrophage polarization in experimental and clinical choroidal neovascularization. Sci Rep. 2016;6: 30933. doi:10.1038/srep30933

97. Crabb JW, Miyagi M, Gu X, Shadrach K, West KA, Sakaguchi H, et al. Drusen proteome analysis: an approach to the etiology of age-related macular degeneration. Proc Natl Acad Sci U S A. 2002;99: 14682–7. doi:10.1073/pnas.222551899

98. Johnson L V., Ozaki S, Staples MK, Erickson PA, Anderson DH. A potential role for immune complex pathogenesis in drusen formation. Exp Eye Res. 2000;70: 441–449. doi:10.1006/exer.1999.0798

99. Raychaudhuri S, Iartchouk O, Chin K, Tan PL, Tai AK, Ripke S, et al. A rare penetrant mutation in CFH confers high risk of age-related macular degeneration. Nat Genet. 2011;43: 1232–1236. doi:10.1038/ng.976

100. Seddon JM, Yu Y, Miller EC, Reynolds R, Tan PL, Gowrisankar S, et al. Rare variants in CFI, C3 and C9 are associated with high risk of advanced age-related macular degeneration. Nat Genet. 2013;45: 1366–1373. doi:10.1038/ng.2741

101. Clark SJ, Ridge LA, Herbert AP, Hakobyan S, Mulloy B, Lennon R, et al. Tissue-Specific Host Recognition by Complement Factor H Is Mediated by Differential

Activities of Its Glycosaminoglycan-Binding Regions. J Immunol. 2013;190: 2049–2057. doi:10.4049/jimmunol.1201751

102. Clark SJ, Perveen R, Hakobyan S, Morgan BP, Sim RB, Bishop PN, et al. Impaired binding of the age-related macular degeneration-associated complement factor H 402H allotype to Bruch's membrane in human retina. J Biol Chem. 2010;285: 30192–30202. doi:10.1074/jbc.M110.103986

103. Hu J, Bok D. A cell culture medium that supports the differentiation of human retinal pigment epithelium into functionally polarized monolayers. Mol Vis. 2001;7: 14–9. Available: http://www.ncbi.nlm.nih.gov/pubmed/11182021

104. Szklarczyk D, Gable AL, Lyon D, Junge A, Wyder S, Huerta-Cepas J, et al. STRING v11: Protein-protein association networks with increased coverage, supporting functional discovery in genome-wide experimental datasets. Nucleic Acids Res. 2019;47: D607–D613. doi:10.1093/nar/gky1131

Chapter V: Conclusion

Age-related macular degeneration is a devasting disease affecting approximately 170 million people worldwide. Advanced stages of the disease cause a loss of central vision which can progress into blindness. Loss of vision takes an enormous toll on a person's quality of life and has a significant economic impact. Early signs of the disease are easily identified, but few treatments exist to delay the advancement of the disease. Although many risk factors have been identified, the root cause of AMD is not well understood, and it has been challenging to develop models which recapitulate the disease models *in vitro* and *in vivo*, thus hindering the ability to develop drug treatments.

Here we presented two novel wounding platforms that have similar features to advanced AMD. Chronically wounded RPE using EICS resulted in enlarged cell size and multinucleation. However, RPE cells in a chronically wounded state in this model system were always able to repair the lesion, a stark difference compared to the atrophic areas seen in geographic atrophy. To approach this, we then developed a second platform in which we could induce a large, centralized wound to a differentiated RPE monolayer. RPE recovering from a macula-sized wound could not repair the lesion and resulted in areas of RPE atrophy, loss of RPE morphology and loss of pigmentation. Treatment with the ROCK inhibitor Y-27632 greatly improved the ability of RPE to repair.

A major strength of both platforms is that they can be easily scaled up to allow for the screening of dozens of therapeutics. The use of fluorescently labeled iPS derived human RPE provides an unlimited source of cells for experimentation and tracking. The identification of a therapeutic which can improve the ability of RPE to repair could offer an exciting new treatment for patients with AMD. Compounds able to increase the cell density over the

lesioned area, increase the speed at which tight junctions are re-established, or decrease the immune response of chronically wounded RPE using ECIS are of interest. Compounds able to increase cell density and improve RPE function, such as phagocytosis, over the macula-sized wound could also be of potential interest. Our work exploring the effects of aging on RPE transcriptome profiling, highlights the importance of considering age-dependent effects in assay development. Future experiments using these models to study RPE wound repair after aging will be of interest.

Unlike the models presented here, which utilize a single wound size throughout the experiment, gradual enlargement of areas of atrophy is seen in advanced AMD. It may be of interest to develop a system in which the wound size can be enlarged throughout the duration of the experiment. The KillerRed construct, for instance, can trigger cell death via reactive oxygen species when exposed to orange or green light. It may be possible to induce a chronic wounding state in which the wound size can be gradually enlarged over time by enlarging the area exposed to light. Future work developing such an assay could allow for an even more pathologically relevant wound repair system which could be used for therapeutic screens.

Appendix

A. Supplemental Figures

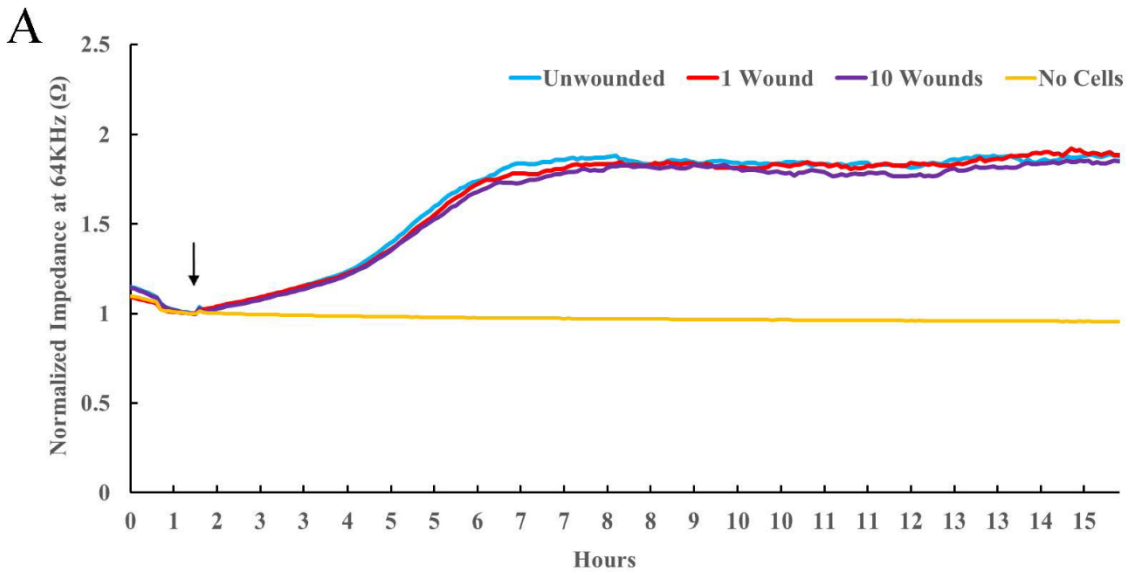

S2-1 Fig. Wounding ECIS electrodes does not affect human fetal RPE attachment. (A) ECIS 8W10E cultureware was coated with laminin and wells were wounded once or ten times. Immediately following last wound treatment, human fetal RPE cells were plated (arrow) at 80,000/cm^2 to assess ability of RPE to attach to wounded electrodes. Impedance at 64,000Hz was normalized to the 1.4-hour time point, when cells were plated. Unwounded wells and a single empty well were used as controls. No significant difference in impedance between unwounded, and 1 or 10 wounds was seen, suggesting no change in the ability of RPE to attach to electrodes post wounding (n=4).

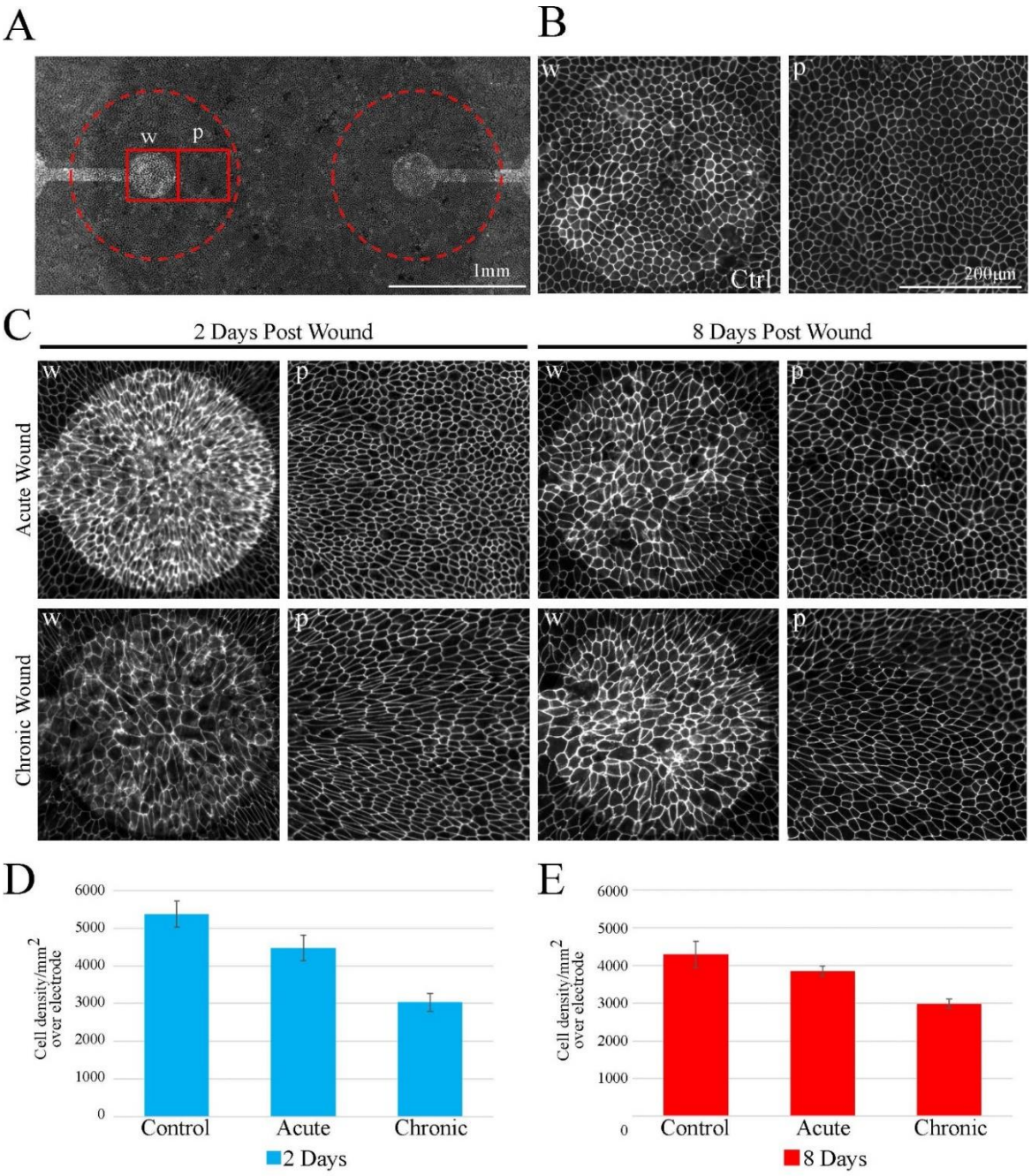

S2-2 Fig. Change in RPE cell size and morphology with acute or chronic wounding. (A) Single 96-well whole mount using ZO-1 antibody to visualize cell morphology. Reflections of gold electrodes are visible. Red dotted circles indicate punch size used for RNA extraction. Solid red boxes indicate locations over the wound (w) or periphery (p). Scale bar is 1 mm (B) Morphology of unwounded RPE control cells over the electrode (w) or periphery. Scale bar is 200 µM. (C) Morphology of RPE cells over the wounded area (w) or periphery (p) at 2-days or 8-days post wounding in acute or chronic wounding conditions. Images are to the same scale as (B). (D) Cell density per mm^2, 2-days after acute or chronic wounding. Data was taken from Fig2 C and normalized to the area over the electrode. (E) Cell density per mm^2, 8-days after acute or chronic wounding. Data was taken from Fig2 C and normalized to the area over the electrode.

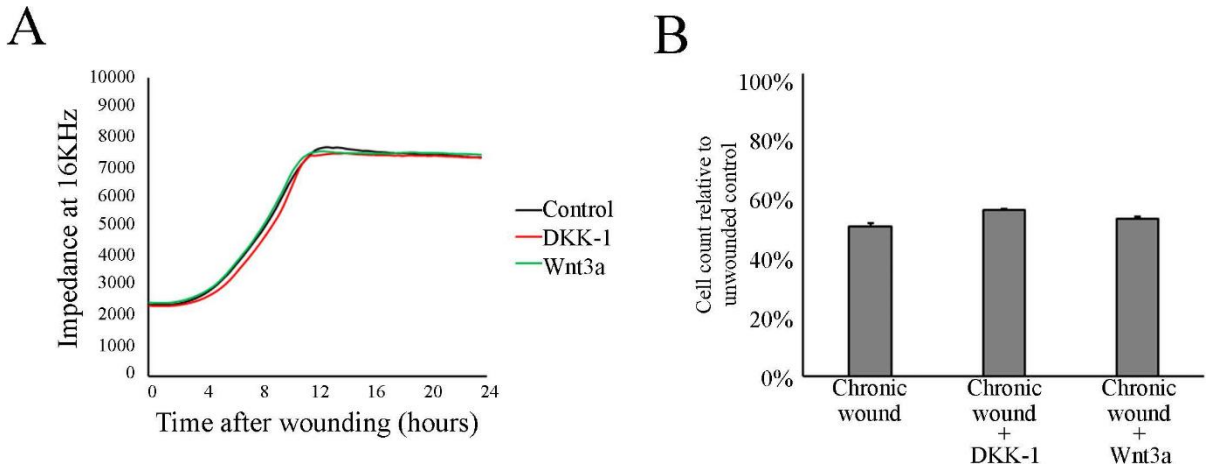

S2-3 Fig. Minimal effect of Wnt3a or DKK-1 on RPE cell wound repair. (A) Real-time impedance recording of RPE cell wound healing supplemented with DKK-1 (200 ng/ml) or Wnt3a (200 ng/ml). The recovery of impedance is not affected by supplementation with either DKK1 or Wnt3a. Each trace is an average of 2 biological replicates. (B) Cell count over the electrode based on Hoechst staining compared to unwounded samples (mean ± SD, n=3).

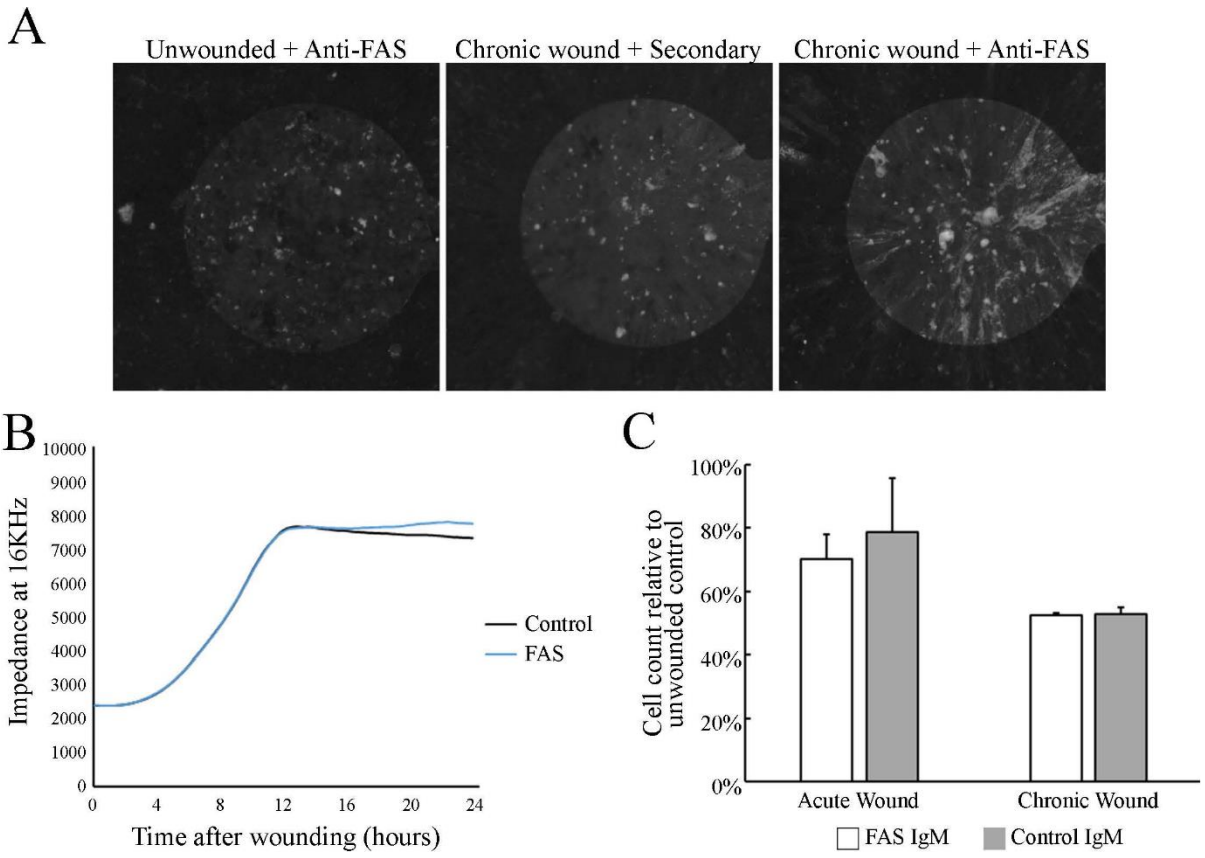

S2-4 Fig. Minimal effect of activating anti-FAS antibody on RPE cell wound repair. (A) Immunostaining of cells expressing FAS after chronic wounding. (B) Real-time impedance recording of RPE cell wound healing supplemented with 500 ng anti-FAS activating antibody. Each trace is an average of 2 biological replicates. (C) Cell count over the electrode based on Hoechst staining relative to unwounded samples (mean ± SD, n=2).

B. Description for Supplemental Files

S2-1 Movie. Real-time imaging of RPE cell wound repair. Wounding was generated using the ECIS system. Phase contrast images were taken every 30-minutes using the Cytation5 (BioTek). The video was generated using Gen3.00 software. Scale bar represents 300 μM.

S2-1 Table. Normalized RPM. The dataset was normalized using the trimmed mean of the M-values method. Genes with reads per million ≥ 1 in three or more samples were selected for further investigation.

S2-2 Table. Changes in gene expression after wounding. Differential expression and statistical analysis were carried out using edgeR. 24-hour unwounded samples were used as control for both 5-hour and 24-hour wounded samples. 8-day unwounded samples were used as the control for 8-day wounded samples.

S2-3 Table. P-values. P-values for Figs 2B and 3C were calculated using a two-tailed homoscedastic student's t-test. P-values for Figs 5B and 6A were calculated using edgeR compared to unwounded controls.

S2-4 Table. Differentially expressed genes after wounding. Genes with FDR ≤ 0.05 and ≥ 2-fold change compared to unwounded controls.

S2-5 Table. Top 100 RPE Genes. Expression levels of the top 100 RPE genes known to decrease in expression after RPE cells undergo epithelial-to-mesenchymal transition.

S2-6 Table. Gene list used in profiles of AMD eyes. Genes are categorized as Early AMD, GA, or CNV and whether the expression was upregulated or downregulated in the original AMD eye profiles by Newman *et al.*

S4-1 Table. Normalized TMM. The dataset was normalized using the trimmed mean of the M-values method. Genes with reads per million ≥ 1 in three or more samples were selected for further investigation.

S4-2 Table. Changes in gene expression after aging. Differential expression and statistical analysis were carried out using edgeR. Young 1-month unwounded controls were used as controls at all age time points.

S4-3 Table. Changes in gene expression after wounding. Differential expression and statistical analysis were carried out using edgeR. Equally aged, unwounded controls were used as controls for each time point.